Chapter – 2

Synthesis and study of antidiabetic and anticancer activities of

1-Aryl-3-(2-aryl-1,3-oxazol-4-yl)- 3-hydroxy-propanones and (E)-1-aryl-3-(2-aryl-1,3-oxazol-4-yl)-propenones.

2.1 Introduction

The research work in this thesis is focused on the chemistry of 1,3-oxazole heterocycle which is a member of the azole family as discussed earlier in Chapter-1. For the synthesis of new compounds, other heterocycles have been built on or attached to the compounds already containing oxazole in their structure with the intention to study various biological activities of the final new hybrid compounds containing two or more heterocycles in their structure.

Oxazole is associated with a number of biological activities due to the number of non-bonding interactions it can undergo. 1,3-Oxazole may undergo weak intermolecular interactions such as π–π stacking, co-ordination bonding, ion-dipole interactions, van der Waals interactions or may exhibit hydrophobic effects depending on its exposure to different types of donor/acceptor atoms or group of atoms or molecules.[1]

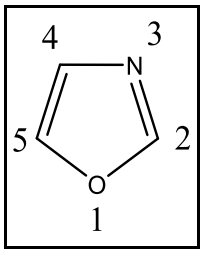

Figure 2.1 ***1,3-Oxazole.***

Following this, the oxazole containing compounds could readily bind with a variety of enzymes and receptors in biological systems as manifested in a wide range of biological activities they possess[1,2] including antibacterial,[3] antifungal,[4,5] antiviral,[6,7] antituberculer,[8,9] anticancer,[10–12] anti-inflammatory,[13] antidiabetic,[14] activities.

Before the structure of penicillin was established it was believed that it contained an oxazole core instead of β-lactam functionality.[15–17] This resulted in the beginning of the interest and development of oxazole chemistry. Some important oxazole containing compounds with significant biological activities have been included in **Figure 2.2**.

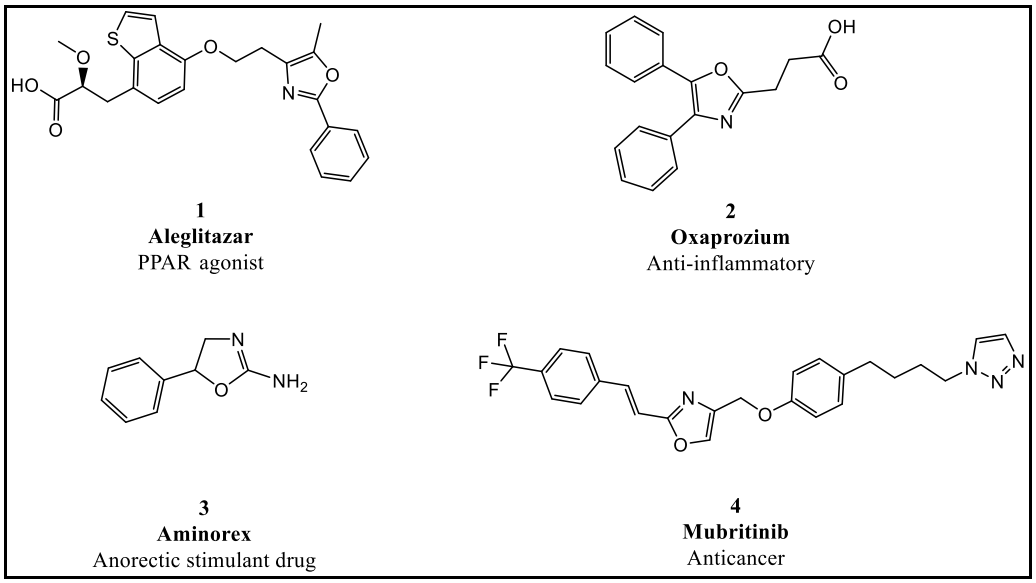

Figure 2.2 ***Oxazole containing drugs.***

A number of natural products, containing oxazole heterocycle have been reported in past few decades. The main source of these natural products is marine invertebrates and marine microorganisms. Many of these oxazole containing marine natural products have complex structural features and structural diversity such as the presence of several stereogenic centres (e.g. **Enigmazole A**) or the presence of macrocyclic rings inclusive or exclusive of oxazole moieties. They are called macrolides in general (**Figure 2.3**). These oxazole natural products have diverse significant biological activities.[18–26]

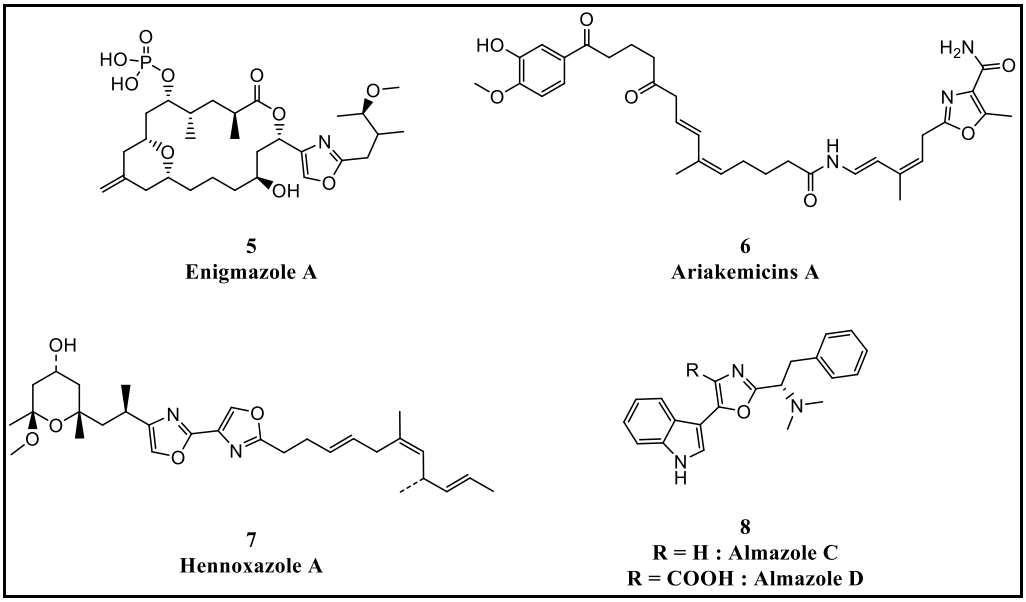

Figure 2.3 ***Marine natural products possessing oxazole.***

Reports on the isolation of natural products having oxazole moiety with various biological activities attracted attention of synthetic organic chemists.[27–30] Challenges involved in the total synthesis of natural products has led to the development of the new synthesis methodologies.[31–35]

Synthesis of Oxazole Compounds

In addition to natural product driven synthesis of oxazole heterocycles there are several important classical synthesis methodologies of oxazole or oxazole compounds such as Robinson-Gabriel oxazole synthesis and Fischer oxazole synthesis are as described in the following section.

Robinson-Gabriel Oxazole Synthesis[36]

2,5-Disubstituted and 2,4,5-trisubstituted oxazole derivatives **10** can be synthesize by the intramolecular condensation and dehydration of N-acyl α-aminoketones **9** in the presence of a dehydrating reagent such as PCl_5 or sulphuric acid. This reaction was first reported by Gabriel in 1907[37] and subsequently by Robinson in 1909[38]. This reaction is thus known as the Robinson-Gabriel cyclodehydration reaction. Other cyclodehydrating reagents include the phosphorus oxychloride ($POCl_3$), polyphosphoric acid (PPA), phosgene ($COCl_2$), $SOCl_2$, trifluoroacetic anhydride, triflic anhydride, P_2O_5, and anhydrous hydrogen fluoride.

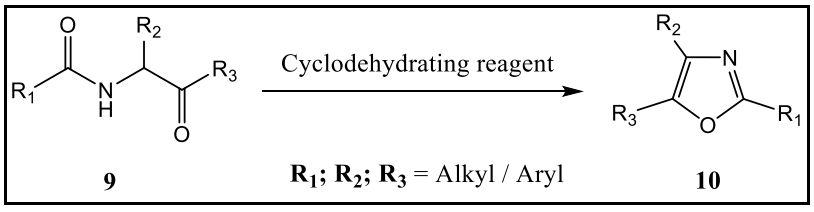

Scheme 2.1

Fischer Oxazole Synthesis[39]

Preparation of 2,5-diaryloxazoles **13** by treatment of equimolar amounts of aromatic aldehyde **11** and aldehyde cyanohydrin **12** in anhydrous ether with dry hydrogen

chloride is a Fischer oxazole synthesis and this reaction was first reported by Fischer in 1896[40]. This method is good for the preparation of diaryl oxazoles and is usually carried out in dry ether by dissolving aromatic aldehydes and aldehyde cyanohydrins and passing dry HCl gas. The synthesized oxazole precipitate out as its hydrochloride salt, which upon water/alcohol treatment can be converted into free oxazoles **13**.

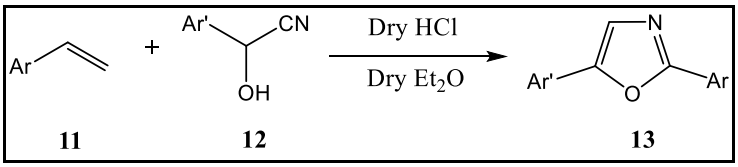

Scheme 2.2

Some of the recently developed important recently developed synthesis methodologies have been described in the following section.

One of the methods involves a quaternary ammonium hydroxide ion exchange resin catalysed reaction of p-toluenesulfonylmethyl isocyanide (TosMIC) with aromatic aldehydes **14** to yield 5-aryloxazoles **15** in high purity[41] (**Scheme 2.3**).

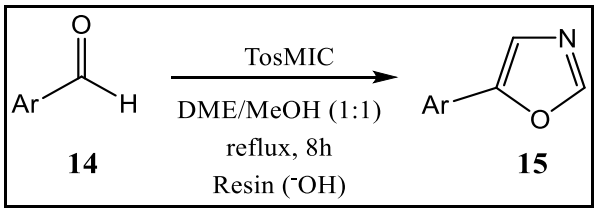

Scheme 2.3

2,5-Disustituted oxazoles **18** were obtained in a gold catalyzed oxidative coupling of alkynes **16** and alkyl/aryl nitriles **17** in good yields[42] (**Scheme 2.4**).

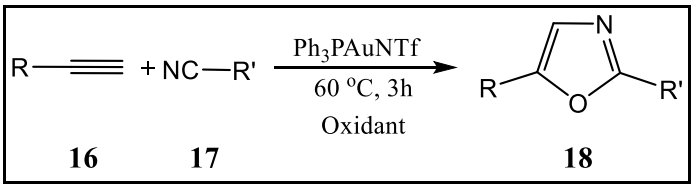

Scheme 2.4

2,5-Disubstituted oxazoles **21** were prepared by a facile one-pot, transition-metal-free t-BuOOH/I_2-mediated domino oxidative cyclization from readily available starting materials aryl alkenes **19** and benzylic amines **20** under mild conditions[43] (**Scheme 2.5**).

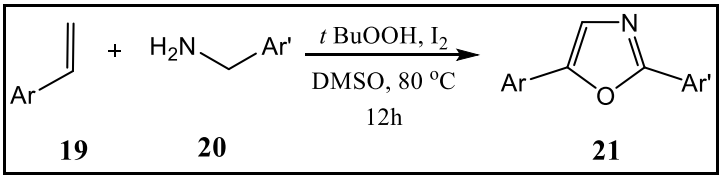

Scheme 2.5

A copper(II)-catalyzed oxidative cyclization of enamides **22** gave 2,5-disubstituted oxazoles **23** via vinylic C-H bond functionalization at room temperature in good yield[44] (**Scheme 2.6**).

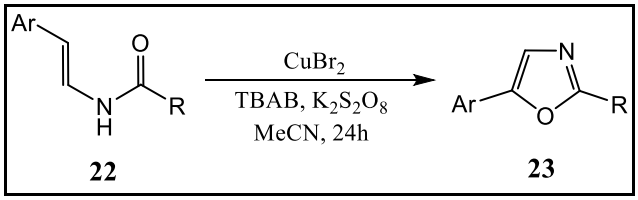

Scheme 2.6

2,5-Disubstituted oxazoles **25** were synthesized in high yields by intramolecular oxidative cyclization of N-styrylbenzamides **24** using hypervalent iodine reagent $PhI(OTf)_2$, generated in situ[45] (**Scheme 2.7**).

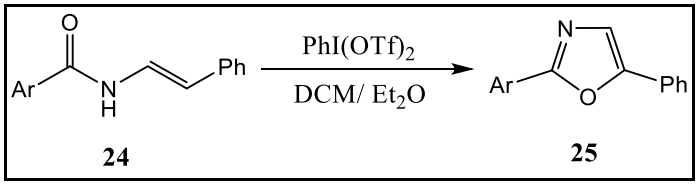

Scheme 2.7

A base-induced transformation reaction of 2-acyl-3-alkyl-2H-azirines **26** provided 2,4,5-substituted oxazoles **27** via a deprotonation-initiated mechanism followed by nucleophilic addition to the imine functionality[46] (**Scheme 2.8**).

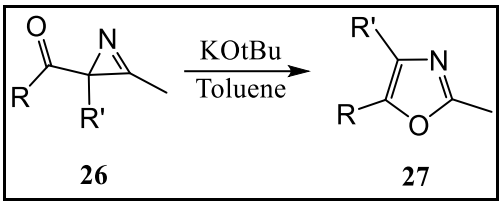

Scheme 2.8

A copper(II) triflate catalyst was used for coupling of α-diazoketones **28** with amides **29** to provide 2,4-disubstituted oxazoles **30**[47] (**Scheme 2.9**).

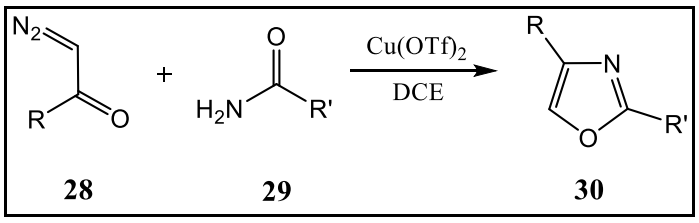

Scheme 2.9

2,4-Disubstituted and 2,4,5-trisubstituted oxazole **33** compounds were synthesized via [2+2+1] annulation of alkynes **31**, nitriles **32** and O-atom in the presence of Tf_2NH using PhIO as an oxygen source[48] (**Scheme 2.10**).

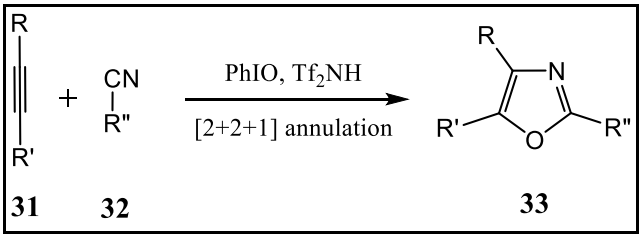

Scheme 2.10

Application of synthesis of 5-substituted-1,3-oxazole **35** using p-toluenesulfonylmethyl isocyanide (TosMIC) **34,** the Van Leusen reagent in the presence of a base on reaction with aldehyde **14** for the synthesis of C3 symmetric 1,3-oxazoles as molecular scaffolds was reported recently[49] (**Scheme 2.11**).

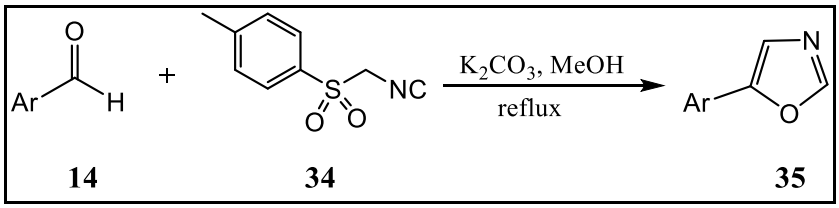

14 **34** **35**

Scheme 2.11

2,4,5-Trisubstituted oxazoles **38** were prepared from propargylic alcohols **36** and amides **37** by an efficient one-pot propargylation/cycloisomerization tandem process with the use of p-toluenesulfonic acid monohydrate (PTSA) as a catalyst[50] (**Scheme 2.12**).

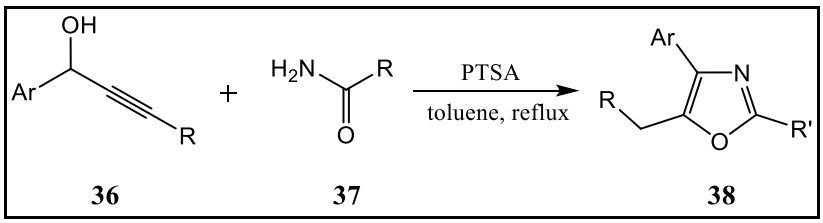

36 **37** **38**

Scheme 2.12

A novel route to synthesize oxazoles **40** was demonstrated via Beckmann rearrangement of α-formyl ketoxime dimethyl acetals **39** as a possible non-amino acid biosynthetic pathway to oxazoles in marine natural products[51] (**Scheme 2.13**).

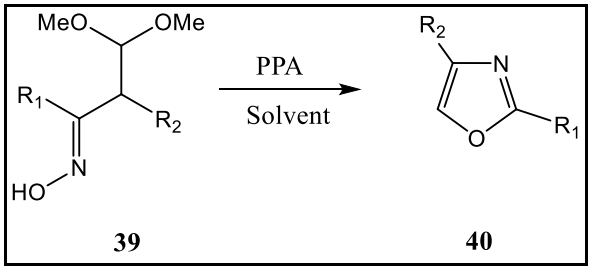

39 **40**

Scheme 2.13

Recently a synthesis of 2-aryl-4-formyl-1,3-oxazoles **44** was reported from α-azido acetophenone **42** under the Vilsmeier conditions. Earlier the reaction was erroneously reported to yield 2-aryl-5-formyl oxazoles.[52] The crystal structure and detailed investigation on the mechanism proposed indicated that the reaction proceeds via the

aziridine **43** and involves rearrangement leading to 2-aryl-4-formyl-1,3-oxazoles in moderate yields[53] (**Scheme 2.14**).

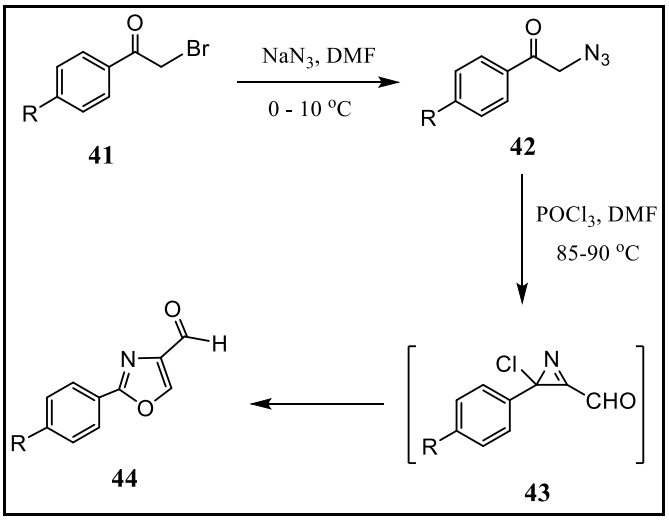

Scheme 2.14

Chalcones

On the other hand 1,3-diaryl/heteroaryl-2-propen-1-ones which are much known as chalcones have special importance as they serve as key synthons in the preparation of several oxygen containing natural products as well as in the synthesis of a number of nitrogen heterocyclic compounds on nucleophilic addition-cyclization reaction sequence.[54] Chalcones themselves exhibit a variety of bioactivity[55,56] which includes anticancer,[57] anti-inflammatory,[58] antiviral,[59] antihypertensive,[60] and antimalarial[61] among the others. Fluoro substituted chalcones in particular have been found to show a good anticancer activity.[62,63] On the other hand heteroaryl chalcones have been reported to exhibit anticancer activity.[64,65] Some of the representative biologically active chalcones are shown in **Figure 2.4.**

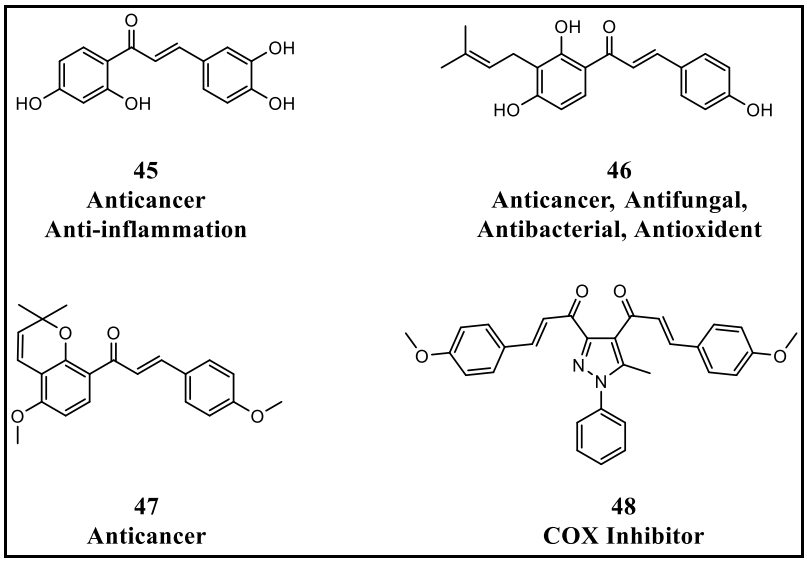

Figure 2.4 ***Representative biologically active chalcone molecules.***

In the present work, the Vilsmeier reagent was employed for the synthesis of 1,3-oxazole-4-carbaldehyde derivatives from the substituted acetophenones. The 1,3-oxazole-4-carbaldehydes prepared by the Vilsmeier reagent have a highly reactive formyl group at position-4 so that they can easily undergo the Claisen-Schmidt condensation reaction with various acetophenones to furnish the corresponding chalcones.

2.2 Results and Discussions

To start with, 2-aryl-1,3-oxazole-4-carbaldehydes **52a-e** were prepared from 4-substitued acetophenones **49** which upon bromination were converted to the corresponding phenacyl bromides **50.** The phenacyl bromides **50** were employed for the preparation of acyl azides **51** in DMF. Without isolating the acyl azides, more of DMF was added followed by the addition of $POCl_3$ under the Vilsmeier reaction conditions to yield 2-aryl-4-formyl-1,3-oxazoles **52**[53] (**Scheme 2.15**).

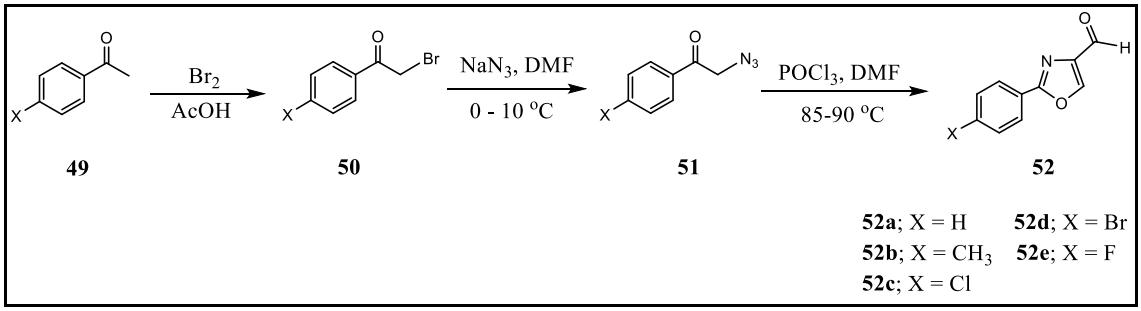

Scheme 2.15

The structures and melting points of all the oxazolyl carbaldehydes were well in agreement with that of the reported ones.[53]

1-(4-Fluoroaryl)-3-heteroaryl propanones and the corresponding propenones were prepared by reacting the 4-substituted acetophenone **53** with aryl substituted 1,3-oxazole-carbaldehydes **52** using the Claisen-Schmidt condensation reaction.

The Claisen-Schmidt reaction between aromatic aldehydes and aryl methyl ketones leads to 1,3-diaryl- 2-propane-1-ones or chalcones readily. The reaction has to proceed via β-hydroxy ketone formation as a primary aldol product, followed by a facile, quick dehydration to give chalcones leading to the thermodynamically stable α,β-unsaturated carbonyl compounds having an extended conjugation with the aryl groups.

For the synthesis of the β-hydroxy ketones **54** the reaction was carried out under kinetically controlled condition nearly at 0 ^oC with a close monitoring of the experiment, β-hydroxy ketones **54** were isolated as white crystalline products[66] (**Scheme 2.16**).

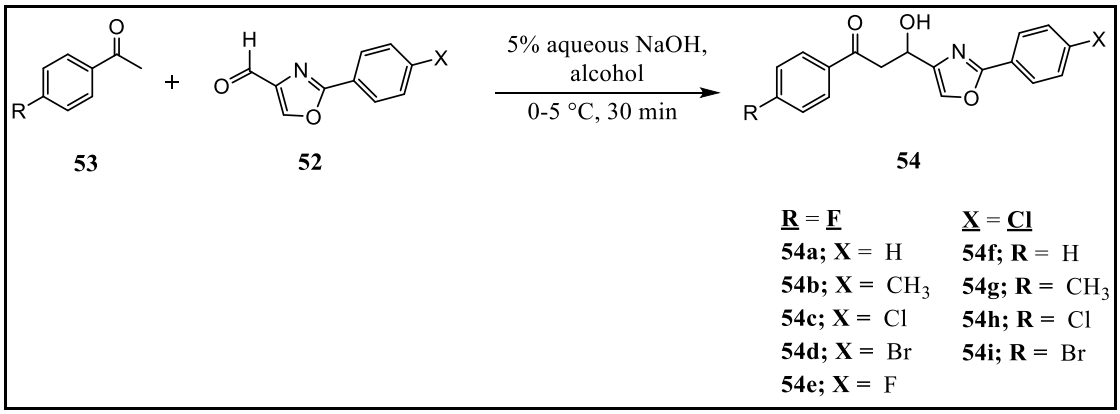

Scheme 2.16

The synthesis of the oxazole substituted chalcones **55** was carried out using 4-substituted acetophenones **53** as the enolizable ketone and aryl oxazole carbaldehydes **52** as enolate acceptors in the Claisen-Schmidt condensation reaction using aqueous alkali by warming the reaction at 50 ^{o}C, to yield the bright yellow compounds[66] (**Scheme-2.17**).

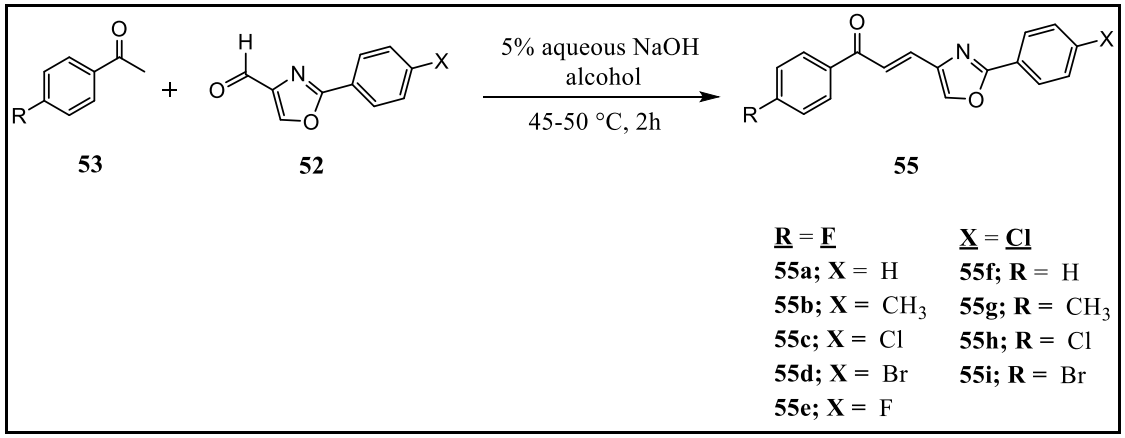

Scheme 2.17

Both the series of compounds namely 3-hydroxy-1-propanones **54(a-i)** and aryl-oxazolyl-propenones **55(a-i)** were characterized using IR, NMR and mass spectrometry.

2.2.1 Spectral Characteristics

The IR spectra of 3-hydroxy-1-propanones **54** show a broad absorption band for -O-H stretching centred at 3220-3325 cm^{-1}. At the higher end for difluoro substituted compound **54e (**R = F, X = F**)**. >C=O stretching is observed at 1680 cm^{-1} and at slightly higher end for the difluoro substituted compound **54e (**R = F, X = F**)** at 1685 cm^{-1}. -C-O stretching are observed at ~1225 cm^{-1} and 1160-1035 cm^{-1}. For propenones **55** the –O-H stretching band is absent and the >C=O stretching band is moved to a lower value of 1660-1670 cm^{-1} on becoming part of the extended conjugation.

Mass spectral analysis of the compounds from both the series show the expected molecular ion peaks clearly. Molecular ion peaks are also base peaks in the case of the chalcones. A characteristic mass peak for 4-fluorophenyl acyl cation at m/z = 123 is observed for some of the fluorinated compounds.

Nuclear Magnetic Resonance (NMR) spectroscopy study for all these compounds was carried out in detail using modern NMR techniques using a 400 MHz NMR instrument.

2.2.1.1 Fluorine NMR

Due to the presence of fluorine in some the newly synthesized heterocyclic moieties, NMR was employed to study ^{19}F NMR as well as ^{19}F coupled-decoupled proton NMR and ^{19}F coupled-decoupled carbon-13 NMR spectral characteristics.

Proton decoupled ^{19}F NMR spectra for the fluorine containing compounds of both the series **54** and **55** showed ^{19}F signals at δ = -104/-105, at the same chemical shift as is observed for 4-fluoroacetophenone itself. The compounds **54e (**R = F, X = F**)** and **55e (**R = F, X = F**)** having fluorine substitution present on both the phenyl rings, ^{19}F NMR spectra show one more signal at δ = -108/-109, slightly up field than the other ^{19}F signal.

Proton coupled ^{19}F were recorded for some representative compounds **54a (**R = F, X = H**)** and **54e (**R = F, X = F**)**. Due to ^{3}J and ^{4}J couplings with the *ortho* and *meta* protons (with respect to the position of F) present on the same aromatic ring, multiplicity for the ^{19}F signal should be a triplet of triplet. In a well resolved spectrum of **54a** (R = F, X =

H) all the nine peaks are observed centred at δ -103.97 (**Figure-2.5a**). For the compound **54e** (R = F, X = F) two identical multiplets with eight peaks each are observed centred at δ -103.88 and -109.26 respectively for fluorine attached to acyl aryl and oxazole aryl rings (**Figure 2.5b**).

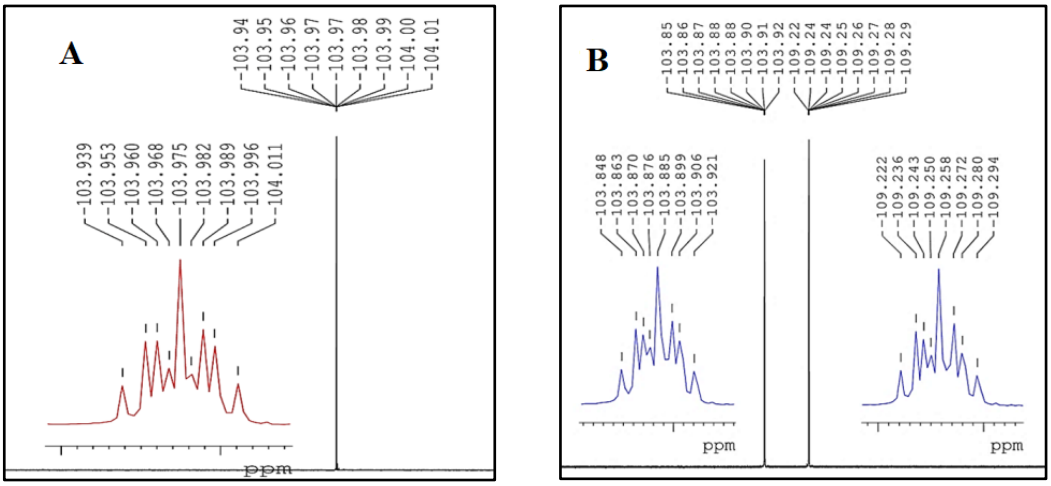

Figure 2.5 ***Proton coupled ^{19}F NMR of compound 54a and 54e.***

2.2.1.2 Proton NMR Study

Proton NMR spectra of 3-hydroxy-1-propanone **54a** (R=F, X=H) show a multiplet at δ 8.04 due to overlapping of signals for ^{19}F coupled proton **b** with that of proton **g** (**Figure-2.6**). For the other compounds (R=F, X≠H), both these protons (**b** and **g**) are observed separately as a doublet of doublet and a doublet respectively having close chemical shifts in this region.

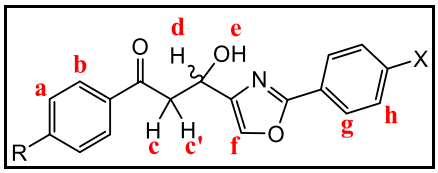

Figure 2.6 ***Proton labels on compounds 54.***

A signal for the protons **f** on the oxazole ring is observed at δ 7.73 as a doublet (^4J=1.2 Hz) due to a long range coupling with the proton **d**. A multiplet is observed for the three adjacent protons for **h** when X = H at δ 7.4. A doublet is observed for proton **h** at δ 7.4 when X ≠ H. The NMR signal for proton **a** *ortho* to fluorine is observed up field

as a triplet at δ 7.16 due to comparable coupling values for the ^{1}H-^{19}F and ^{1}H-^{1}H coupling with the proton **b**.

In the linker three carbon propanone chain, the proton **d** attached to the stereogenic carbinol carbon is observed at δ 5.42 as a multiplet for all the five compounds **54a**-**54i** and is coupled with four other protons: two diastereotopic vicinal protons **c, c'** situated on the methylene carbon, with the vicinal hydroxyl proton **e** and with the oxazole proton **f** having a long range coupling ^{4}J=1.2 Hz.

The hydroxyl proton **e** is observed between δ 3.8-3.6 as a doublet due to vicinal coupling ^{3}J = 3.6 Hz. Both the diastereotopic protons **c, c'** on the methylene carbon are observed as a doublet of doublet due to germinal coupling ^{2}J = 18.0 Hz between themselves and the vicinal coupling ^{3}J = 8.8 Hz or ^{3}J = 3.2 Hz with proton **d** depending on different dihedral angels formed; *anti* periplanar and *syn* periplanar respectively.

The deuterium exchange experiment was carried out to confirm the chemical shift of the hydroxy proton **e.** It also resulted in a reduced multiplicity of the NMR signal for proton **d**.

^{19}F-decoupled proton NMR of the compounds **54** resulted in simplification of the aromatic region protons with clear doublets due to the *ortho* coupling ^{3}J= 8.8 Hz between proton **a** and proton **b**. Because of the decoupling frequency incident on the sample, the long range small coupling between the oxazole proton **f** and the proton **d** on the stereogenic centre is vanished.

Aryl-oxazolyl-propenones **55(a-i)** do not have any sp^3 carbons therefore proton NMR spectra do not possess signals in the up field region present in the earlier case and all the protons signals for these compounds are observed between δ 8.9-7.1.

Overall the PMR spectra of these compounds have similar features for the aromatic protons with the comparable chemical shift values of the respective protons in the compounds with hydroxy ketone linker chain. The newly generated double bond connects both the aromatic ends bringing them in conjugation with the formation of unsaturated carbonyl middle linker chain.

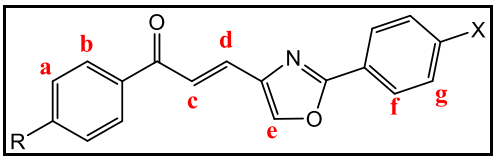

Figure 2.7 ***Compounds 55 with protons labelled.***

The protons **c** and **d** (**Figure-2.7**) on the double bond appear at δ 7.7 and 7.9 respectively. The assignment is based on the fact that the proton **d** connected carbon should have lower electron density due to electron withdrawing carbonyl functionality in conjugation. The vicinal coupling constant ^{3}J observed is 15 Hz for these protons (**c, d**) indicating the formation of thermodynamically more stable *trans* stereo-isomers.

In fluorine coupled proton NMR spectra of these compounds, the protons **b** and **f** (**Figure-2.7**) are observed downfield together as a mulptiplet between δ 8.2-8.1 for **55a** (R = F, X = H) and **55e** (R = F, X = F). For the other compounds (R = F, X ≠ H), the protons **b** and **f** show separate signals in the same region. The oxazole proton **e** is observed as a singlet in absence of the long range coupling. The protons **g** are observed as a doublet (R = F, X ≠ H) between d 7.3-7.6 and as a multiplet when X = H for three protons. The protons **a** appear as a triplet at δ 7.2 with both the ^{3}J = 8.8 Hz. Interestingly, for the compound **55e** (R = F, X = F), both the protons **a** and **g** (**Figure-2.7**) have exactly identical chemical shift and appear as a clean triplet at δ 7.20 and collapse to a doublet in ^{19}F decoupling experiments. In the decoupling experiments, the signal for proton **b** observed at a low field is also simplified to a doublet for the other compounds (R = F, X ≠ F) and for the proton **f** too for the compound **55e** where (R = F, X = F).

2.2.1.3 Carbon NMR Interpretation

Carbon 13 NMR experiments were carried out for characterization of the newly synthesized compounds and to study ^{19}F-^{13}C splitting due to ^{1}J, ^{2}J, ^{3}J couplings with the aromatic carbons of the aromatic ring possessing fluorine.

In the aryl-heteroaryl-hydroxyl propanones **54**, the carbonyl carbon **e** (**Figure-2.8**) is observed at δ~ 198. ^{19}F attached carbon **a** is observed most down field at δ 166

compared to the other aromatic carbons as a doublet having ^{1}J coupling with ^{19}F measured to be 255-250 Hz. The chemical shift value of δ ~116 is assigned to carbon **b** based on the doublet with ^{2}J = 22 Hz for its ^{13}C-^{19}F coupling. Carbon **c** are observed at δ~131 with ^{3}J = 9-10 Hz. The quaternary aromatic carbon **d** shows a doublet due to its coupling with fluorine having coupling constant ^{4}J = 3 Hz with the chemical shift value of δ = 133-134.

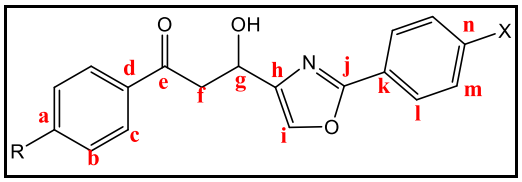

Figure 2.8 ***Carbon labels on compound 54.***

The assignment of the oxazole quaternary carbon **h** was possible with the help of DEPT, HSQC (**Figure 2.9**), and HMBC experiments. The carbon signal observed at δ~ 143 is assigned to **h** as it shows HMBC correlation (see spectral section) with the sole oxazole proton situated on carbon **i**. The carbon **i** has chemical shift at δ 134. The rest of the aromatic carbons **k, l, m, n** are observed in between δ 124-133 except for the case when X =F.

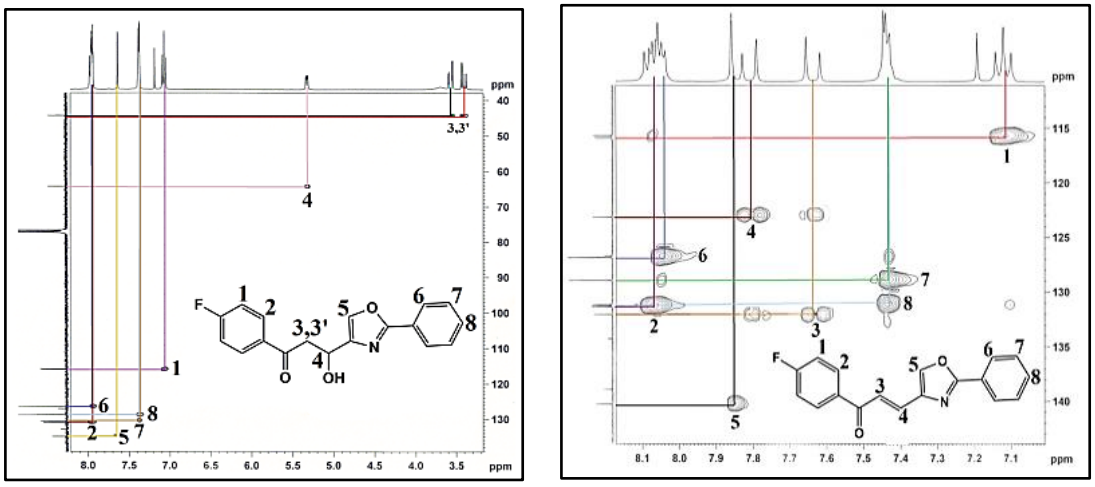

Figure 2.9 ***HSQC 2D-NMR of compound 54a and 55a.***

Carbon 13 NMR spectra of compound **54e** with (R = F, X = F) has comparable couplings with fluorine as are observed for the other fluorine containing aromatic ring. Carbon **n** is observed at δ 164 as a doublet with ^{1}J = 249 Hz while the doublet for

carbon **m** is found at δ 115 having ^{2}J =22 Hz, and is overlapping with the signal for carbon **b.** Carbon **l** is observed at δ 128.5 with ^{3}J = 8 Hz and the farthest fluorine coupled carbon **k** has chemical shift δ 123.7 with ^{4}J = 3 Hz. Thus similar to ^{19}F NMR signals, ^{13}C NMR signals of difluoro compound **54e** (R = F, X = F) has an identical pattern of coupling for the two fluorine containing rings with change in the chemical shift values.

Carbon 13 NMR were also studied for the aryl-oxazolyl-propenones **55**. Introduction of the double bond in the linker and extended conjugation in the molecule results in change in chemical shift value of carbonyl carbon **e** shifting it up field by ~10 ppm to δ 188 ppm.

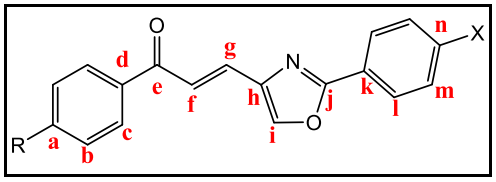

Figure 2.10 ***Carbon labels on compound 55.***

The chemical shift of carbon **i** (**Figure-2.10**) in these compounds is also affected and is observed at δ 140 from its earlier position of δ 135 in its parent hydroxy ketones **54**. The chemical shift of the newly appearing unsaturated carbons were assigned to δ 132 for carbon **f** and δ 123 for carbon **g** based on 2D HSQC (**Figure 2.9**) experiments supported by DEPT. ^{19}F-^{13}C couplings ^{1}J, ^{2}J, ^{3}J and ^{4}J are found to be identical as were observed in the earlier case.

The Physical data (Yields, mp) of newly synthesized compounds are presented in **Table 2.1.**

Table 2.1 ***Physical data (Yield, mp) of newly synthesized compounds*.**

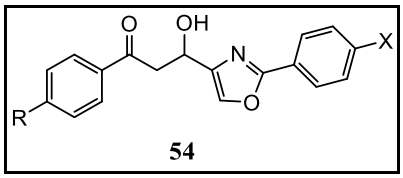

54

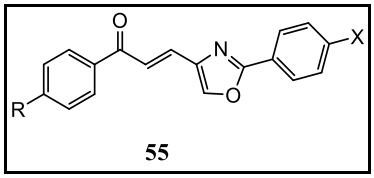

55

-R	-X	ID	Molecular formula	Yield	Mp	ID	Molecular formula	Yield	Mp
F	**H**	**54a**	$C_{18}H_{14}FNO_3$	69 %	150 **°C**	**55a**	$C_{18}H_{12}FNO_2$	58 %	110 **°C**
F	**CH_3**	**54b**	$C_{19}H_{16}FNO_3$	82 %	148 **°C**	**55b**	$C_{19}H_{14}FNO_2$	58 %	157 **°C**
F	**Cl**	**54c**	$C_{18}H_{13}ClFNO_3$	84 %	158 **°C**	**55c**	$C_{18}H_{11}ClFNO_2$	64 %	144 **°C**
F	**Br**	**54d**	$C_{18}H_{13}BrFNO_3$	78 %	144 **°C**	**55d**	$C_{18}H_{11}BrFNO_2$	62 %	139 **°C**
F	**F**	**54e**	$C_{18}H_{13}F_2NO_3$	69 %	138 **°C**	**55e**	$C_{18}H_{11}F_2NO_2$	68 %	143 **°C**
H	**Cl**	**54f**	$C_{18}H_{14}ClNO_3$	78 %	160 **°C**	**55f**	$C_{18}H_{12}ClNO_2$	67 %	178 **°C**
CH_3	**Cl**	**54g**	$C_{19}H_{16}ClNO_3$	80 %	164 **°C**	**55g**	$C_{19}H_{14}ClNO_2$	61 %	187 **°C**
Cl	**Cl**	**54h**	$C_{18}H_{13}Cl_2NO_3$	82 %	168 **°C**	**55h**	$C_{18}H_{11}Cl_2NO_2$	73 %	174 **°C**
Br	**Cl**	**54i**	$C_{18}H_{13}BrClNO_3$	86 %	197 **°C**	**55i**	$C_{18}H_{11}BrClNO_2$	69 %	149 **°C**

2.2.2 Single Crystal X-ray Study

One of the β-hydroxy ketones **54e** (R = F, X = F) and one α,β-unsaturated compound **55b** (R = F, X = CH_3) were crystallized from ethanol to obtain crystal suitable for X-ray diffraction. Single crystal X–ray diffraction study of the crystals of these compounds was carried out. The triclinic (space group P-1) crystals of the β-hydroxy ketone **54e** exhibit the structure as seen in its ORTEP diagram (**Figure 2.11)**. The intermolecular hydrogen bonding is observed between H10---N20 (2.053 Å). There are two sets of intermolecular π-π stacking interactions were observed between electron π-cloud of C5---C19 (3.337 Å), C6---C22 (3.338 Å) and C6---C6 (3.400 Å) (**Figure 2.13**). The crystal is also governed by three sets of C-H5---O11 (2.321 Å), C-H8A---O11 (2.644 Å), C-H8B---O10 (2.647 Å) interactions and N20---O10 (2.823 Å). The intermolecular interactions between F12---H5 (2.441Å) results into 1D chain formation and this 1D chains are further linked to form 2D network through π---π stacking interactions between phenyl and oxazole rings results in an attractive 2D zig-zag molecular packing pattern (**Figure 2.14**).

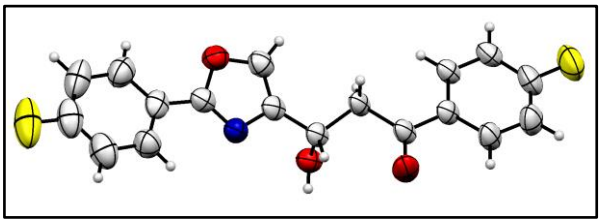

Figure 2.11 ***ORTEP diagram of 54e.***

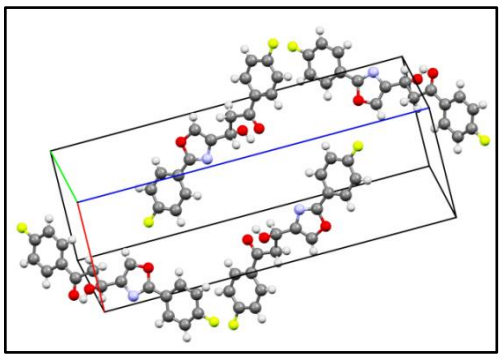

Figure 2.12 ***Unit cell of compound 54e.***

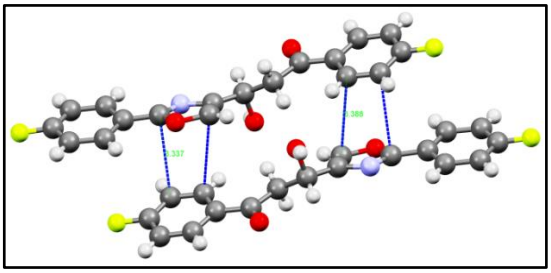

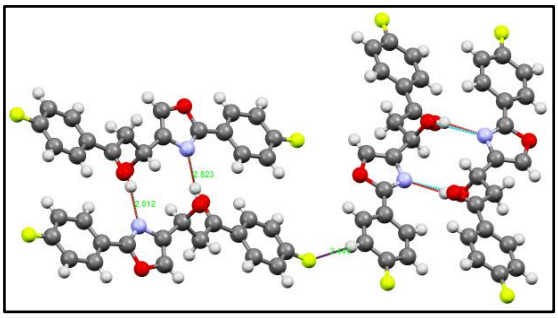

Figure 2.13 ***π---π stacking interaction and hydrogen bonding of compound 54e.***

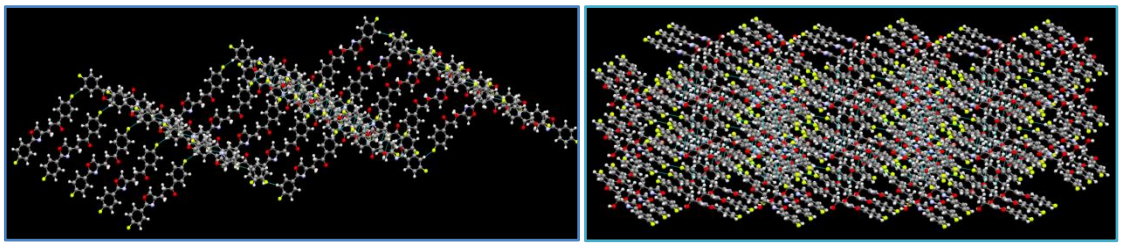

Figure 2.14 ***Molecular packing pattern of compound 54e.***

While in the case of α,β-unsaturated compound **55b,** the monoclinic (space group P21/n) crystals exhibit the orientation as shown (**Figure 2.15** and **2.16)**. The intermolecular CH---π interactions observed between electron π-cloud of C18---H14 (2.739 Å) (**Figure 2.17**). The intermolecular interactions between F23---H22 (2.531Å) and O13---H10 (2.515 Å) are also observed and form 1D linear chain. This 1D chains are further linked to form 2D framework through the intermolecular CH---π interactions between aromatic hydrogen and phenyl ring carbon (**Figure 2.18**).

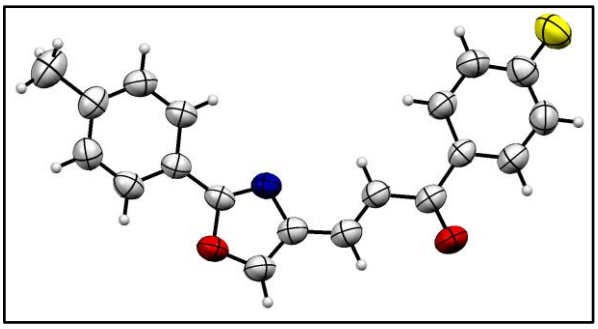

Figure 2.15 ***ORTEP diagram of 55b.***

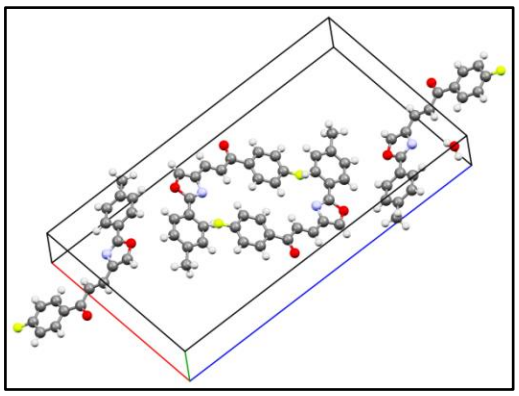

Figure 2.16 ***unit cell of compound 55b.***

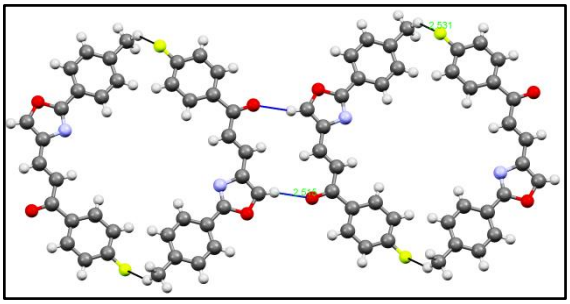

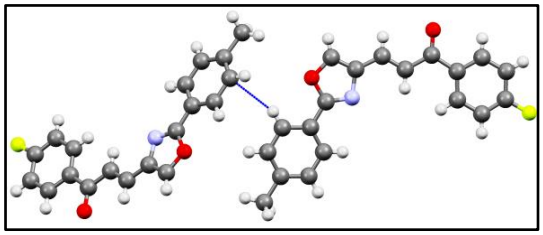

Figure 2.17 ***CO---H and CH---π interactions of compound 55b.***

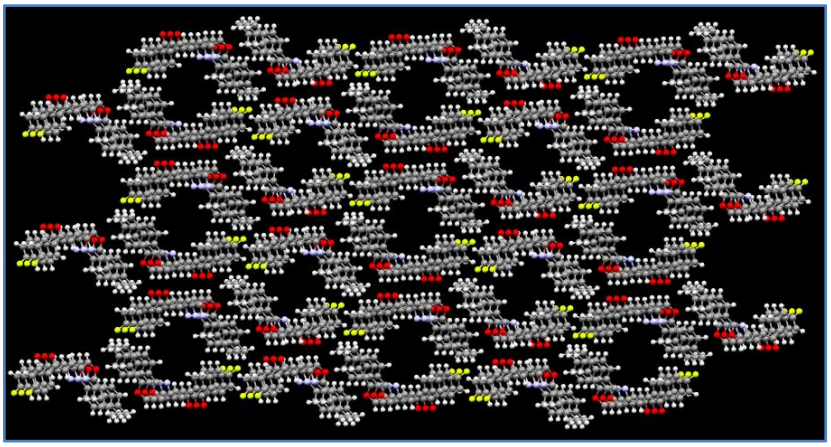

Figure 2.18 ***Molecular packing pattern of compound 55b.***

2.2.3 Anticancer Activity Study

On the basis of the literature reports on the anticancer activity of oxazoles as well as that for chalcones, anticancer activity of the newly synthesized compounds were subjected to *in-vitro* anticancer activity study.

The compounds were screened for their anticancer activities under the screening project at the Development Therapeutic Program (DTP), National Cancer Institute (NCI), Chemotherapeutic Research division, United States of America (USA) against full NCI 60 cell line panel representing the nine human systems as Leukaemia, Melanoma and cancers of Lung, Colon, Brain, Breast, Ovary, Kidney and Prostate (six cell lines of Leukaemia, six cell lines of CNS cancer, nine cell lines of Lung cancer, eight cell lines of Renal cancer, seven cell lines of Colon cancer, eight cell lines of Melanoma, six cell lines of Ovarian cancer, two cell lines of Prostate cancer and eight cell lines of Breast cancer) according to the applied protocol.

To begin with the structures of all the newly prepared eighteen compounds were submitted to the NCI website for their selection. The structures are generally selected for screening based on their ability to add diversity to the NCI small molecule compound collection. The structures with unique heterocyclic ring systems are particularly given attention. The screening process is of two steps, starting with the screening of all compounds against the 60 cell lines at one dose of $1x10^{-5}$ M concentration. The results from the single dose screen are reported as a mean graph and available for analysis by the COMPARE program. Compounds which exhibit significant growth inhibition are evaluated against the 60 cell panel at five concentration levels. The compounds are added at a concentration ($1x10^{-5}$ M) and the culture incubated for 48 h. A protein binding dye sulforhodamine B is used to determine the end point. Results of each test compound are shown as percentage growth of the treated cells when compared with untreated control cells. The methodology description of the experiments is included in the experimental section of this chapter.

Out of all the submitted compounds, three of the 3-hydroxy-1-propanones **54** and seven of the aryl-oxazolyl-propenones **55** (**Figure 2.19**) were selected for *in vitro* screening at a single dose of $1x10^{-5}$ M concentration.

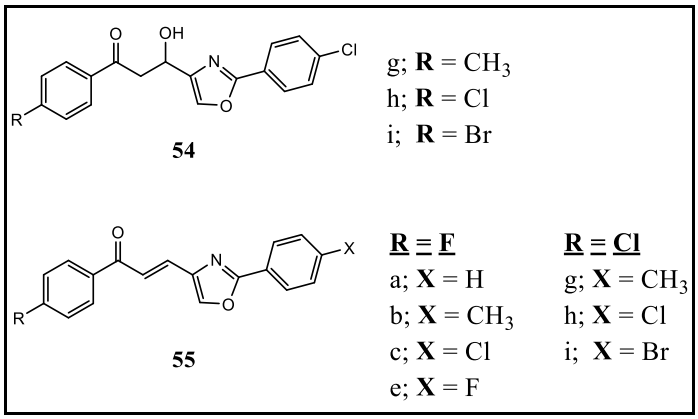

Figure 2.19 ***Selected compounds from 54 and 55 for anticancer activity.***

Interpretation of One-Dose Data

The one-dose data are reported as a mean graph of the percent growth of treated cells. The number reported for the one-dose assay is growth relative to the no-drug control, and relative to the time zero number of cells. This allows detection of both growth inhibition (values between 0 and 100) and lethality (values less than 0). For example, a value of 100 means no growth inhibition. A value of 40 would mean 60% growth inhibition. A value of 0 means no net growth over the course of the experiment. A value of -40 would mean 40% lethality. A value of -100 means all cells are dead. Results represent the % growth inhibition of the selected compounds. The anticancer activity results of 3-hydroxy-1-propanones **54** (**g, h, i**) are presented in graph form (**Figure 2.19)**. For a particular compound the cell lines for with greater than 20% growth inhibition are included in the results.

The results of the single dose anticancer screening of all the ten selected compounds in form of one dose mean graphs are included in appendix at the end of the thesis (**Sheets 1-10**).

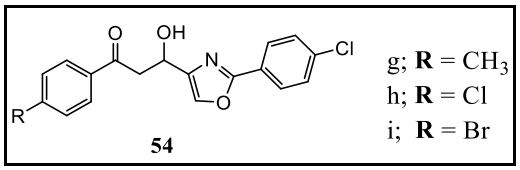

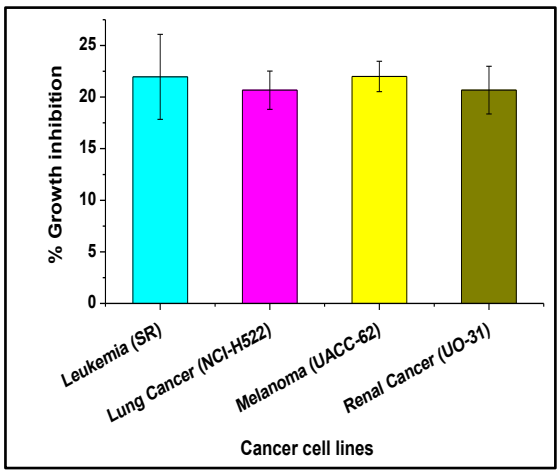

Compound 54g

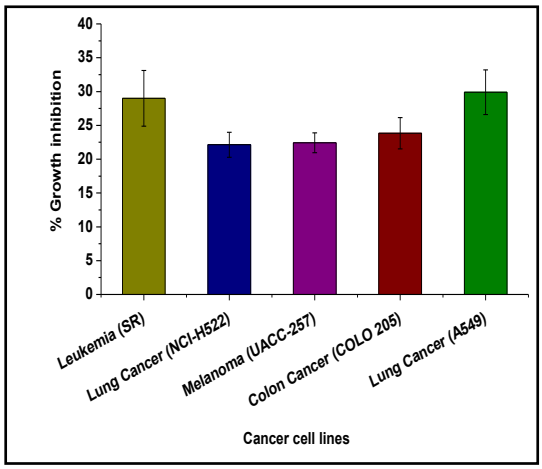

Compound 54h

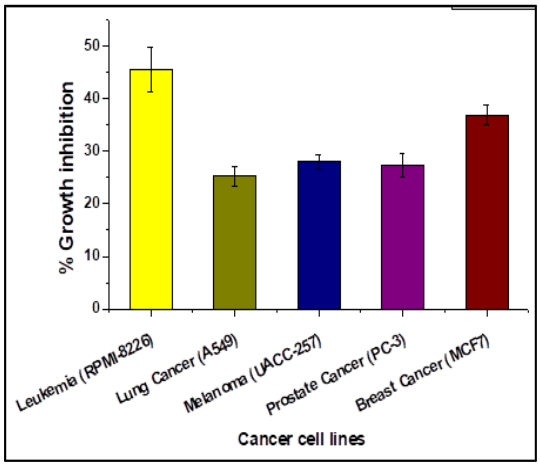

Compound 54i

Figure 2.19 ***Anticancer activity results of compounds from 54.***

Compound **54g (**R = Cl, X = CH_3**)** showed about 25% inhibition against Leukemia(SR), Lung cancer (H522), Melanoma (UACC-62) and Renal cancer (UO-31) cell lines (**Figure 2.19**). Compound **54h (**R = Cl, X = Cl**)** showed 27% and 32% inhibition against Leukemia(SR) and Lung cancer (H522) cell line respectively (**Figure 2.19**). Compound **54i (**R = Cl, X = Br**)** showed 46% inhibition against Leukemia (RPMI-8226) cancer cell line and 37% inhibition for Breast (MCF7) cancer cell line (**Figure 2.19**).

The results of the one dose screening for the tested seven compounds of **55 (a, b, c, e, g, h, i)** are projected in **Figure 2.20.**

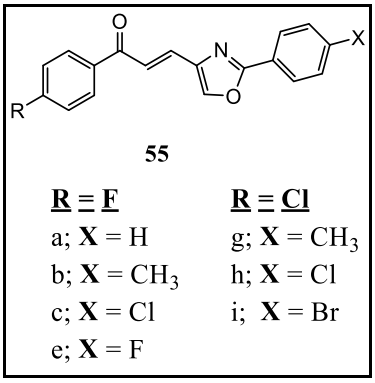

55

R = F	R = Cl
a; X = H	g; X = CH_3
b; X = CH_3	h; X = Cl
c; X = Cl	i; X = Br
e; X = F	

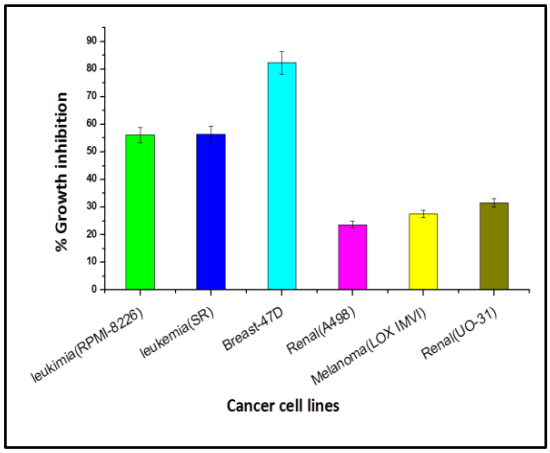

Compound 55a

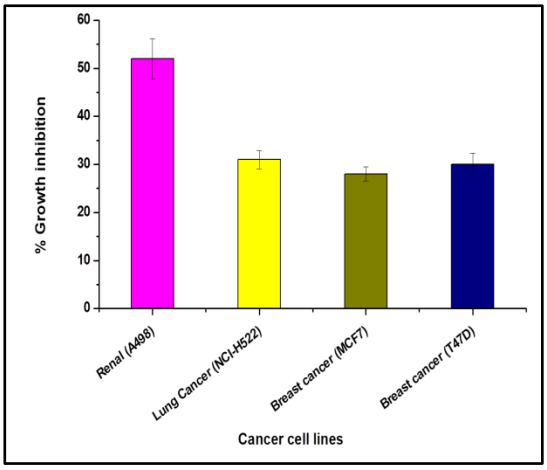

Compound 55b

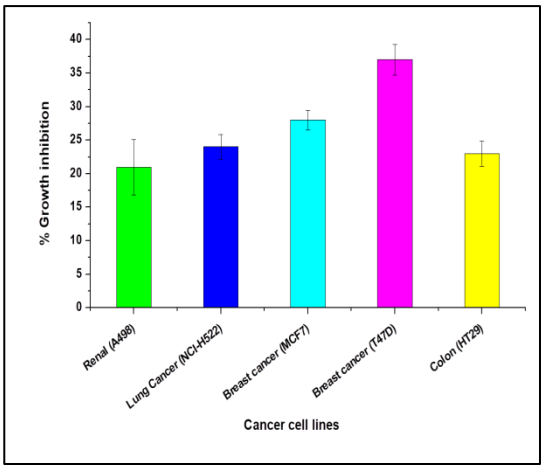

Compound 55c

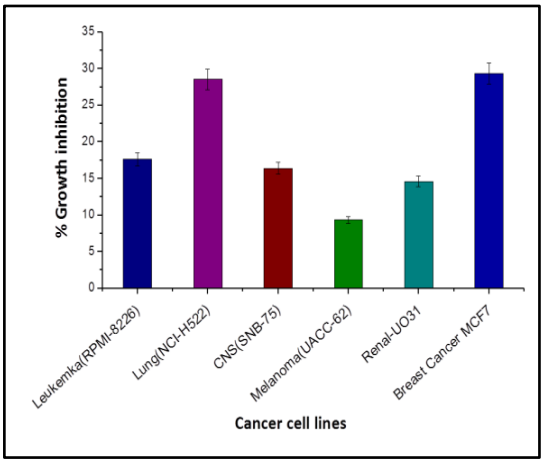

Compound 55e

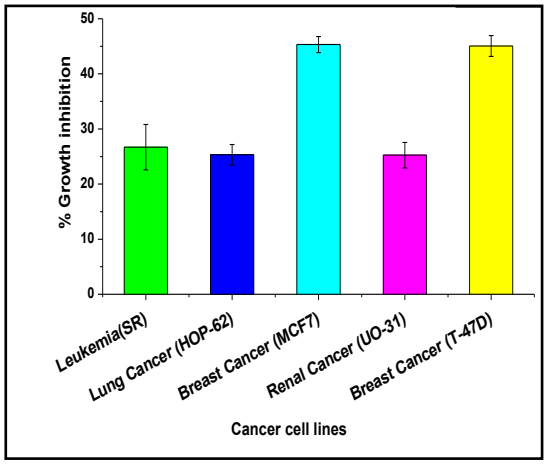

Compound 55g

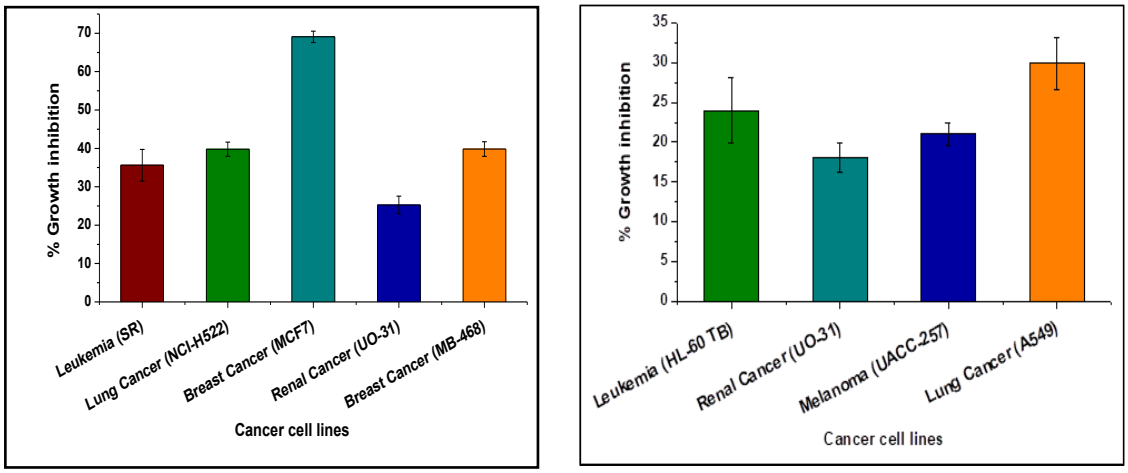

Compound 55h **Compound 55i**

Figure 2.20 ***Anticancer activity results of compounds from 55.***

Compound **55a (**R = F, X = F**)** and **55c (**R = F, X = Cl**)** showed 80% and 37% inhibition against Breast cancer (T-47D) cell line respectively, while compound **55b (**R = F, X = CH_3**)** showed 52% inhibition against Renal cancer (A498) cell line (**Figure 2.20**). Compound **55e (**R = F, X = F**)** inhibits Lung cancer (NCI-H522) and Breast cancer (MCF7) by 26% (**Figure 2.20**). Compound **55g (**R = F, X = Cl**)** showed 45% inhibition for Breast cancer cell lines namely (T-47D) and (MCF7) and compound **55g (**R = Cl, X = CH_3**)** showed 30% inhibition for Lung cancer (A549) cell line (**Figure 2.20**). Compound **55g** showed about 25% inhibition for Lung cancer (NCI-H522), Lung cancer (SR), Melanoma (UACC-62), Renal (UO-31) (**Figure 2.20**). While compound **55h (**R = Cl, X = Cl**)** showed 25% inhibition of Leukaemia (SR) cell line and Lung cancer (A549) cell line (**Figure 2.20**). Compound **55i (**R = Cl, X = Br**)** showed 45% inhibition of Leukaemia (RPMI-8226) cancer cell line (**Figure 2.20**).

Anticancer activity shows noteworthy results for all the ten selected compounds. From both the series of compounds aryl-oxazolyl-propenones showed better activity as compare to 3-hydroxy-1-propanones. The highest activity (% inhibition) was observed for compounds **55a (**R = F, X = F**)** and **55c (**R = F, X = Cl**)** against Breast cancer cell line T47D. Both the compounds showed 80% and 37% inhibition against Breast cancer (T-47D) cell lines respectively. While compound **55b (**R = F, X = CH_3) showed 52% inhibition against Renal (A498) cancer cell line.

2.2.4 Antidiabetic Activity Study

In continuation with the interest in study of antidiabetic activity [14,67–69] of new chemical entities, all the newly synthesized compounds **54(a-i)** and **55(a-i)** containing bioactive 1,3-oxazole heterocycle, the substituted aromatic rings and a three carbon linker chains with different polar groups, were subjected to *in vivo* oral glucose tolerance test on male C57 mice with the testing facility available at the Zydus Research Centre, Ahmedabad. The serum glucose was monitored at different time intervals from 0 to 240 minutes and the results were computed. The procedure is included in experimental section. The results are as summarized in **Table-2.2** and are presented as F**igure 2.21 and Figure 2.22** in graphical form.

Table 2.2 ***Oral glucose tolerance test results.***

Treatment (10mg/kg, IP)	**Baseline corrected Area under Curve glucose (mg/dl*240min)**			**% Change against vehicle control in Baseline corrected Area under Curve glucose (mg/dl*240min)**			**Statistical Significance**
Vehicle Control	35007		1730				
54a	21118	±	3163	-39.7	±	10.5	**p < 0.05**
54b	33576	±	2610	-4.1	±	8.9	Nil
54c	18413	±	2144	-47.4	±	8.2	**p < 0.05**
54d	31683	±	1858	-9.5	±	7.3	Nil
54e	40641	±	7869	16.1	±	23.0	Nil
46f	23956	±	5355	-31.6	±	16.2	Nil
54g	16969	±	4643	-51.5	±	14.4	**P<0.05**
54h	30427	±	3399	-13.1	±	10.9	Nil
54i	20268	±	2026	-42.1	±	7.9	**P<0.05**
55a	35261	±	1032	0.7	±	5.8	Nil
55b	34836	±	2951	-0.5	±	9.8	Nil
55c	22699	±	4939	-35.2	±	15.1	**P<0.05**
55d	45810	±	2636	30.9	±	9.1	Nil
55e	33944	±	4530	-3.0	±	13.9	Nil
55f	20675	±	4011	-40.9	±	12.6	**P<0.05**
55g	25569	±	4263	-27.0	±	13.2	Nil
55h	28799	±	4938	-17.7	±	15.0	Nil
55i	17314	±	2541	-50.5	±	9.1	**P<0.05**
	Mean		**SEM**	**Mean**		**SEM**	

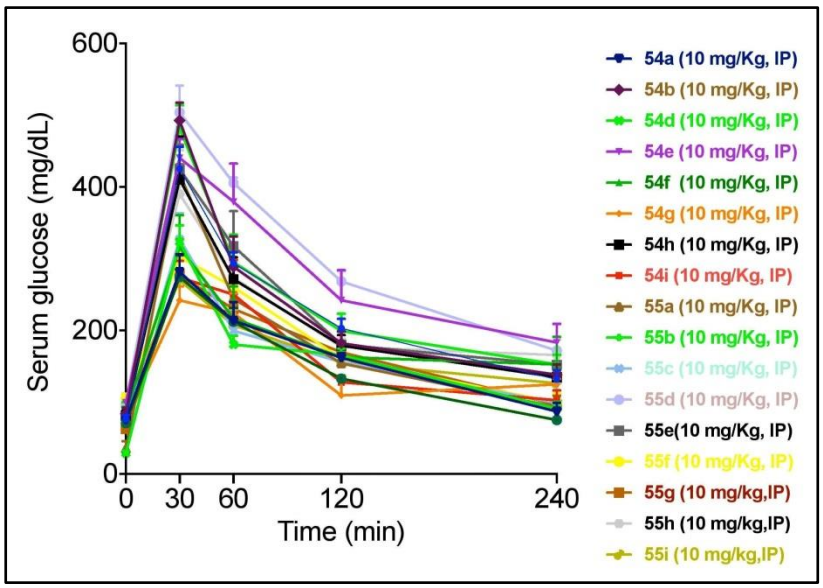

Figure 2.21 ***Serum glucose measurements during 240 min.***

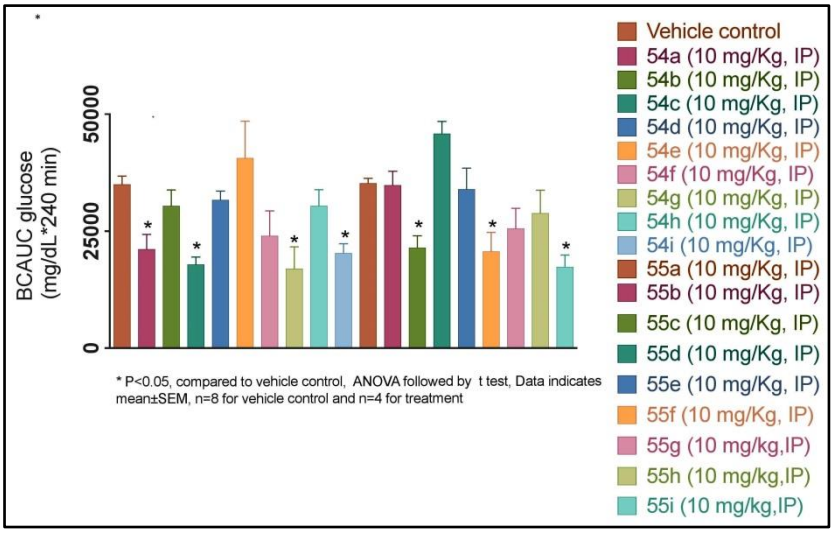

Figure 2.22 ***Base line corrected area under curve.***

Antidiabetic activity study of 3-hydroxy-1-propanones **54a-i** and aryl-oxazolyl-propenones **55a-i** showed excellent results as seven of the total eighteen compounds namely **54a (**R = F, X = F**)**, **54c (**R = F, X = Cl**)**, **54g (**R = Cl, X = CH_3**)**, **46i (**R = Cl, X = Br**)**, **55c (**R = F, X = Cl**)**, **55f (**R = Cl, X = H**)**, **55i (**R = Cl, X = Br**)** showed significant glucose lowering activity (**$p<0.05$**) with respect to the vehicle control (**Table 2.2** and **Figure 2.22**).

2.2.5 Molecular Docking Study

Molecular docking studies were performed to find out the binding interactions of the synthesized compounds with the active site of PPAR-α and PPAR-γ. Validation of the docking protocol was carried out by observing the orientation of the standard compounds in the active site of the proteins. This was done in collaboration and with the help of the computation facility available at the Faculty of Pharmacy, The M. S. University of Baroda.

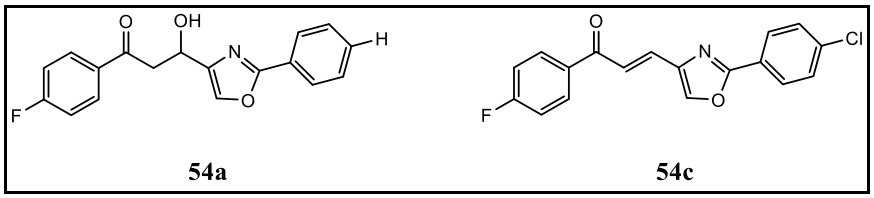

Figure 2.23

Wy 14643 (PPAR-α agonist) was used as the standard compounds in docking studies of the test compounds in the active site of PPAR-α. Wy 14643 has G-score of -12.28 which formed four hydrogen bonds with Tyr 464, His 440, Ser 280 and Tyr 314 residues which are the essential interactions for PPAR-α selectivity. Compounds **54a (**R = F, X = F**)** and **54c (**R = F, X = Cl**)** showed G-scores of -9.92 and -9.53 respectively. The phenyl and 4-chlorophenyl rings attached to the oxazole ring of compounds **54a (**R = F, X = F**)** and **54c (**R = F, X = Cl**)** respectively, were oriented towards Cys 275, Cys 276, Leu 321 residues. Oxygen of hydroxyl group of compound **54a (**R = F, X = F**)** formed two hydrogen bonds with Tyr 464 and His 440 residues as shown in **Figure 2.24a**. Whereas the oxygen of hydroxyl group of compound **54c (**R = F, X = Cl**)** showed hydrogen bond with Phe 273 residue and oxygen of carbonyl of compound **54c (**R = F, X = Cl**)** formed two hydrogen bonds with Tyr 314 and Ser 280 residues as shown in **Figure. 2.24b**. Formation of the hydrogen bond with Tyr 464, Tyr 314 and Ser 280 by compounds **54a (**R = F, X = H**)** and **54c (**R = F, X = Cl**)** could be one of the reasons for their antidiabetic activity.

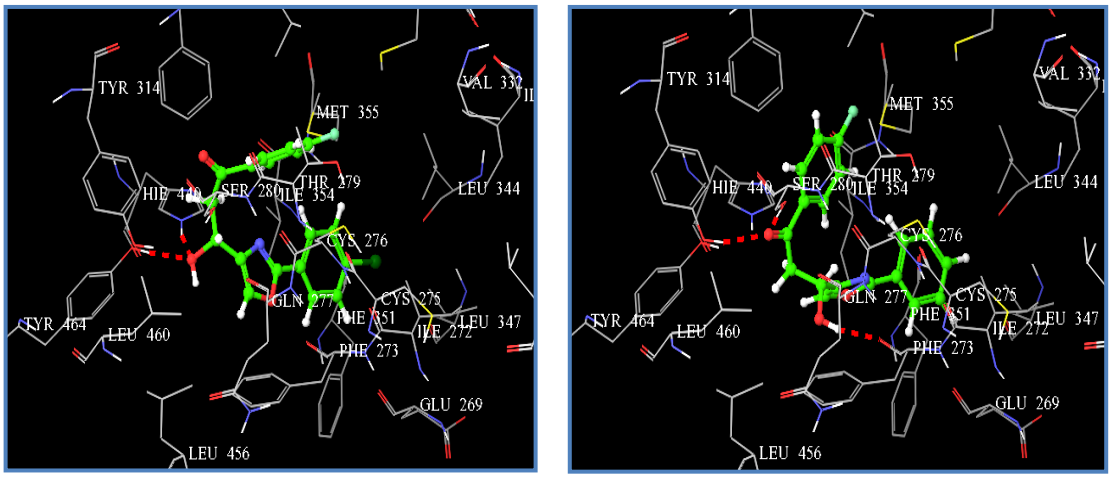

Figure 2.24 ***a) Orientation of compound (54a) in the active site of PPAR-α, b) Orientation of compound (54c) in the active site of PPAR-α.***

Roziglitazone was used as a standard compound for the docking studies of the test compounds in the active site of PPAR-γ. Roziglitazone has a G-score of -13.06 having three hydrogen bonds with Tyr 473, His 449 and Ser 289 residues. The terminal phenyl ring of roziglitazone showed π-π interactions with Phe 363 residue. Compounds **54a (**R = F, X = F**)** and **54c (**R = F, X = Cl**)** showed G-scores of -9.71 and -9.87 respectively. The oxygen of the hydroxyl group of compound **54a (**R = F, X = F**)** showed one hydrogen bond with Tyr 473 residue as shown in **Figure-2.25a**, whereas the oxygen of hydroxyl group of compound **54c (**R = F, X = Cl**)** formed two hydrogen bonds with Tyr 473 and His 449 residues as shown in **Figure-2.25b**. Hydrogen bonds formed by the hydroxyl group of compound **54a (**R = F, X = F**)** and **54c (**R = F, X = Cl**)** with Tyr 473 suggests that the hydroxyl group at this position is suitable and might be assisting for their good PPAR-γ agonistic activity. The phenyl ring of compounds **54a (**R = F, X = F**)** and **54c (**R = F, X = Cl**)** also formed π-π interactions with the Phe 363 residue. Thus, it is clear from the docking studies that compounds **54a (**R = F, X = F**)** and **54c (**R = F, X = Cl**)** bind perfectly in the same active site of PPAR-γ in which roziglitazone was bound.

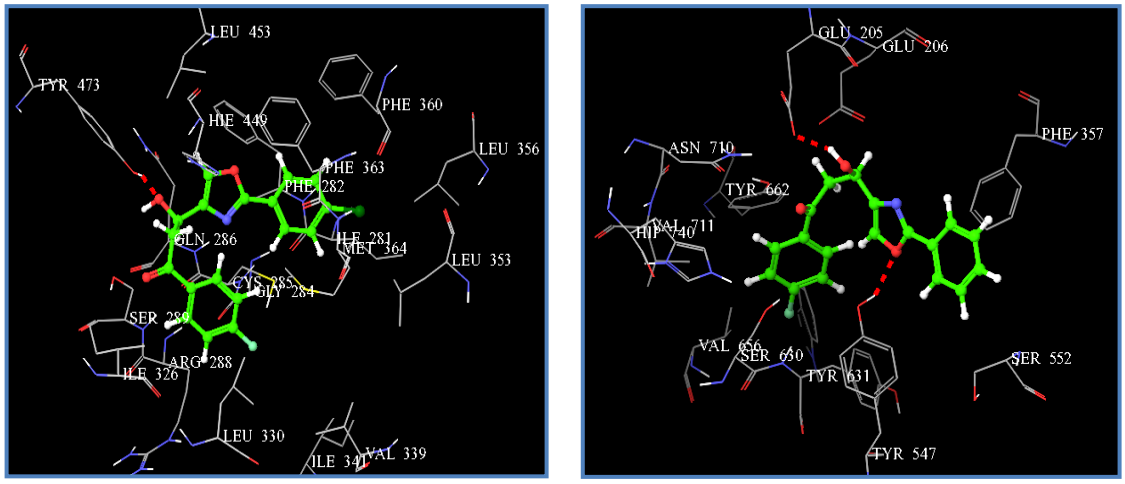

Figure 2.25 ***a) Orientation of compound (54a) in the active site of PPAR-γ, b) Orientation of compound (54c) in the active site of PPAR-γ.***

2.3 Conclusion

Several new oxazole containing 3-hydroxy-1-propanones and aryl-oxazolyl-propenones with the inclusion of an important heterocycle 1,3-oxazole and with the two types of linkers connecting the substituted aromatic and heteroaromatic parts have been synthesized from the corresponding 2-aryl-1,3-oxazole-4-carbaldehydes and 4-substituted acetophenones. All the new compounds were fully characterized by using various spectro analytical techniques. The final new compounds' NMR characteristics are studied in detail with the emphasis on ^{19}F NMR and signal assignments are made using 2D NMR techniques. The X–ray crystal diffraction study of one of the 3-hydroxy-1-propanones and one aryl-oxazolyl-propenones has been carried out. The final new 3-hydroxy-1-propanone and aryl-oxazolyl-propenone entities **54(a-i)** and **55(a-i)** were screened for anticancer and antidiabetic activities. Among them, compounds **54a**, **54c**, **54g**, **54i**, **55c**, **55f**, **55i** were found to show promising glucose lowering activity whereas some of the newly synthesized compounds show noteworthy activity against a number of different cancer cell lines. The highest activity (% inhibition) was observed for compounds **55a** and **55c** against Breast cancer cell line T47D.

2.4 Experimental

General

The chemicals were used as received from local companies without further purification. Organic solvents were purified by distillation prior to use.

Column chromatography was carried out using silica gel (60-120 mesh). Thin layer chromatography was performed on the pre-coated silica gel 60 F_{254} aluminium sheets. Melting points are determined in open capillary and are uncorrected.

FT-IR spectra were recorded on Perkin Elmer FTIR spectrometer between 4000-400 cm^{-1} in solid state as KBr discs. The NMR spectra were recorded on 400 MHz Bruker Avance-III instrument and chemical shifts are given in parts per million. In the NMR data for ^{19}F decoupled ^{1}H NMR experiments, the data for the affected signals only are included. ^{19}F chemical shift values are of ^{1}H decoupled ^{19}F signals.

Mass spectra were recorded on Thermo-Fischer DSQ II GCMS instrument. X-ray diffraction data for the compounds were collected at room temperature using a Bruker Smart Apex CCD diffractometer.

General Procedure for the Synthesis of 2-aryl-1,3-oxazole-4-carbaldehyde.[53]

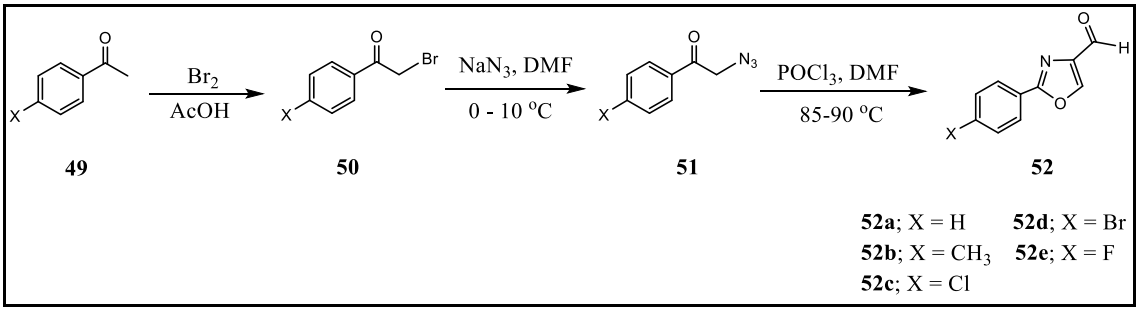

In an ice-cooled magnetically stirred solution of 4-substituted acetophenones **49** (10 ml, 0.0833 mole) in glacial acetic acid (25 ml) bromine (4.08 ml, 0.0833 mole) in 10 ml glacial acetic acid was added drop wise within half an hour by addition funnel at 10-15 °C. After the addition the reaction mixture was stirred at room temperature for 1 hour. When the colour of the reaction mixture becomes yellow an ice water was added to get white crystalline product **50**, which was filtered, washed with chilled water and dried in a desiccator.

In a 250-mL, two-necked, round-bottomed flask, sodium azide (3.16 g, 55 mmol) was added in one portion to an ice-cooled (10–15 °C), magnetically stirred solution of arylacyl bromide **42** (50 mmol) in DMF (50 mL). After stirring for 30 min, the acyl bromide was completely converted into the phenacyl azide **51** (TLC 10% EtOAc in petroleum ether). Then, $POCl_3$ (14 mL, 150 mmol) was added dropwise at 10–15 °C within 30–45 min. The reaction mixture was allowed to attain room temperature (30 °C) and was stirred for 3–4 h. After this time, the reaction mixture was heated slowly to 90–95 °C and stirred for 2–3 h. The reaction mixture was then cooled to room temperature and poured into an ice– water mixture (500 mL). The mixture was stirred for 1 h and extracted with $CHCl_3$ (3 x 100 mL). The organic layer was washed with aqueous $NaHCO_3$ solution to remove the formed benzoic acid and with water and brine and then dried over anhydrous Na_2SO_4. The solvent was removed, and the residue was column chromatographed (5% EtOAc/petroleum ether) to yield 2-aryloxazole-4-carbaldehydes **52a-e** as crystalline products. Yields: 28-39 %.

General Procedure for the Synthesis of 3-hydroxy-1-(4-fluorophenyl)-3-(2-aryl-1,3-oxazol-4-yl)-propanone 54. [66]

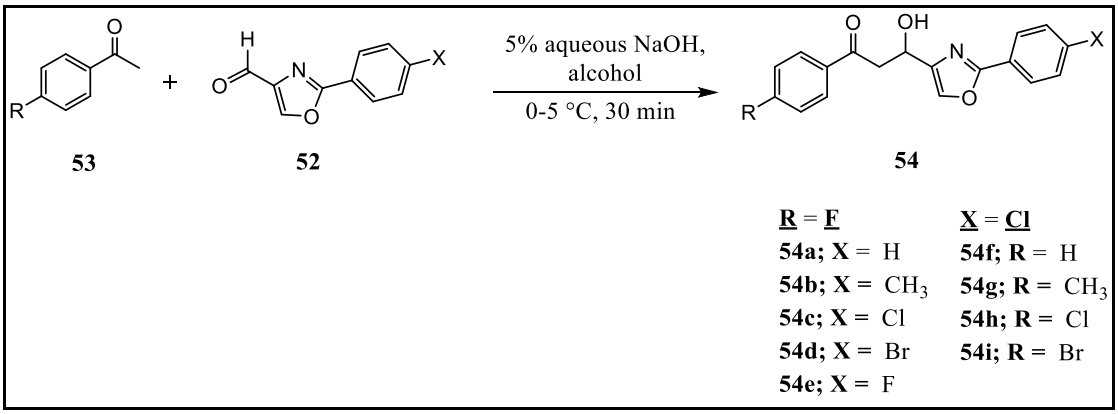

53 **52** **54**

R = **F**	**X** = **Cl**
54a; X = H	**54f; R** = H
54b; X = CH_3	**54g; R** = CH_3
54c; X = Cl	**54h; R** = Cl
54d; X = Br	**54i; R** = Br
54e; X = F	

To a magnetically stirred mixture of an 4-substituted acetophenones **53** (0.01 mol) in ethanol (95%, 20 ml) and NaOH (0.012 mol) in10 ml water kept at 0-5 °C in a 250 ml conical flask, a solution of respective 2-aryl-1,3-oxazole-4-carbaldehyde **54** (0.01 mol) in 20 ml ethanol was added drop wise using addition funnel during 20-30 minutes keeping the temperature below 5 °C . Stirring was continued for 30-60 minutes when the crystalline product started separating out. When the reaction completed (TLC : 10% E.A.), ice water (100 ml) was added for the complete precipitation of white products which were then filtered, washed with cold water and crystallized from alcohol. Yield: 70-84%.

1-(4-Fluorophenyl)-3-hydroxy-3-(2-phenyloxazol-4-yl)propanone 54a.

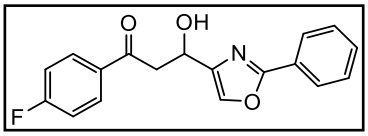

Compound **54a** was prepared following the general procedure described above by treating 2-phenyl-1,3-oxazole-4-carbaldehyde **52a** (1.73g, 0.01 mol) in ethanol with 4-fluoroacetophenone **53** (1.38g, 0.01 mol) and NaOH (0.5 g, 0.012 mol) in 10 ml water. Yield = 2.13g, 69%; White Solid; M.P. = 150 °C; **IR (KBr) cm^{-1}** : 3078, 2975, 1681, 1108, 942, 885, 775; **^{1}H NMR (400 MHz, $CDCl_3$, δ ppm)**: 3.49 (1H, dd, (1H of $-CH_2$), $^1J_{HH}$ = 18 Hz, $^2J_{HH}$ = 8.8 Hz , 3.65 (1H, dd, (1H of $-CH_2$), $^1J_{HH}$ = 18 Hz, $^3J_{HH}$ = 3.2 Hz), 3.85 (1H, d (-OH proton), $^3J_{HH}$ =3.2 Hz) , 5.42 (1H, m, (-CH), $^2J_{HH}$ = 8.8 Hz, $^3J_{HH}$= 3.2 Hz, $^5J_{HH}$ = 1.2 Hz), 7.15 (2H, t, F sub. Ar-H), 7.46 (3H, m, Ar-H), 7.72 (1H, d, oxazole H, $^4J_{HH}$ = 1.2 Hz), 8.04 (4H, m, Ar-H); **^{19}F decoupled ^{1}H NMR (400 MHz,**

$CDCl_3$, δ ppm): 7.15 (2H, d, Ar-H), 7.42 (3H, t (br), Ar-H), 7.72 (1H, s, oxazole-H), 8.02 (2H, d, Ar-H), 8.05 (2H, d, Ar-H); **^{19}FNMR (376 MHz, $CDCl_3$, δ ppm)**: -103.00; **^{13}CNMR (100 MHz, $CDCl_3$, δ ppm)**: 44.3, 64.3, 115.9 (d, $^2J_{CF}$ = 22 Hz), 126.4, 127.1, 128.8, 130.6, 130.9 (d, $^3J_{CF}$ = 9 Hz), 132.9, 134.2 (d, $^4J_{CF}$ = 3 Hz), 143.4 , 161.9, 166.1 (d, $^1J_{CF}$ = 254 Hz), 198.5; **EI-Mass**: m/z calculated for $C_{18}H_{14}O_3NF$: 310.77, found: (m/z) 310.77 $(M)^+$.

1-(4-Fluorophenyl)-3-hydroxy-3-(2-(4-Methylphenyl)-oxazol-4-yl)-propanone 54b.

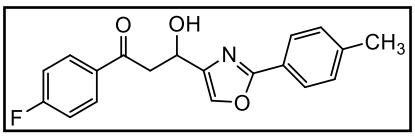

Compound **54b** was prepared following the general procedure described above by treating 2-(4-methylphenyl)-1,3-oxazole-4-carbaldehyde **52b** (1.87g, 0.01 mol) in ethanol with 4-fluoro acetophenone **53** (1.38g, 0.01 mol) and NaOH (0.5 g, 0.012 mol) in 10 ml water. Yield = 2.65g, 82%; White Solid; M.P. = 148°C; **IR (KBr) cm^{-1}** : 3215, 3081, 1680, 1593, 1073, 777; **^{1}H NMR (400 MHz, $CDCl_3$, δ ppm)**: 2.42 (3H, s, (-CH_3), 3.49 (1H, dd, (1H of -CH_2), $^1J_{HH}$ = 18 Hz, $^2J_{HH}$ = 8.8 Hz), 3.66 (1H, dd, (1H of -CH_2), $^1J_{HH}$ = 18 Hz, $^4J_{HH}$ = 3.2 Hz), 3.74 (1H, d, -OH, $^3J_{HH}$ = 4.4 Hz), 5.41 (1H, m, -CH, $^2J_{HH}$ = 8.8 Hz, $^3J_{HH}$ = 4.4 Hz , $^4J_{HH}$ = 3.2 Hz, $^5J_{HH}$ = 0.8 Hz), 7.16 (2H, t, F-sub. Ar-H), 7.27 (2H, t, Ar-H), 7.70 (1H, d, oxazole-H, $^5J_{HH}$ = 0.8 Hz), 7.92 (2H, d, Ar-H), 8.05 (2H, m, F- sub Ar-H); **^{19}F decoupled ^{1}H NMR (400 MHz, $CDCl_3$, δ ppm)**: 7.16 (2H, d, Ar-H), 7.27 (2H, d, Ar-H), 7.70 (1H, s, oxazole-H), 7.92 (2H, d, Ar-H), 8.05 (2H, d, Ar-H); **^{19}F NMR : (376 MHz, $CDCl_3$, δ ppm)**: -103.8; **^{13}C NMR (100 MHz, $CDCl_3$, δ ppm)** : 21.5, 44.3, 64.3, 115.8 (d, $^2J_{CF}$ = 22 Hz), 124.6, 126.3, 129.5, 130.9, (d, $^3J_{CF}$ = 9 Hz), 132.9 (d, $^4J_{CF}$ = 3 Hz), 134.4, 140.7, 143.4, 162.1, 166.0 (d, $^1J_{CF}$ = 250 Hz), 198.4; **EI-Mass**: m/z calculated for $C_{19}H_{16}FNO_3$: 324.88, found: (m/z) 324.88 $(M)^+$.

3-(2-(4-Chlorophenyl)-oxazol-4-yl)-1-(4-fluorophenyl)-3-hydroxy-propanone 54c.

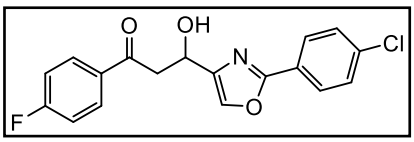

Compound **54c** was prepared following the general procedure described above by treating 2-(4-chlorophenyl)-1,3-oxazole-4-carbaldehyde **52c** (2.07g, 0.01 mol) in ethanol with 4-fluoro acetophenone **53** (1.38g, 0.01 mol) and NaOH (0.5 g, 0.012 mol) in 10 ml water. Yield = 2.89g, 84%; White Solid; M.P. = 158 °C; **IR (KBr) cm^{-1}** : 3078, 2975, 1681, 1108, 942, 885, 775; **^{1}H NMR (400 MHz,**

$CDCl_3$, δ ppm): 3.49 (1H, dd, (1H of -CH_2), $^1J_{HH}$ = 18 Hz, $^2J_{HH}$ = 8.8 Hz , 3.64 (1H, dd, (1H of -CH_2), $^1J_{HH}$ = 18 Hz, $^4J_{HH}$ = 3.2 Hz), 3.77 (1H, d (-OH proton), $^3J_{HH}$ = 4.4 Hz) , 5.41 (1H, m, (-CH), $^2J_{HH}$ = 8.8 Hz, $^3J_{HH}$ = 4.4 Hz $^4J_{HH}$ = 3.2 Hz, $^5J_{HH}$ = 0.8 Hz), 7.21 (2H, t, F sub. Ar-H), 7.44 (2H, m, Ar-H), 7.73 (1H, d, oxazole H, $^5J_{HH}$ = 0.8 Hz), 7.97 (2H, m, Ar-H), 8.03 (2H, m, Ar-H), **^{19}F decoupled ^{1}H NMR (400 MHz, $CDCl_3$, δ ppm)**: 7.17 (2H, d, Ar-H), 7.45 (2H, d, Ar-H), 7.73 (1H, s, oxazole-H), 7.97 (2H, d, Ar-H), 8.05 (2H, d, Ar-H); **^{19}FNMR (376 MHz, $CDCl_3$, δ, ppm)**: -105.19; **^{13}CNMR (100 MHz, $CDCl_3$, δ ppm)**: 44.2, 64.3, 115.5 (d, $^2J_{CF}$ = 22 Hz), 125.8, 127.6, 129.1, 130.8 (d, $^3J_{CF}$ = 9 Hz), 132.9 (d, $^4J_{CF}$ = 3 Hz), 135.0, 136.5, 143.8, 160.9, 166.1 (d, $^1J_{CF}$ = 249 Hz), 198.4; **EI-Mass**: m/z calculated for $C_{18}H_{13}ClFNO_3$: 344.54, found: (m/z) 344.54 $(M)^+$.

3-(2-(4-Bromophenyl)-oxazol-4-yl)-1-(4-fluorophenyl)-3-hydroxy propanone 54d.

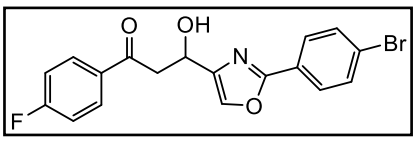

Compound **54d** was prepared following the general procedure described above by treating 2-(4-bromophenyl)-1,3-oxazole-4-carbaldehyde **52d** (2.52g, 0.01 mol) in ethanol with 4-fluoro acetophenone **53** (1.38g, 0.01 mol) and NaOH (0.5 g, 0.012 mol) in 10 ml water. Yield = 3.27g, 78%; White Solid; M.P. = 144 ^oC; **IR (KBr) cm^{-1}**: 3215, 3081, 680, 1593, 1073, 777; **^{1}H NMR (400 MHz, $CDCl_3$, δ ppm)**: 3.49 (1H, dd, (1H of -CH_2), $^1J_{HH}$ = 18 Hz, $^2J_{HH}$ = 8.8 Hz , 3.65 (1H, dd, (1H of -CH_2), $^1J_{HH}$ = 18 Hz, $^4J_{HH}$ = 3.2 Hz), 3.77 (1H, d (-OH proton, $^3J_{HH}$ = 4.4 Hz) , 5.41 (1H, m, (-CH), $^2J_{HH}$ = 8.8 Hz, $^3J_{HH}$ = 3.2 Hz, $^5J_{HH}$ = 1.2 Hz) , 7.17 (2H, t, F sub. Ar-H) , 7.61 (2H, m, Ar-H) , 7.74 (1H, d, oxazole H, $^5J_{HH}$ = 1.2 Hz), 7.90 (m, 2H, Ar-H), 8.05 (2H, m, F- sub Ar-H); **^{19}F decoupled ^{1}H NMR (400 MHz, $CDCl_3$, δ ppm)**: 7.17 (2H, d, Ar-H), 7.62 (t (br), 2H, Ar-H), 7.74 (1H, s, oxazole-H), 7.90 (2H, d, Ar-H), 8.05 (2H, d, Ar-H); **^{19}F NMR (376 MHz, $CDCl_3$, δ ppm)**: -103; **^{13}C NMR (100 MHz, $CDCl_3$, δ ppm)**: 44.2, 64.3, 115.5 (d, $^2J_{CF}$ = 22 Hz), 125.8, 127.6, 129.1, 130.8 (d, $^3J_{CF}$ = 9 Hz), 132.9 (d, $^4J_{CF}$ = 3 Hz), 135.0, 136.5, 143.8, 160.9, 166.1 (d, $^1J_{CF}$ = 249 Hz), 198.4; **EI-Mass**: m/z calculated for $C_{18}H_{13}BrFNO_3$: 390.20, found: (m/z) 390.20 $(M)^+$.

1-(4-Fluorophenyl)-3-(2-(4-fluorophenyl)-oxazol-4-yl)-3-hydroxy propanone 54e.

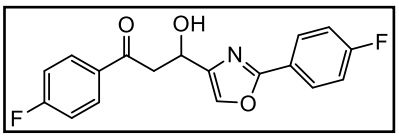

Compound **54e** was prepared following the general procedure described above by treating 2-(4-fluorophenyl)-1,3-oxazole-4-carbaldehyde **52e** (1.91g, 0.01 mol) in ethanol with 4-fluoro acetophenone **53** (1.38g, 0.01 mol) and NaOH (0.5 g, 0.012 mol) in 10 ml water. Yield = 2.26g, 69%; White Solid; M.P. = 138 ^{o}C; **IR (KBr) cm^{-1}**: 3070, 1684, 1598, 1031, 841, 746; **^{1}H NMR (400 MHz, CDCl$_3$, δ ppm)**: 3.49 (1H, dd, (1H of -CH$_2$), $^{1}J_{HH}$ = 18 Hz, $^{2}J_{HH}$ = 8.8 Hz , 3.65 (1H, dd, (1H of –CH$_2$), $^{1}J_{HH}$ = 18 Hz, $^{4}J_{HH}$ = 3.2 Hz), 3.73 (1H, d (-OH proton), $^{3}J_{HH}$ = 4.4 Hz) , 5.41 (1H, m, (-CH), $^{2}J_{HH}$ = 8.8 Hz, $^{3}J_{HH}$ = 4.4 Hz, $^{4}J_{HH}$ = 3.2 Hz, $^{5}J_{HH}$ = 0.8 Hz), 7.21 (4H, m, Ar-H), 7.72 (1H, d, oxazole H, $^{5}J_{HH}$ = 0.8 Hz), 8.04 (4H, m, Ar-H); **^{19}F decoupled ^{1}H NMR (400 MHz, CDCl$_3$, δ ppm)**: 7.16 (4H, m, Ar-H), 7.72 (1H, s, oxazole-H), 8.04 (4H, m, Ar-H); **^{19}F NMR (376 MHz , CDCl$_3$, δ ppm)**: -103.8, -109.2; **^{13}C NMR (100 MHz, CDCl$_3$, δ, ppm)**: 44.2, 64.2, 115.8 (d, $^{2}J_{CF}$ = 22 Hz), 116.0 (d, $^{2}J_{CF}$ = 22 Hz), 123.7 (d, $^{4}J_{CF}$ = 3 Hz), 128.5 (d, $^{3}J_{CF}$ = 8 Hz), 130.9 (d, $^{3}J_{CF}$ = 8 Hz), 132.9 (d, $^{4}J_{CF}$ = 3 Hz), 134.8, 143.6, 161.09, 164.0 (d, $^{1}J_{CF}$ = 249 Hz), 166.1 (d, $^{1}J_{CF}$ = 250 Hz), 198.4; **EI-Mass**: m/z calculated for $C_{18}H_{13}F_2NO_3$: 328.84, found: (m/z) 328.84 $(M)^+$.

3-(2-(4-Chlorophenyl)-oxazol-4-yl)-3-hydroxy-1-phenyl-propanone 54f.

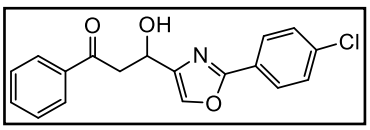

Compound **54f** was prepared following the general procedure described above by treating 2-Chlorophenyl-1,3-oxazole-4-carbaldehyde **52c** (2.07g, 0.01 mol) in ethanol with acetophenone **53** (1.20g, 0.01 mol) and NaOH (0.5 g, 0.012 mol) in 10ml water. Yield = 2.5g, 76%; White Solid; M.P. = 160 ^{o}C; **IR (KBr) cm^{-1}** : 3048, 2962, 1678, 1115, 937, 886, 748; **^{1}H NMR (400 MHz, CDCl$_3$, δ ppm)** : 3.52 (1H, dd, (1H of -CH$_2$), $^{1}J_{HH}$ = 18 Hz, $^{2}J_{HH}$ = 8.8 Hz , 3.69 (1H, dd, (1H of -CH$_2$), $^{1}J_{HH}$ = 18 Hz, $^{3}J_{HH}$ = 3.2 Hz), 3.82 (1H, d (-OH proton), $^{3}J_{HH}$ =3.2 Hz) , 5.42 (1H, m, (-CH), $^{2}J_{HH}$ = 8.8 Hz, $^{3}J_{HH}$= 3.2 Hz, $^{4}J_{HH}$ = 0.8 Hz), 7.47 (5H, m, Ar-H), 7.72 (1H, d, oxazole H, $^{4}J_{HH}$ = 0.8 Hz), 7.98 (2H, d, Ar-H), 8.01 (2H, m, Ar-H); **^{13}C NMR (100 MHz, CDCl$_3$, δ ppm)** : 44.3, 64.3, 115.9, 125.8, 127.7, 128.2, 128.7, 129.0, 133.7, 135.03, 136.53, 143.9, 160.9, 200.1 ; **EI-Mass**: m/z calculated for $C_{18}H_{14}ClNO_3$: 327.16, found: (m/z) 327.16 $(M)^+$.

3-(2-(4-Chlorophenyl)-oxazol-4-yl)-3-hydroxy-1-(4-methylphenyl)propanone 54g.

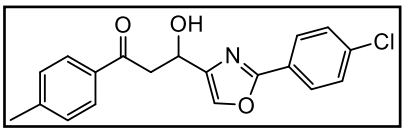

Compound **54g** was prepared following the general procedure described above by treating 2-(4-chlorolphenyl)-1,3-oxazole-4-carbaldehyde **52c** (2.07g, 0.01 mol) in ethanol with 4-methyl acetophenone **53** (1.35g, 0.01 mol) and NaOH (0.5 g, 0.012 mol) in 10 ml water. Yield = 2.9g, 80%; White Solid; M.P. = 164^{o}C; IR (KBr) cm^{-1} : 3214, 3084, 1682, 1591, 1073, 776; **^{1}H NMR (400 MHz, CDCl$_3$, δ ppm)** : 2.49 (s, 3H, (-CH_3) protons), 3.48 (1H, dd, (1H of -CH_2), $^{1}J_{HH}$ = 18 Hz, $^{2}J_{HH}$ = 8.4 Hz), 3.66 (1H, dd, (1H of -CH_2), $^{1}J_{HH}$ = 18 Hz, $^{4}J_{HH}$ = 3.2 Hz), 3.88 (1H, d (-OH proton), $^{3}J_{HH}$ = 4.4 Hz), 5.40 (1H, t, (-CH), $^{2}J_{HH}$ = 8.4 Hz, $^{3}J_{HH}$ = 4.4 Hz , $^{4}J_{HH}$ = 3.2 Hz, $^{5}J_{HH}$ = 1.2 Hz), 7.14 (2H, d, Ar-H), 7.44 (2H, m, Ar-H), 7.73 (1H, d, oxazole H, $^{5}J_{HH}$ = 1.2 Hz), 7.91 (2H, d, Ar-H), 7.98 (2H, m, Ar-H); **^{13}C NMR (100 MHz, CDCl$_3$, δ ppm)** : 21.7, 44.1, 64.4, 125.9, 127.7, 128.3, 129.0, 129.4, 133.9, 135.0, 136.5, 143.9, 144.7, 160.9, 199.8; **EI-Mass**: m/z calculated for $C_{19}H_{16}ClNO_3$: 341.08, found: (m/z) 341.08 $(M)^+$.

1-(4-Chlorophenyl)-3-(2-(4-chlorophenyl)-oxazol-4-yl)-3-hydroxy-propanone 54h

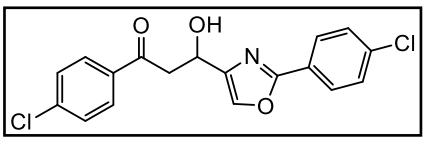

Compound **54h** was prepared following the general procedure described above by treating 2-(4-chlorophenyl)-1,3-oxazole-4-carbaldehyde **52c** (2.07g, 0.01 mol) in ethanol with 4-chloro acetophenone **53** (1.54g, 0.01 mol) and NaOH (0.5 g, 0.012 mol) in 10 ml water. Yield = 3.0g, 82%; White Solid; M.P. = 168 ^{o}C; **IR (KBr) cm^{-1}** : 3068, 1974, 1686, 1110, 948, 765; **^{1}H NMR (400 MHz, CDCl$_3$, δ ppm)** : 3.50 (1H, dd, (1H of -CH_2), $^{1}J_{HH}$ = 18 Hz, $^{2}J_{HH}$ = 8.8 Hz , 3.64 (1H, dd, (1H of -CH_2), $^{1}J_{HH}$ = 18 Hz, $^{4}J_{HH}$ = 3.2 Hz), 3.77 (1H, d (-OH proton), $^{3}J_{HH}$ = 4.4 Hz) , 5.41 (1H, m, (-CH), $^{2}J_{HH}$ = 8.8 Hz, $^{3}J_{HH}$ = 4.4 Hz $^{4}J_{HH}$ = 3.2 Hz, $^{5}J_{HH}$ = 1.2 Hz), 7.46 (4H, m, Ar-H), 7.73 (1H, d, oxazole H, $^{5}J_{HH}$ = 1.2 Hz), 7.97 (4H, m, Ar-H), **^{13}C NMR (100 MHz, CDCl$_3$, δ ppm)** : 44.3, 64.2, 125.7, 127.7, 128.8, 129.1, 131.5, 134.7, 135.0, 136.6, 140.3, 143.7, 161.0, 198.7; **EI-Mass**: m/z calculated for $C_{18}H_{13}Cl_2NO_3$: 361.06, found: (m/z) 361.06 $(M)^+$.

1-(4-Bromophenyl)-3-(2-(4-chlorophenyl)-oxazol-4-yl)-3-hydroxy-propanone 54i.

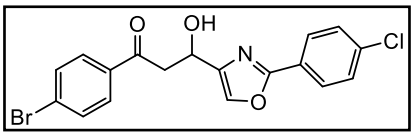

Compound **54i** was prepared following the general procedure described above by treating 2-(4-chlorophenyl)-1,3-oxazole-4-carbaldehyde **52c** (2.07g, 0.01 mol) in ethanol with 4-bromo acetophenone **53** (1.99g, 0.01 mol) and NaOH (0.5 g, 0.012 mol) in 10 ml water. Yield = 3.5g, 86%; White Solid; M.P. = 197 ^{o}C; IR (KBr) cm^{-1} : 3071, 1970, 1679, 1107, 881, 774; **^{1}H NMR (400 MHz, CDCl$_3$, δ ppm)** : 3.48 (1H, dd, (1H of -CH$_2$), $^{1}J_{HH}$ = 18 Hz, $^{2}J_{HH}$ = 8.8 Hz , 3.63 (1H, dd, (1H of -CH$_2$), $^{1}J_{HH}$ = 18 Hz, $^{4}J_{HH}$ = 3.2 Hz), 3.77 (1H, d (-OH proton), $^{3}J_{HH}$ = 4.4 Hz) , 5.40 (m , 1H, (-CH), $^{2}J_{HH}$ = 8.8 Hz, $^{3}J_{HH}$ = 4.4 Hz $^{4}J_{HH}$ = 3.2 Hz, $^{5}J_{HH}$ = 0.8 Hz), 7.44 (2H, d, Ar-H), 7.64 (2H, dd, Ar-H), 7.73 (1H, d, oxazole H, $^{5}J_{HH}$ = 0.8 Hz), 7.88 (2H, d, Ar-H), 7.97 (2H, d, Ar-H), **^{13}C NMR (100 MHz, CDCl$_3$, δ ppm)** : 44.3, 64.2, 125.8, 127.7, 129.0, 129.1, 129.7, 132.0, 135.0, 135.2, 136.6, 143.7, 161.0, 198.9; **EI-Mass**: m/z calculated for $C_{18}H_{11}BrClNO_3$: 405.9, found: (m/z) 405.9 $(M)^{+}$.

General Procedure for the Synthesis of 1-aryl-3-(2-phenyl-oxazol-4-yl)-propenones 55.[66]

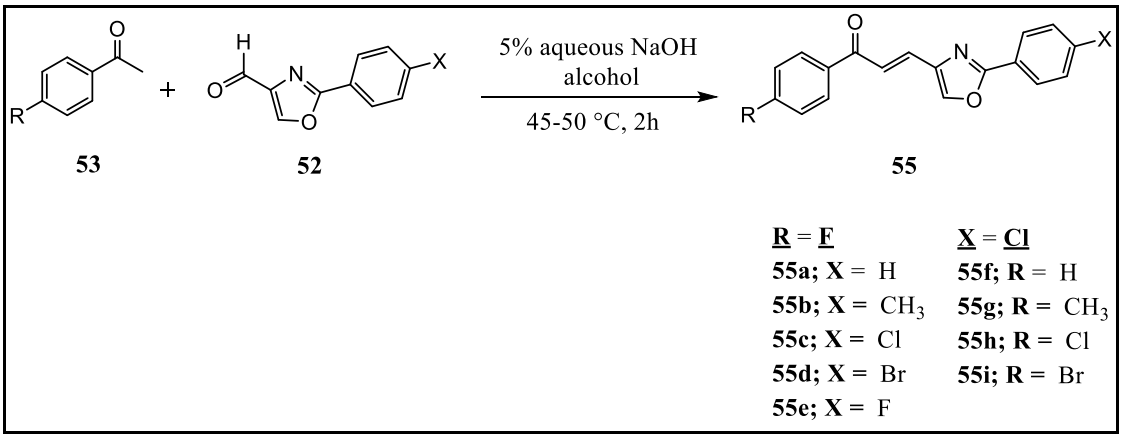

To a magnetically stirred mixture of an 4-substituted acetophenone **53** (0.01 mol) in ethanol (95%, 80 ml) and NaOH (0.012 mol) in 10 ml water kept at 0-5 ^{o}C in a 250 ml conical flask, a solution of 2-aryl-oxazole-4-carbaldehyde **52** (0.01 mol) in 20 ml ethanol was added dropwise using addition funnel during 20-30 minutes keeping the temperature below 5 ^{o}C. The reaction mixture was allowed to attain room temperature,

after which water bath was warmed to 45-50 °C and maintained for further 2 hours to complete the reaction (TLC: 10% E.A.). Reaction mixture than was poured into ice cold water to precipitate the product as yellow solids, which were then filtered, dried and crystallized from ethanol. Yield: 56-68%.

1-(4-Fluorophenyl)-3-(2-phenyloxazol-4-yl)-propenone 55a.

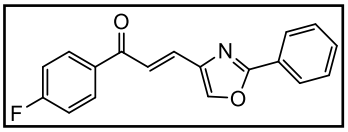

Compound **55a** was prepared following the general procedure described above by treating 2-phenyl-1,3-oxazole-4-carbaldehyde **52a** (1.73g, 0.01 mol) in ethanol with 4-fluoroacetophenone **53** (1.38g, 0.01 mol) and NaOH (0.5 g, 0.012 mol) in 10 ml water. Yield = 1.69g, 58%; Light Yellow Solid; M.P. = 110 °C; **IR (KBr) cm^{-1}**: 3137, 3074, 1622, 1549, 1153, 1103; **^{1}H NMR (400 MHz, $CDCl_3$, δ ppm)** : 7.56 (5H, m, Ar-H), 7.81 (2H, d, (-CH=CH-)), $^{1}J_{HH}$ = 14.8 Hz (trans-H)), 7.94 (1H, s, oxazole-H), 8.14 (4H, m, Ar-H); **^{19}F decoupled ^{1}H NMR (400 MHz, $CDCl_3$, δ ppm)** : 7.20 (2H, d, Ar-H), 7.52 (s (br), 3H, Ar-H), 7.72 (1H, d, (-CH=CH-)), 7.89 (1H, d, (-CH=CH-)), 7.94 (1H, s, oxazole-H), 8.16 (d (br), 4H, Ar-H); **^{19}F NMR : (376 MHz, $CDCl_3$, δ ppm)** : -105.28; **^{13}C NMR (100 MHz, $CDCl_3$, δ ppm)** : 115.7 (d, $^{2}J_{CF}$ = 22 Hz), 123.1, 126.6, 126.8, 128.9, 131.1 (d, $^{3}J_{CF}$ = 9 Hz), 131.3, 132.0, 134.2 (d, $^{4}J_{CF}$ = 3 Hz), 138.8, 140.2, 162.5, 165.7 (d, $^{1}J_{CF}$ = 249 Hz), 188.3; **EI-Mass**: m/z calculated for $C_{18}H_{12}FNO_2$: 292.76, found: (m/z) 292.76 $(M)^+$.

3-(2-(4-Methylphenyl)oxazol-4-yl)-1-(4-fluorophenyl)-propenone 55b.

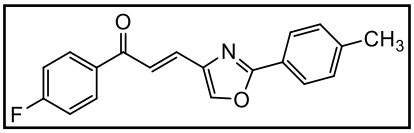

Compound **55b** was prepared following the general procedure described above by treating 2-(4-methylphenyl)-1,3-oxazole-4-carbaldehyde **52b** (1.87g, 0.01 mol) in ethanol with 4-fluoro acetophenone **53** (1.38g, 0.01 mol) and NaOH (0.5 g, 0.012 mol) in 10 ml water. Yield = 1.78g, 58%; Light Yellow Solid; M.P. = 157°C; **IR (KBr) cm^{-1}** : 3152, 3098, 1563, 1024, 833, 778; **^{1}H NMR (400 MHz, $CDCl_3$, δ ppm)** : 2.45 (s,1H , -CH_3), 7.25 (m , 4H, Ar-H), 7.80 (2H, d, (-CH=CH-), $^{1}J_{HH}$ = 15.2 Hz (trans-H)), 7.92 (1H, s, Oxazole-H), 8.09 (4H, m, Ar-H); **^{19}F decoupled ^{1}H NMR (400 MHz, $CDCl_3$, δ, ppm)** : 7.20 (2H, d, Ar-H), 7.29 (2H, d, Ar-H), 7.71 (1H, d, (-CH=CH-)), 7.87 (1H, d, (-CH=CH-)), 7.91 (1H, s, oxazole-H), 8.01 (2H, d, Ar-H), 8.15 (2H, d, Ar-H); **^{19}F NMR (376 MHz, $CDCl_3$, δ, ppm)** : -105.35; **^{13}C NMR**

(100 MHz, $CDCl_3$, δ, ppm) : 21.6, 115.7 (d, $^2J_{CF}$ = 22 Hz), 122.8, 124.0, 126.7, 129.6, 131.2 (d, $^3J_{CF}$ = 9Hz), 134.2 (d, $^4J_{CF}$ = 3 Hz), 138.8, 140.0, 141.5, 162.8, 165.7 (d, $^1J_{CF}$ = 253 Hz), 188.2; **EI-Mass**: m/z calculated for $C_{19}H_{15}FNO_2$: 307.10, found: (m/z) 307.10 $(M)^+$.

3-(2-(4-Chlorophenyl)oxazol-4-yl)-1-(4-fluorophenyl)-propenone 55c.

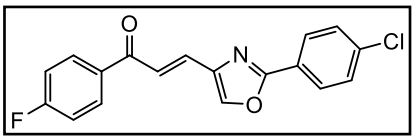

Compound **55c** was prepared following the general procedure described above by treating 2-(4-chlorophenyl)-1,3-oxazole-4-carbaldehyde **52c** (2.07g, 0.01 mol) in ethanol with 4-fluoro acetophenone **53** (1.38g, 0.01 mol) and NaOH (0.5 g, 0.012 mol) in 10 ml water. Yield = 2.05g, 64%; Yellow Solid; M.P. = 144 °C; **IR (KBr) cm^{-1}** : 3153, 3065, 1619, 1597, 1043, 834, 777; **^{1}H NMR (400 MHz, $CDCl_3$, δ ppm)** : 7.34 (4H, m, Ar-H), 7.79 (2H, d, (-CH=CH-), $^1J_{HH}$ = 15.2 Hz (trans-H)), 7.93 (1H, s, oxazole-H), 8.11 (4H, m, Ar-H); **^{19}F decoupled ^{1}H NMR (400 MHz, $CDCl_3$, δ ppm)** : 7.20 (2H, d, Ar-H), 7.50 (2H, d, Ar-H), 7.71 (1H, d, (-CH=CH-)), 7.88 (1H, d, (-CH=CH-)), 7.94 (1H, s, oxazole-H), 8.07 (2H, d, Ar-H), 8.15 (2H, d, Ar-H), **^{19}F NMR (376 MHz, $CDCl_3$, δ ppm)** : -105.16; **^{13}C NMR (100 MHz, $CDCl_3$, δ ppm)** : 115.7 (d, $^2J_{CF}$ = 22 Hz), 123.2, 125.2, 128.1, 129.2, 131.2 (d , $^3J_{CF}$ = 9 Hz), 131.8, 134.2 (d, $^4J_{CF}$ = 3Hz), 137.2, 139.0, 140.2, 161.6, 165.7 (d, $^1J_{CF}$ = 249Hz), 188.2; **EI-Mass**: m/z calculated for $C_{18}H_{12}ClFNO_2$: 326.53, found: (m/z) 326.53 $(M)^+$.

3-(2-(4-Bromophenyl)oxazol-4-yl)-1-(4-fluorophenyl)-propenone 55d.

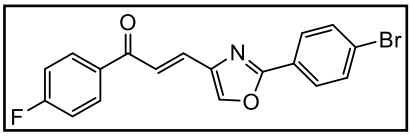

Compound **55d** was prepared following the general procedure described above by treating 2-(4-bromophenyl)-1,3-oxazole-4-carbaldehyde **52d** (2.52g, 0.01 mol) in ethanol with 4-fluoro acetophenone **53** (1.38g, 0.01 mol) and NaOH (0.5 g, 0.012 mol) in 10 ml water. Yield = 2.31g, 62%; Light Yellow Solid; M.P. = 139°C; **IR (KBr) cm^{-1}** : 3144, 2946, 1670, 1590, 829, 789; **^{1}H NMR (400 MHz, $CDCl_3$, δ ppm)** : 7.43 (4H, m, Ar-H), 7.79 (2H, d, (-CH=CH-)), $^1J_{HH}$ = 14.8 Hz (trans-H)), 7.94 (1H, s Oxazole - H), 8.08 (4H, m, Ar-H); **^{19}F decoupled ^{1}H NMR (400 MHz, $CDCl_3$, δ ppm)** : 7.20 (2H, d, Ar-H), 7.66 (2H, d, Ar-H), 7.70 (1H, d, (-CH=CH-)), 7.87 (1H, d, (-CH=CH-)), 7.94 (1H, s, oxazole-H), 8.00 (2H, d, Ar-H), 8.15 (2H, d, Ar-H); **^{19}F NMR (376 MHz, $CDCl_3$, δ ppm)** : -105.14; **^{13}C NMR (100 MHz, $CDCl_3$, δ**

ppm) : 115.8 (d , $^{2}J_{CF}$ = 22 Hz), 123.2, 125.6, 125.7, 128.2, 131.2 (d, $^{3}J_{CF}$ = 9 Hz), 131.9, 132.2, 134.1 (d, $^{4}J_{CF}$ = 3 Hz), 139.0, 140.0, 140.3, 161.6, 165.7 (d, $^{1}J_{CF}$ = 249 Hz), 188.2; **EI-Mass**: m/z calculated for $C_{18}H_{12}BrFNO_2$: 372.90, found: (m/z) 372.90 $(M)^{+}$.

3-(2-(4-Fluorophenyl)oxazol-4-yl)-1-(4-fluorophenyl)-propenone 55e.

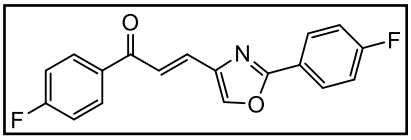

Compound **55e** was prepared following the general procedure described above by treating 2-(4-fluorophenyl)-1,3-oxazole-4-carbaldehyde **52e** (1.91g, 0.01 mol) in ethanol with 4-fluoro acetophenone **53** (1.38g, 0.01 mol) and NaOH (0.5 g, 0.012 mol) in 10 ml water. Yield = 2.11g, 68%; Yellow Solid; M.P. = 143°C; **IR (KBr) cm^{-1}** : 3152, 3098, 1659, 1563, 1024, 833, 778; **^{1}H NMR (400 MHz, $CDCl_3$, δ ppm)** : 7.23 (4H, m, Ar-H), 7.79 (2H, d, (-CH=CH-), $^{1}J_{HH}$ = 15.2 Hz (trans-H)), 7.93 (1H, s, oxazole-H), 8.13 (4H, m, Ar-H), **^{19}F decoupled ^{1}H NMR (400 MHz, $CDCl_3$, δ ppm)** : 7.20 (2H, d, Ar-H), 7.29 (2H, d, Ar-H), 7.71 (1H, d, (-CH=CH-), 7.87 (1H, d, (-CH=CH-)), 7.91 (1H, s, oxazole-H), 8.01 (2H, d, Ar-H), 8.15 (2H, d, Ar-H); **^{19}F NMR (376 MHz, $CDCl_3$, δ ppm)** : -105.20, -108.12; **^{13}C NMR (100 MHz, $CDCl_3$, δ ppm)** : 115.8 (d, $^{2}J_{CF}$ = 22 Hz), 116.1 (d , $^{2}J_{CF}$ = 22 Hz), 123.1 (d, $^{4}J_{CF}$ = 3 Hz), 129.0 (d, $^{3}J_{CF}$ = 8 Hz), 131.2 (d, $^{3}J_{CF}$ = 9 Hz), 132.0, 134.2 (d, $^{4}J_{CF}$ = 3 Hz), 138.96, 140.2, 161.7, 164.4 (d, $^{1}J_{CF}$ = 249 Hz), 166.3 (d, $^{1}J_{CF}$ = 249 Hz), 188.2; **EI-Mass**: m/z calculated for $C_{18}H_{12}F_2NO_2$: 311.09, found: (m/z) 311.09 $(M)^{+}$.

3-(2-(4-Chlorophenyl)oxazol-4-yl)-1-phenyl-propenone 55f.

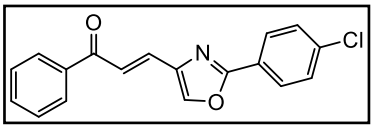

Compound **55f** was prepared following the general procedure described above by treating 2-(4-chlorophenyl)-1,3-oxazole-4-carbaldehyde **52c** (2.07g, 0.01 mol) in ethanol with acetophenone **53** (1.20g, 0.01 mol) and NaOH (0.5 g, 0.012 mol) in 10 ml water. Yield = 2.1g, 67%; Yellow Solid; M.P. = 178 °C; **IR (KBr) cm^{-1}**: 3159, 3045, 1629, 1597, 1087, 824, 775; **^{1}H NMR (400 MHz, $CDCl_3$, δ ppm)**: 7.52 (m, 6H, Ar-H), 7.79 (2H, d, -CH=CH-), $^{1}J_{HH}$ = 15.2 Hz (trans-H)), 7.93 (1H, d, oxazole-H), 8.10 (4H, m, Ar-H); **^{13}CNMR (100 MHz, $CDCl_3$, δ ppm)**: 123.7, 125.3, 128.1, 128.6, 129.2, 131.7, 133.0, 137.2, 139.1, 140.1, 189.9; **EI-Mass**: m/z calculated for $C_{18}H_{12}ClNO_2$: 309.06, found: (m/z) 309.06 $(M)^{+}$.

3-(2-(4-Chlorophenyl)-oxazol-4-yl)-1-(4-methylphenyl)-propenone 55g.

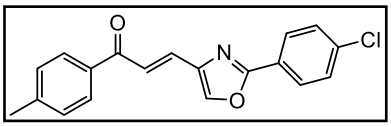

Compound **55g** was prepared following the general procedure described above by treating 2-(4-chlorophenyl)-1,3-oxazole-4-carbaldehyde **52c** (1.87g, 0.01 mol) in ethanol with 4-methyl acetophenone **53** (1.35g, 0.01 mol) and NaOH (0.5 g, 0.012 mol) in 10 ml water. Yield = 2.0g, 61%; Light Yellow Solid; M.P. = 187°C; **IR (KBr) cm^{-1}**: 3149, 3089, 1569, 1034, 838, 777; **^{1}H NMR (400 MHz, $CDCl_3$, δ ppm)**: 2.46 (s,1H , -CH_3), 7.33 (2H, d, Ar-H), 7.49 (2H, dd, Ar-H), 7.78 (2H, d, (-CH=CH-), $^{1}J_{HH}$ = 15.2 Hz (trans-H)), 7.92 (1H, s, Oxazole-H), 8.03 (4H, m, Ar-H); **^{13}C NMR (100 MHz, $CDCl_3$, δ, ppm)**: 21.7, 123.2, 125.3, 128.1, 128.8, 129.2, 129.3, 131.3, 135.2, 137.1, 139.2, 140.0, 143.9, 161.5, 189.4; **EI-Mass**: m/z calculated for $C_{19}H_{14}ClNO_2$: 323.07, found: (m/z) 323.07 $(M)^+$.

1-(4-Chlorophenyl)-3-(2-(4-chlorophenyl)-oxazol-4-yl)-propenone 55h.

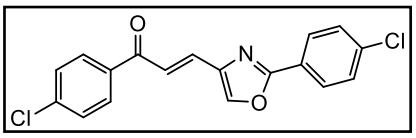

Compound **55h** was prepared following the general procedure described above by treating 2-(4-chlorophenyl)-1,3-oxazole-4-carbaldehyde **52c** (2.07g, 0.01 mol) in ethanol with 4-chloro acetophenone **53** (1.54g, 0.01 mol) and NaOH (0.5 g, 0.012 mol) in 10 ml water. Yield = 2.5g, 73%; Yellow Solid; M.P. = 174 °C; **IR (KBr) cm^{-1}**: 3158, 3047, 1621, 1586, 1049, 824, 779; **^{1}H NMR (400 MHz, $CDCl_3$, δ ppm)**: 7.33 (2H, d, Ar-H), 7.49 (2H, d, Ar-H) 7.78 (2H, d, (-CH=CH-), $^{1}J_{HH}$ = 15.2 Hz (trans-H)), 7.92 (1H, s, oxazole - H), 8.05 (4H, m, Ar-H); **^{13}CNMR (100 MHz, $CDCl_3$, δ ppm)**: 123.7, 125.3, 128.1, 128.8, 129.2, 129.3, 131.3, 135.2, 137.2, 139.2, 140.0, 143.9, 161.5, 189.4; **EI-Mass**: m/z calculated for $C_{18}H_{11}Cl_2NO_2$: 343.01, found: (m/z) 343.01 $(M)^+$.

1-(4-Bromophenyl)-3-(2-(4-chlorophenyl)-oxazol-4-yl)-propenone 55i.

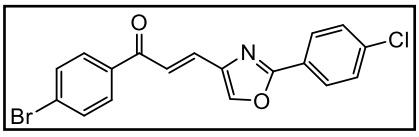

Compound **55i** was prepared following the general procedure described above by treating 2-(4-chlorophenyl)-1,3-oxazole-4-carbaldehyde **52c** (2.07g, 0.01 mol) in ethanol with 4-bromo acetophenone **53** (1.99g, 0.01 mol) and NaOH (0.5 g, 0.012 mol) in10 ml water. Yield = 2.7g, 69%; Yellow Solid; M.P. = 149 °C; **IR (KBr) cm^{-1}**: 3158, 3061, 1617, 1588, 1090, 831, 778; **^{1}H NMR (400 MHz,**

$CDCl_3$, δ ppm): 7.50 (2H, d, Ar-H), 7.67 (2H, d, Ar-H), 7.78 (2H, d, (-CH=CH-), $^1J_{HH}$ = 15.2 Hz (trans-H)), 7.94 (1H, s, oxazole -H), 7.98 (2H, d, Ar-H), 8.07 (2H, d, Ar-H); **^{13}CNMR (100 MHz, $CDCl_3$, δ ppm)**: 125.9, 126.4, 127.5, 128.5, 128.6, 129.0, 129.2, 129.7, 131.9, 132.2, 135.0, 135.4, 136.3, 143.3, 197.4; **EI-Mass**: m/z calculated for $C_{18}H_{12}BrClNO_2$: 386.90, found: (m/z) 386.90 $(M)^+$.

Experimental For Anticancer Assay

This includes Standard Procedure Followed by NCI (USA) for Screening. The human tumour cell lines of the cancer screening panel are grown in RPMI 1640 medium containing 5% fatal bovine serum and 2 mM L-glutamine. For a typical screening experiment, cells are inoculated into 96 well microtiter plates in 100 µL at plating densities ranging from 5,000 to 40,000 cells/well depending on the doubling time of individual cell lines. After cell inoculation, the microtiter plates are incubated at 37° C, 5 % CO_2, 95 % air and 100 % relative humidity for 24 h prior to addition of experimental drugs.

After 24 h, two plates of each cell line are fixed *in situ* with TCA, to represent a measurement of the cell population for each cell line at the time of drug addition (Tz). Experimental drugs are solubilized in dimethyl sulfoxide at 400-fold the desired final maximum test concentration and stored frozen prior to use. At the time of drug addition, an aliquot of frozen concentrate is thawed and diluted to twice the desired final maximum test concentration with complete medium containing 50 µg/ml gentamicin. Additional four, 10-fold or ½ log serial dilutions are made to provide a total of five drug concentrations plus control. Aliquots of 100 µl of these different drug dilutions are added to the appropriate microtiter wells already containing 100 µl of medium, resulting in the required final drug concentrations.

Following drug addition, the plates are incubated for an additional 48 h at 37°C, 5 % CO2, 95 % air, and 100 % relative humidity. For adherent cells, the assay is terminated by the addition of cold TCA. Cells are fixed *in situ* by the gentle addition of 50 µl of cold 50 % (w/v) TCA (final concentration, 10 % TCA) and incubated for 60 minutes at 4°C. The supernatant is discarded, and the plates are washed five times with tap water

and air dried. Sulforhodamine B (SRB) solution (100 µl) at 0.4 % (w/v) in 1 % acetic acid is added to each well, and plates are incubated for 10 minutes at room temperature. After staining, unbound dye is removed by washing five times with 1 % acetic acid and the plates are air dried. Bound stain is subsequently solubilized with 10 mM trizma base, and the absorbance is read on an automated plate reader at a wavelength of 515 nm. For suspension cells, the methodology is the same except that the assay is terminated by fixing settled cells at the bottom of the wells by gently adding 50 µl of 80 % TCA (final concentration, 16 % TCA). Using the seven absorbance measurements [time zero, (Tz), control growth, (C), and test growth in the presence of drug at the five concentration levels (Ti)], the percentage growth is calculated at each of the drug concentrations levels. Percentage growth inhibition is calculated as:

[(Ti-Tz)/(C-Tz)] x 100 for concentrations for which Ti>/=Tz

[(Ti-Tz)/Tz] x 100 for concentrations for which Ti<Tz

Experiment Protocol of Antidiabetic Activity

Oral glucose tolerance test was carried out in male C57 mice of 8-10 weeks age. Glucose load (3g/kg, solution in deionized water) was administered in overnight fasted mice 30 min after compound administration. Compounds were formulated in 0.5% carboxymethyl cellulose Na (Sodium-CMC) in water, and administered by intraperitoneal (IP) route. Mice were bled at the time points indicated in the results under isofluorane anaesthesia by retro orbital bleeding, and the glucose concentration in the serum was measured using glucose oxidase-peroxidase method by spectrophotometer.

Baseline corrected area under the curve for glucose excursion during OGTT for 240 min was calculated using Graph Pad. The study is conducted in two parts. Data for both the vehicles were clubbed so that n=8 for vehicle and n=4 for individual treatments. There were no significant differences between two vehicle control groups that could affect the interpretation of data. The data was expressed as mean± standard error of mean. The AUC data was subjected to one way ANOVA, followed by Dunnet t test. The level of significance, $p<0.05$, was considered for the significant differences in

AUC against the vehicle control group. The statistical analysis was done using Graph Pad Prism software.

Experimental Procedure of Molecular Docking Study

All the molecular modelling studies were carried out using Maestro 9.0 molecular modelling software. The chemical structures of the compounds were sketched using ChemDraw 8.0 software.[70] Open Babel 2.3.0[71] software was used to convert the structures into mol2 format and then all the structures were imported in Maestro 9.0 software. The structures were cleaned up and energy minimization process was carried out for all the structures using OPLS 2005 force field in standard module "Ligprep 2.3". Wy 14643 (PPAR-α agonist), roziglitazon (PPAR-γ agonist) were used as the standard compounds in docking studies which were built and minimized as per the same protocol. These minimized structures were used to dock in the active site of PPAR-α, PPAR-γ using standard module "Glide 5.5". The crystal structures 1K7L, 3BC5 were downloaded from RCSB for PPAR-α, PPAR-γ respectively. The "protein preparation wizard" module was used for refinement of the crystal structures by removing heteroatoms and water molecules. After the refinement process, the receptor grid for individual protein was prepared by using standard option "Receptor grid generation". Default settings were maintained during receptor grid generation in which the van der Waals radii and partial charge cut off were scaled to 0.8 and 0.25 respectively. The minimized structures were docked in the active site of the target proteins using extra precision method.

2.5 Spectral Data

Compound 54a

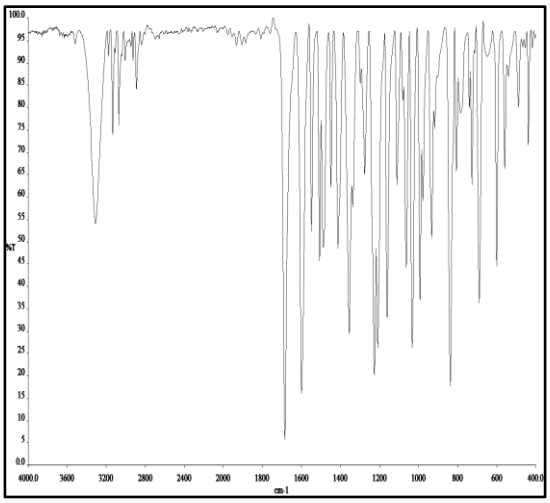

Spectrum 1. IR of compound 54a

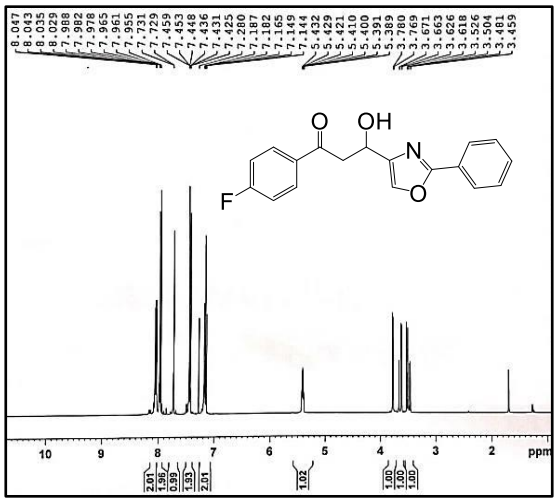

Spectrum 2. ^{1}H NMR of compound 54a

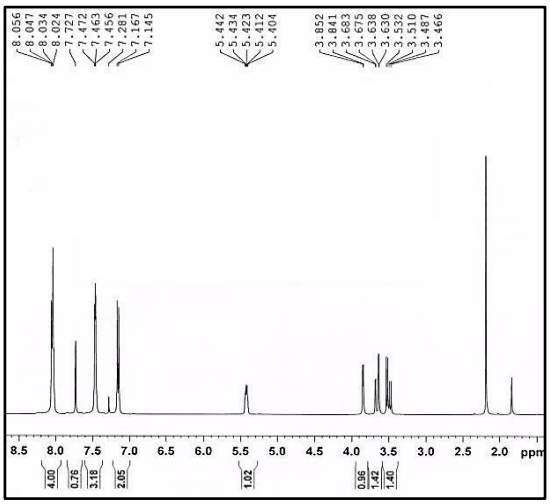

Spectrum 3. ^{19}F decoupled ^{1}H NMR of 54a

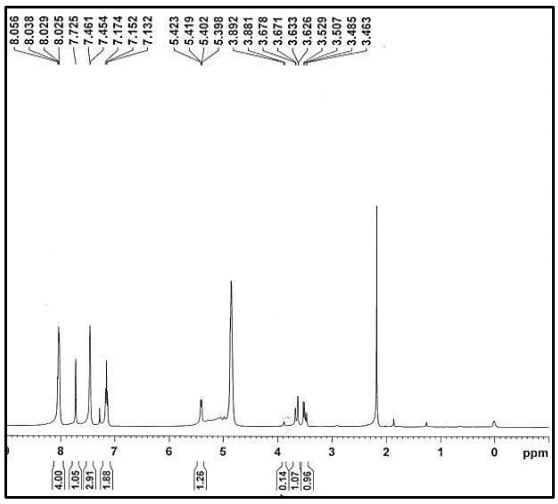

Spectrum 4. D_2O exchange of compound 54a

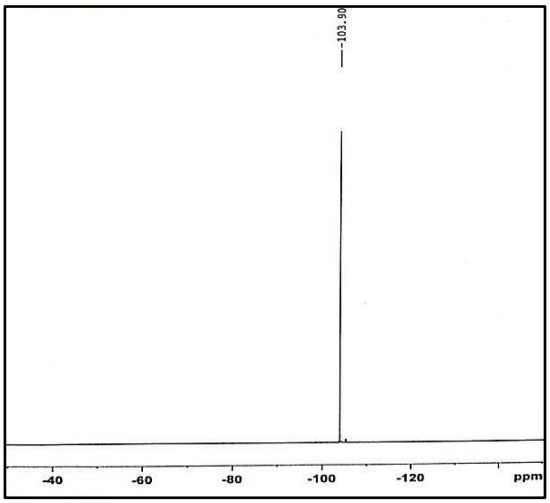

Spectrum 5. ^{19}F NMR of compound 54a

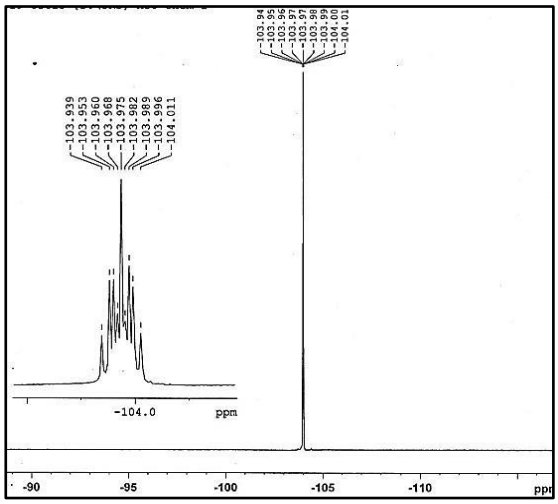

Spectrum 6. ^{19}F coupled NMR of compound 54a

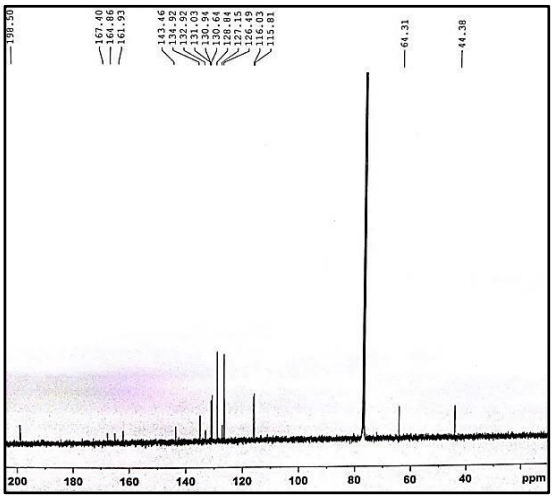

Spectrum 7. ^{13}C NMR of compound 54a

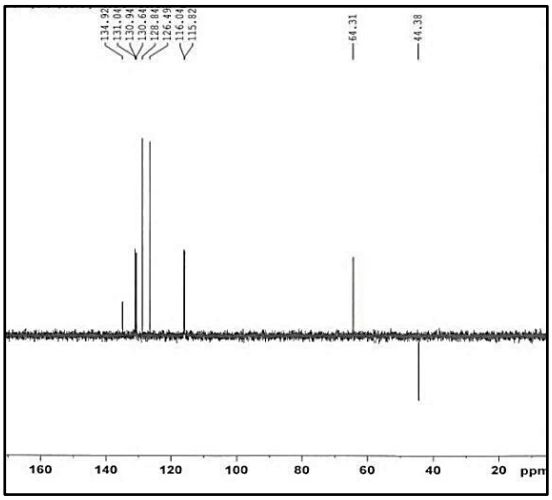

Spectrum 8. DEPT 135 of compound 54a

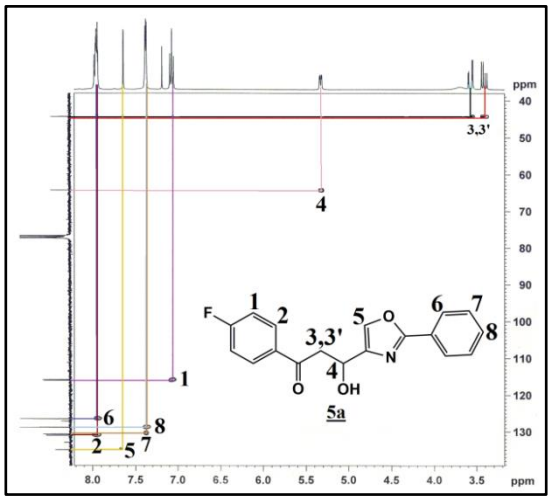

Spectrum 9. HSQC of compound 54a

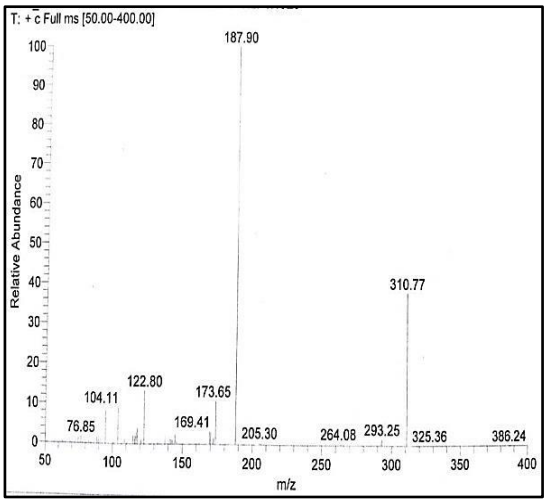

Spectrum 10. MASS of compound 54a

Compound 54b

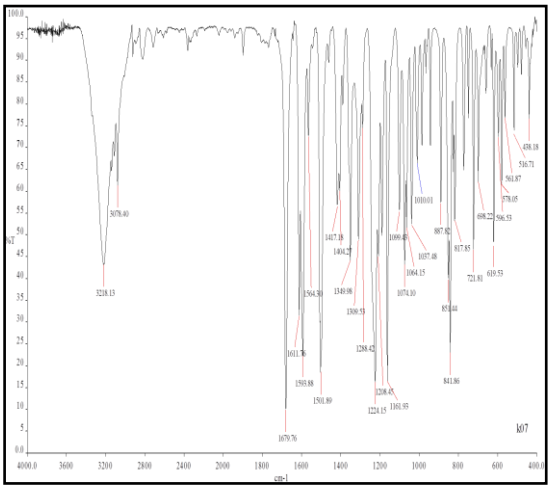

Spectrum 11. IR of compound 54b

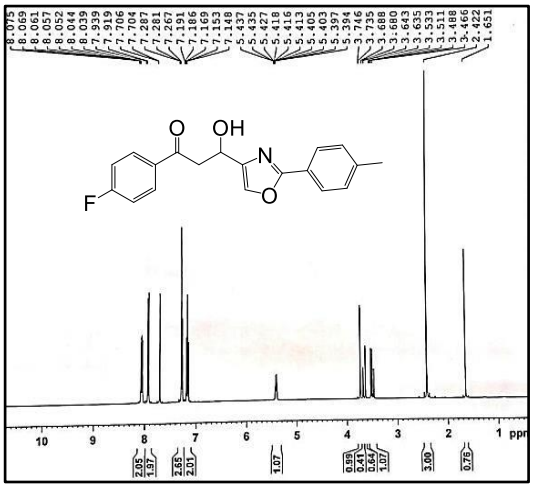

Spectrum 12. ^{1}H NMR of compound 54b

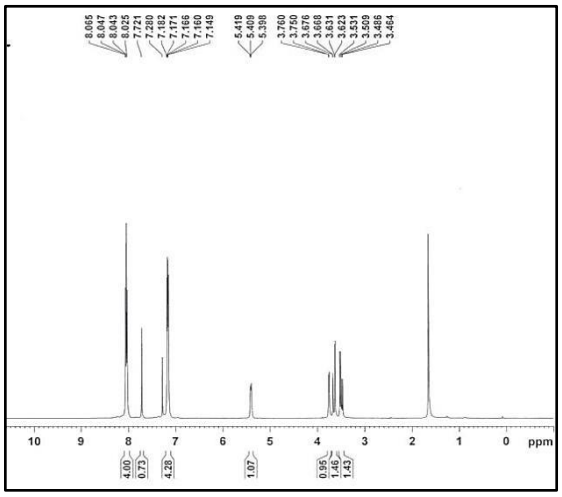

Spectrum 13. ^{19}F decoupled ^{1}H NMR of 54b

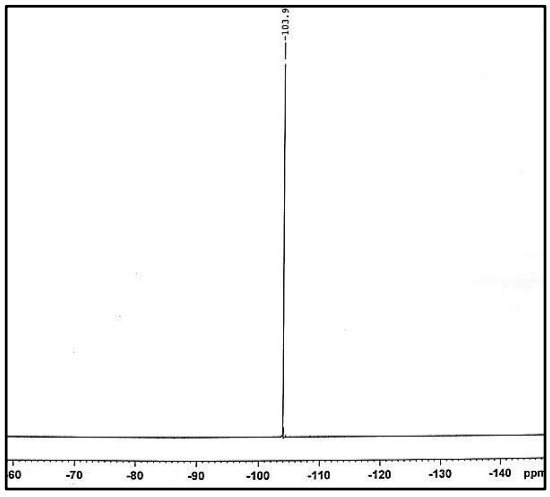

Spectrum 14. ^{19}F NMR of compound 54b

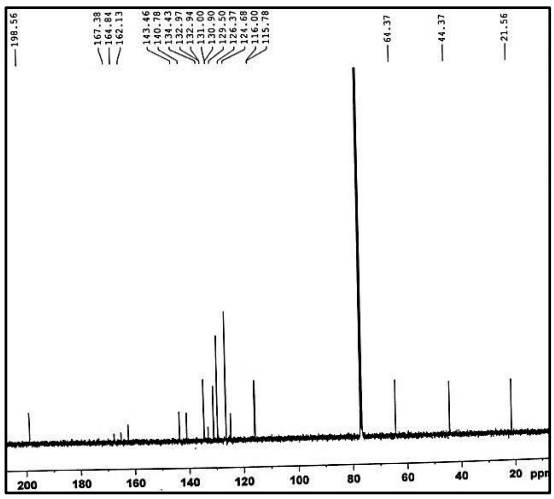

Spectrum 15. ^{13}C NMR of compound 54b

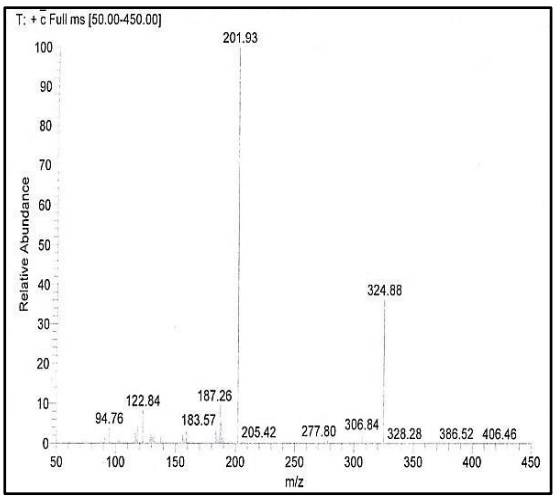

Spectrum 16. MASS of compound 54b

Compound 54c

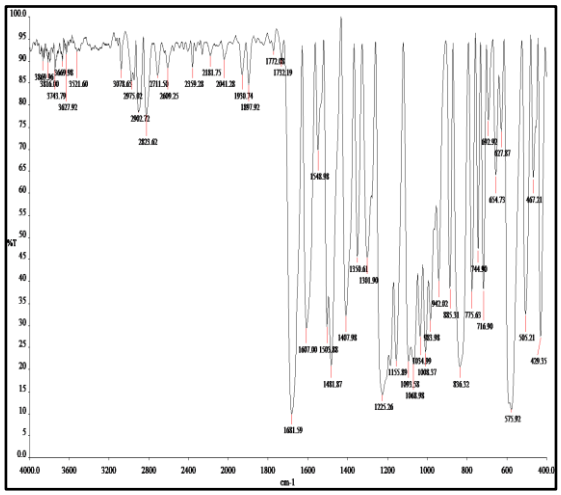

Spectrum 17. IR of compound 54c

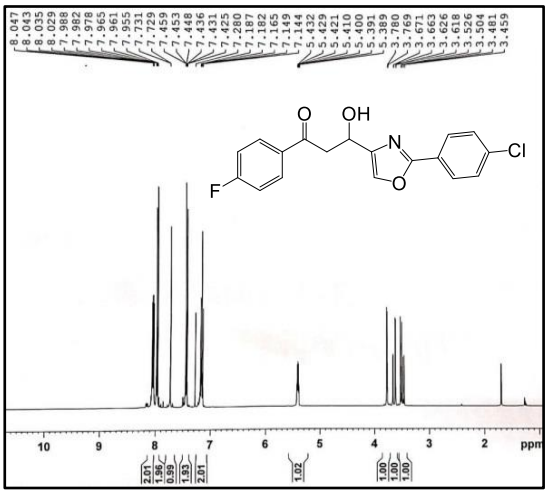

Spectrum 18. ^{1}H NMR of compound 54c

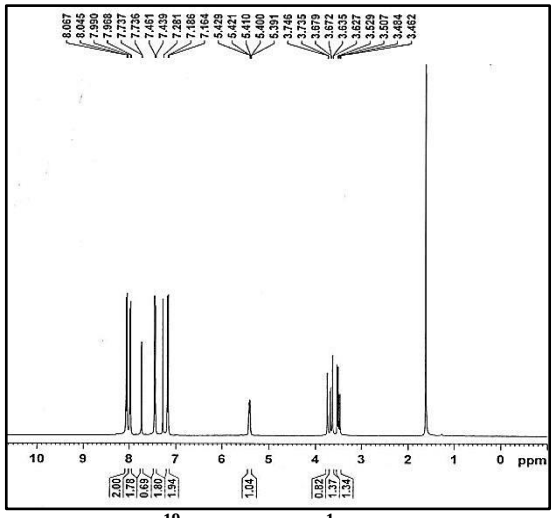

Spectrum 19. ^{19}F decoupled ^{1}H NMR of 54c

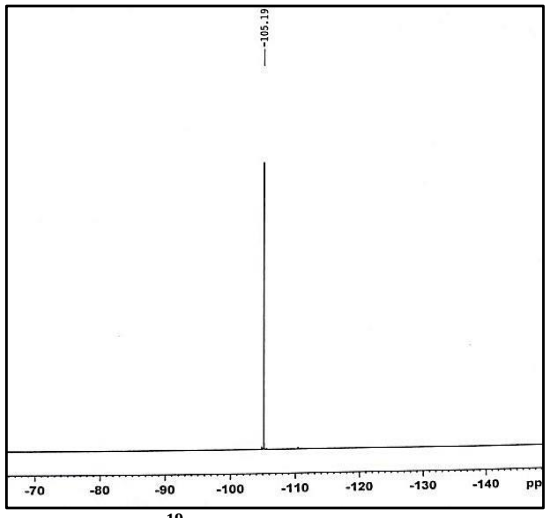

Spectrum 20. ^{19}F NMR of compound 54c

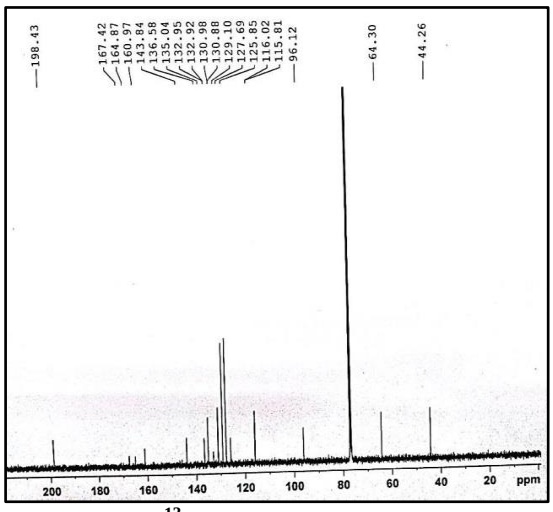

Spectrum 21. ^{13}C NMR of compound 54c

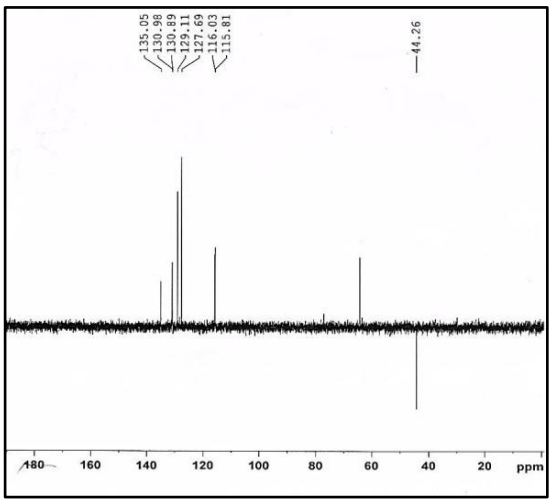

Spectrum 22. DEPT 135 of compound 54c

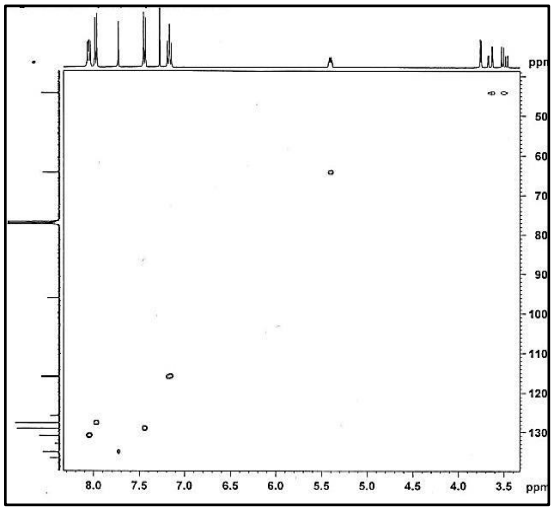

Spectrum 23. HSQC of compound 54c

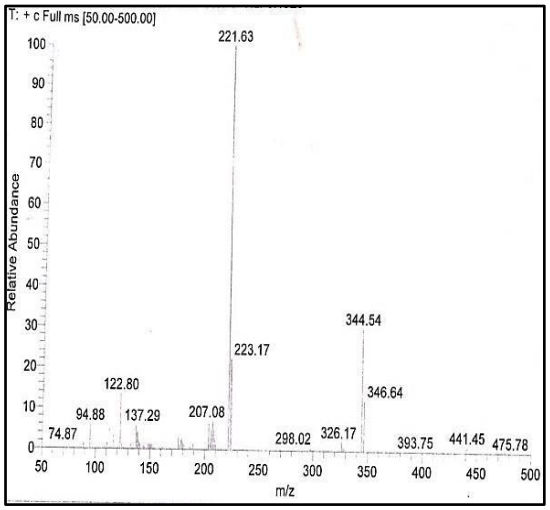

Spectrum 24. MASS of compound 54c

Compound 54d

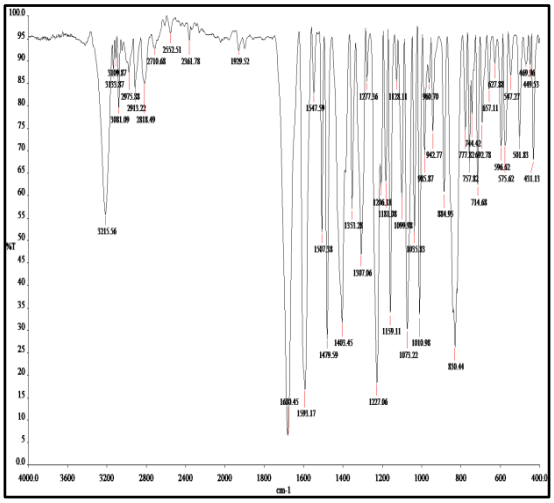

Spectrum 25. IR of compound 54d

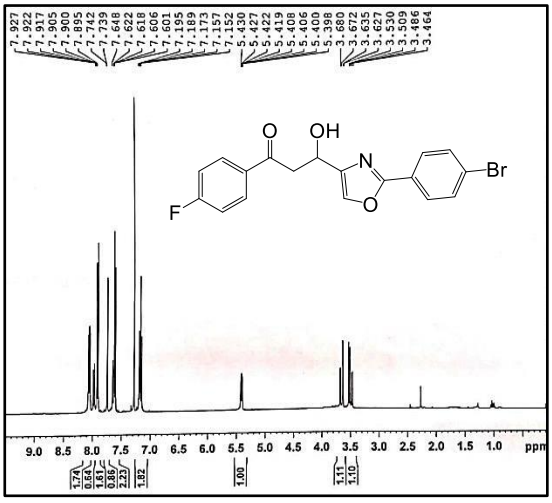

Spectrum 26. ^{1}H NMR of compound 54d

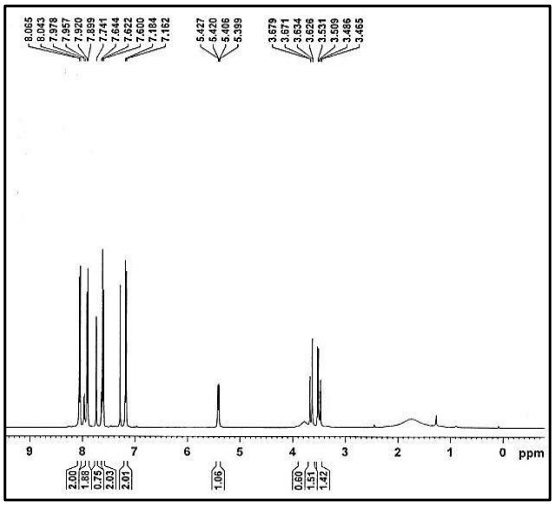

Spectrum 27. ^{19}F decoupled ^{1}H NMR of 54d

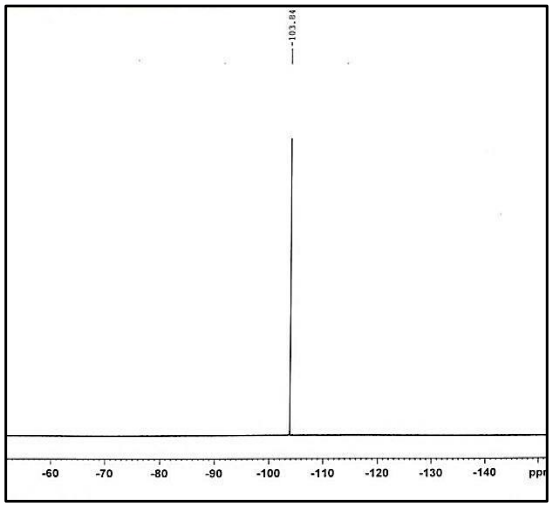

Spectrum 28. ^{19}F NMR of compound 54d

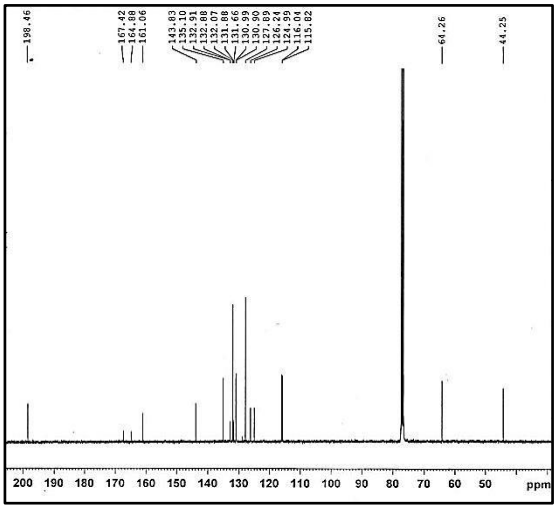

Spectrum 29. ^{13}C NMR of compound 54d

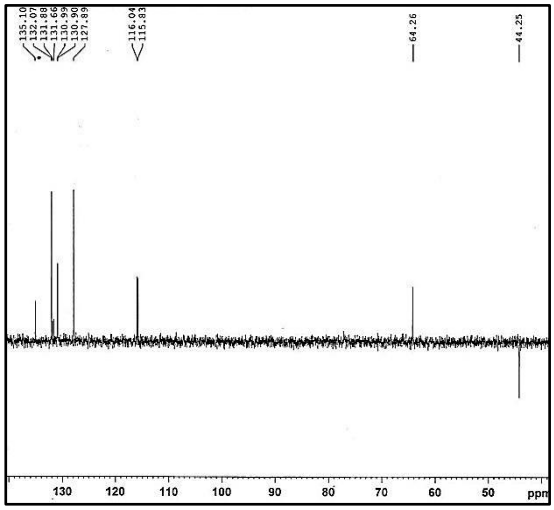

Spectrum 30. DEPT 135 of compound 54d

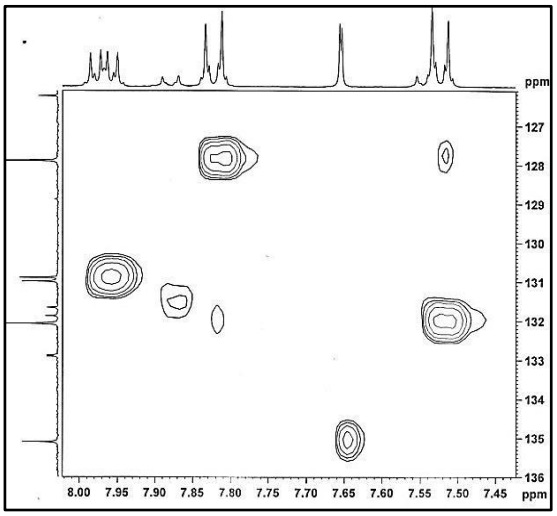

Spectrum 31. HSQC of compound 54d

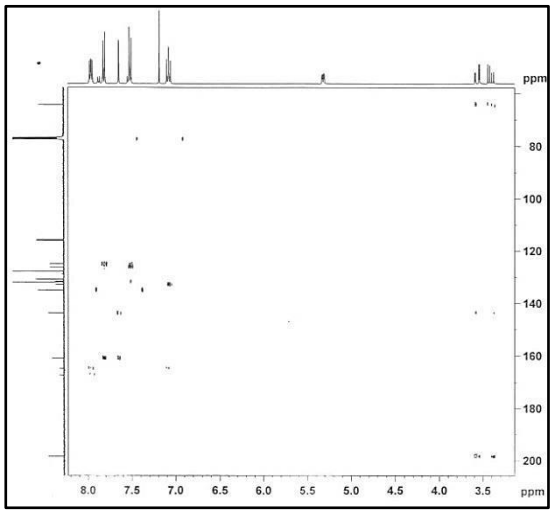

Spectrum 32. HMBC of compound 54d

Compound 54e

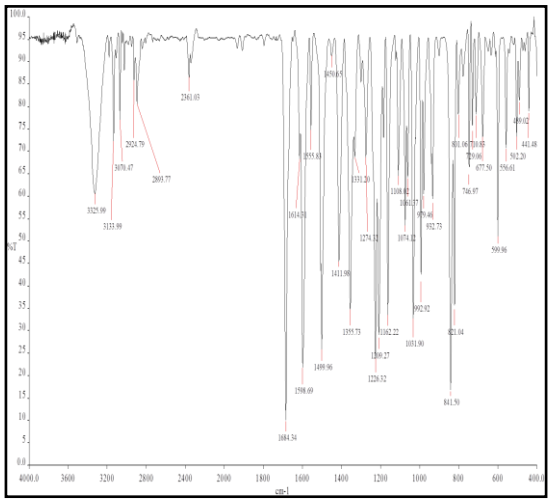

Spectrum 33. IR of compound 54e

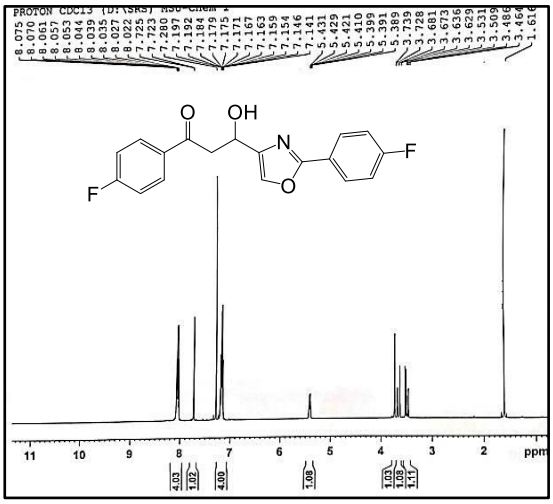

Spectrum 34. ^{1}H NMR of compound 54e

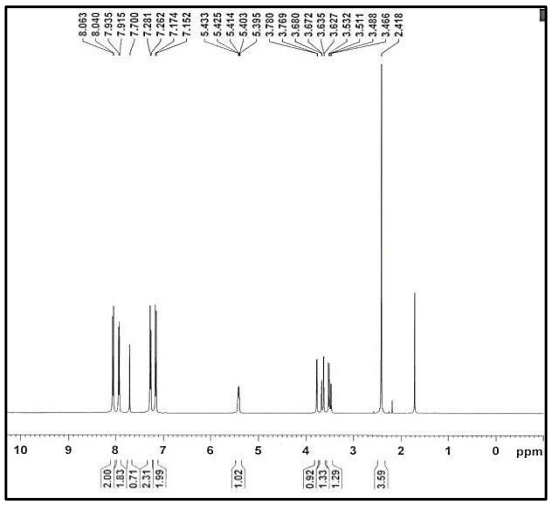

Spectrum 35. ^{19}F decoupled ^{1}H NMR of 54e

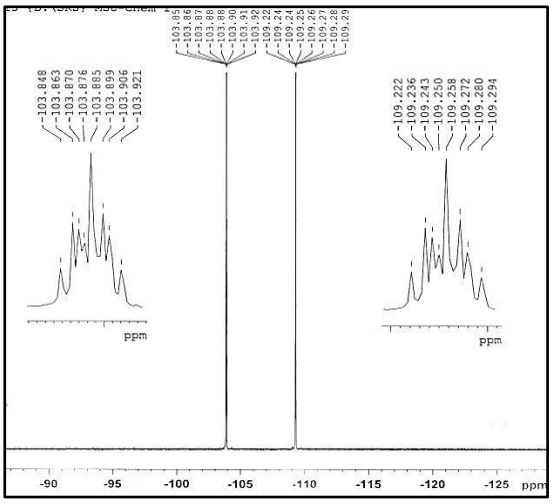

Spectrum 36. ^{19}F coupled NMR of 54e

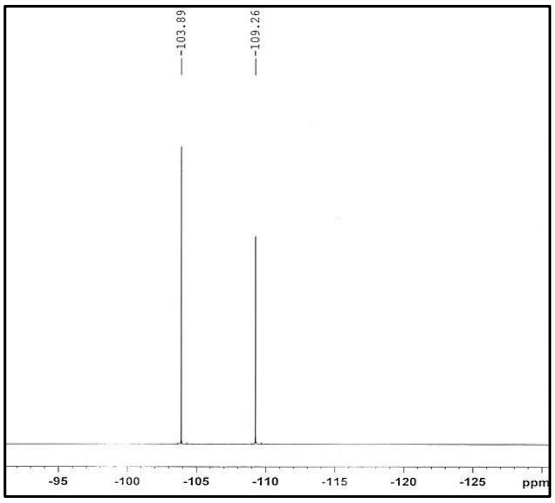

Spectrum 37. ^{19}F coupled NMR of 54e

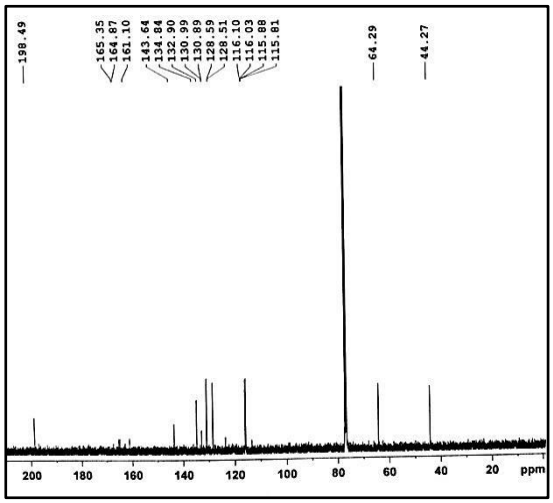

Spectrum 38. ^{13}C NMR of compound 54e

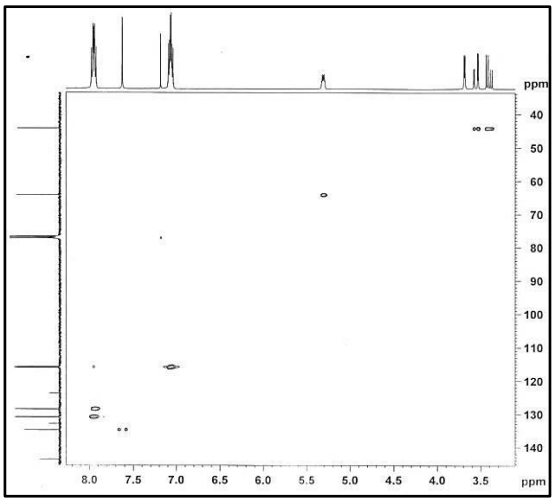

Spectrum 39. HSQC of compound 54e

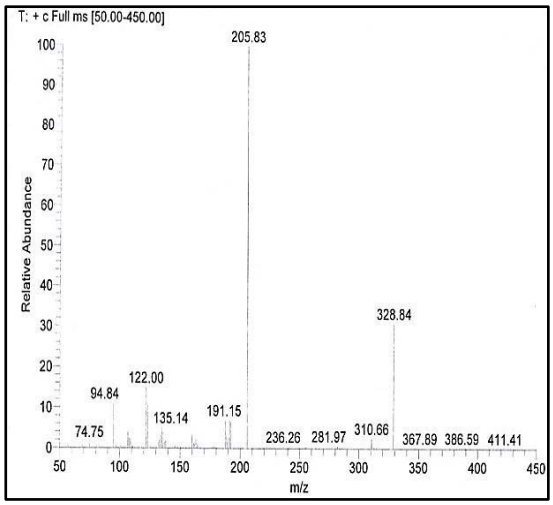

Spectrum 40. MASS of compound 54e

Compound 54f

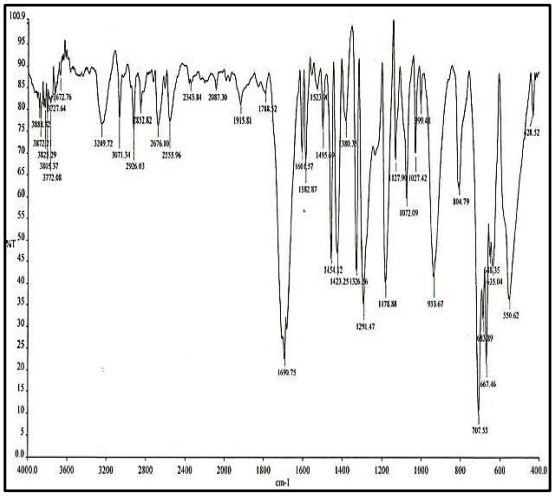

Spectrum 41. 19F decoupled 1H NMR of 54f

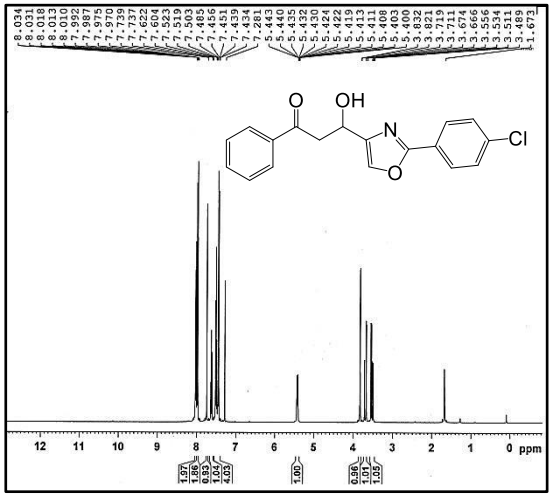

Spectrum 42. ^{1}H NMR of compound 54f

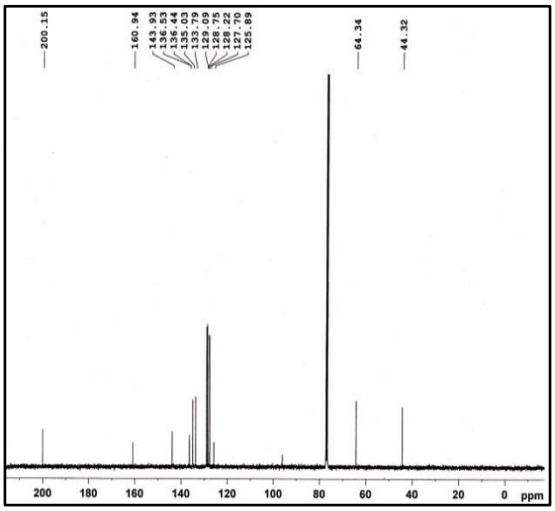

Spectrum 43. ^{13}C NMR of compound 54f

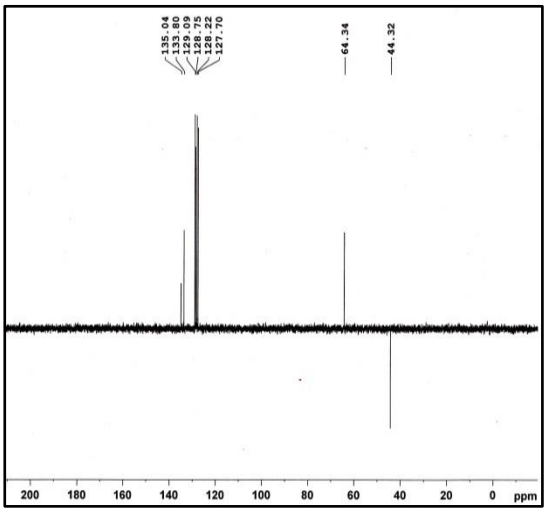

Spectrum 44. DEPT 135 of compound 54f

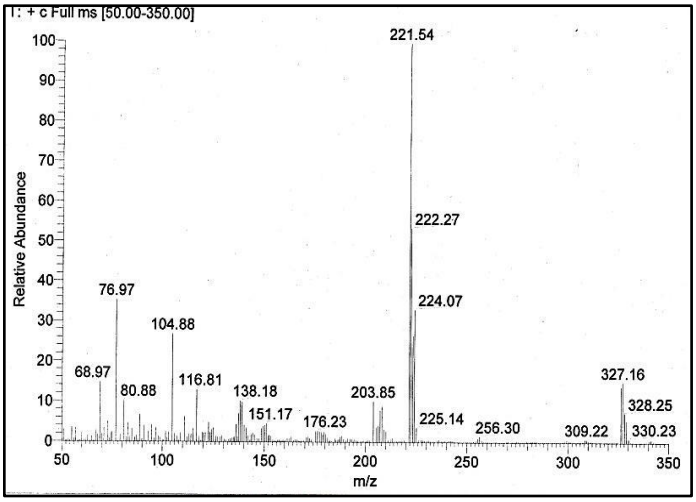

Spectrum 45. MASS of compound 54f

Compound 54g

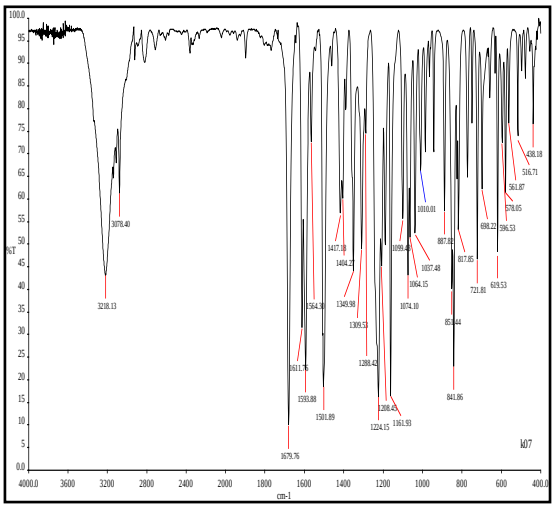

Spectrum 46. IR of compound 54g

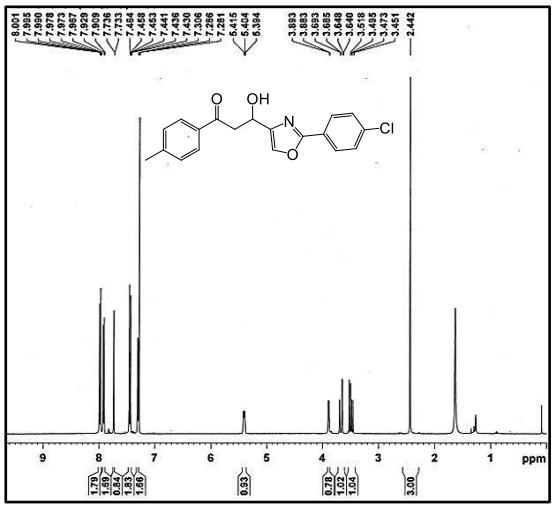

Spectrum 47. ^{1}H NMR of compound 54g

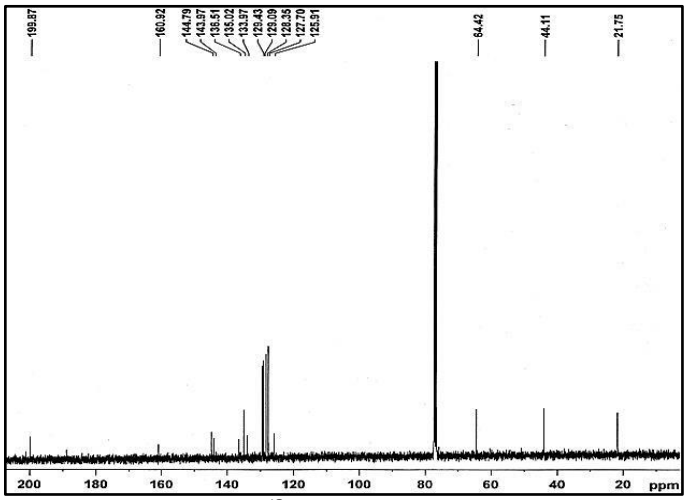

Spectrum 48. ^{13}C NMR of compound 54g

Compound 54h

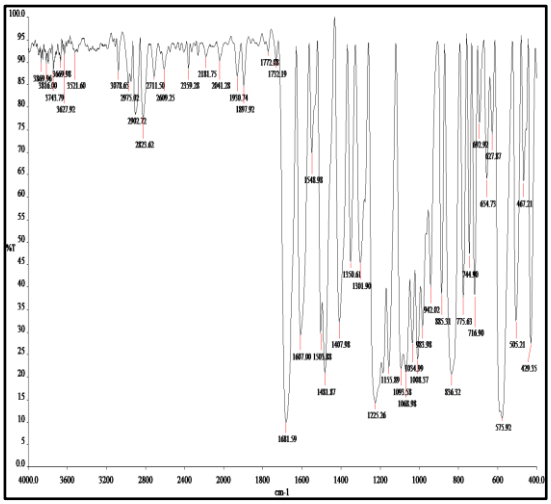

Spectrum 49. IR of compound 54h

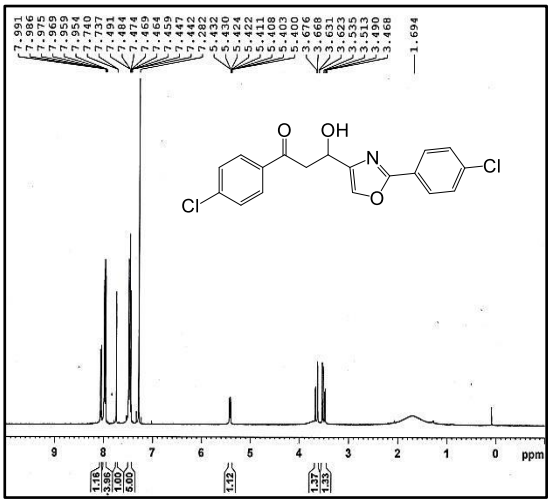

Spectrum 50. ^{1}H NMR of compound 54h

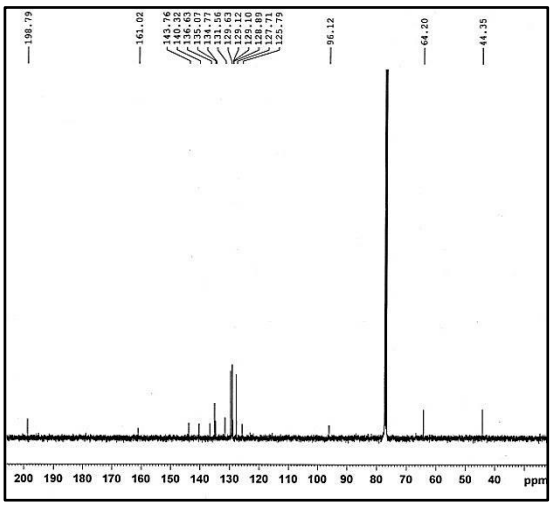

Spectrum 51. ^{13}C NMR of compound 54h

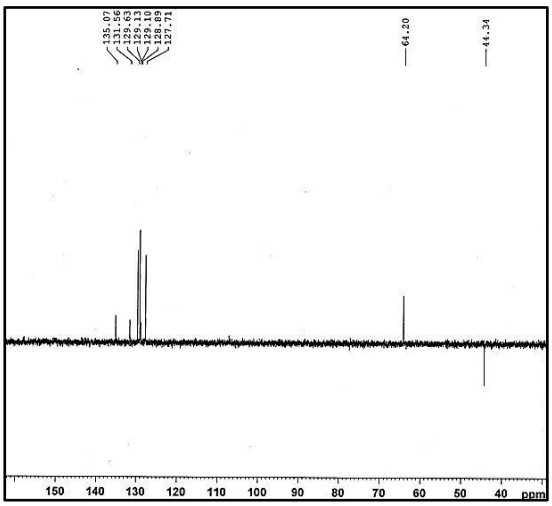

Spectrum 52. DEPT 135 of compound 54h

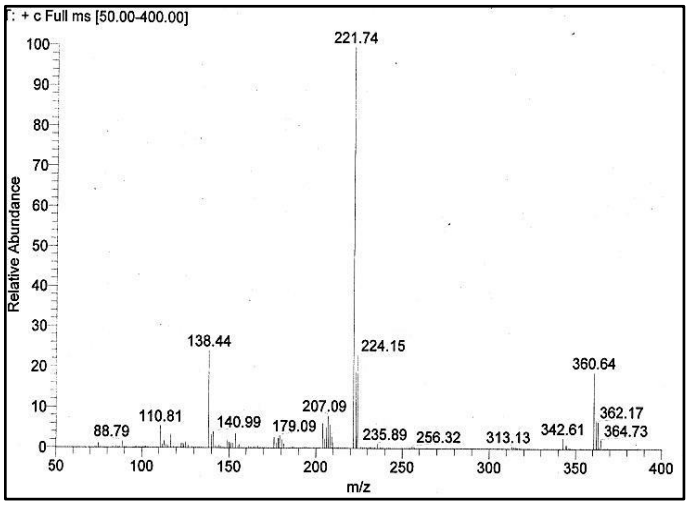

Spectrum 53. MASS of compound 54h

Compound 54i

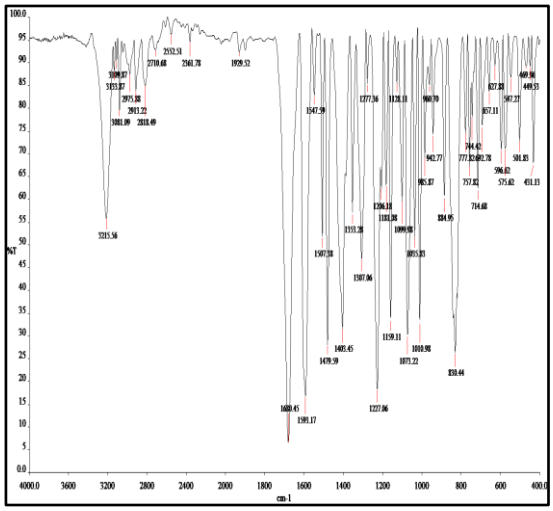

Spectrum 54. IR of compound 54i

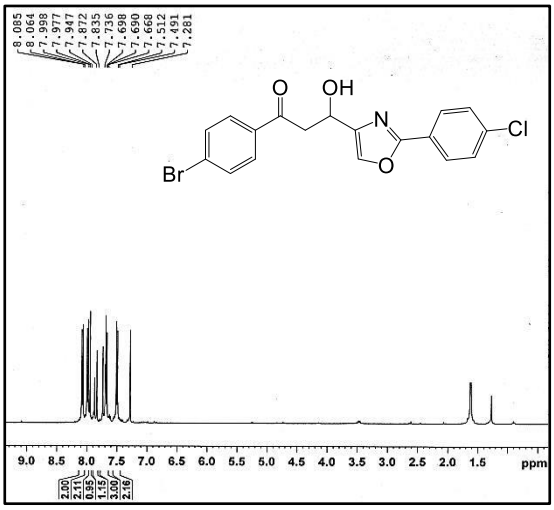

Spectrum 55. ^{1}H NMR of compound 54i

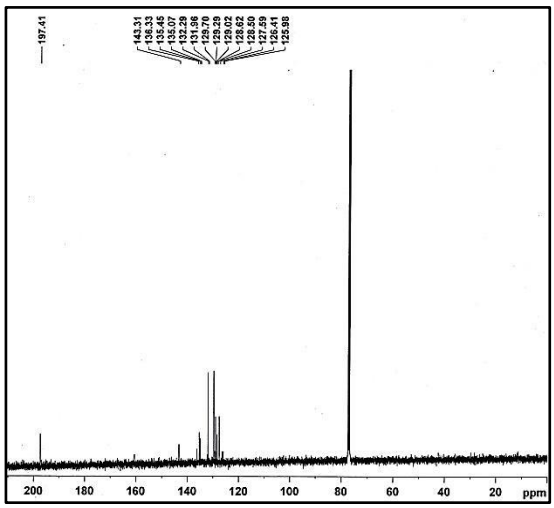

Spectrum 56. ^{13}C NMR of compound 54i

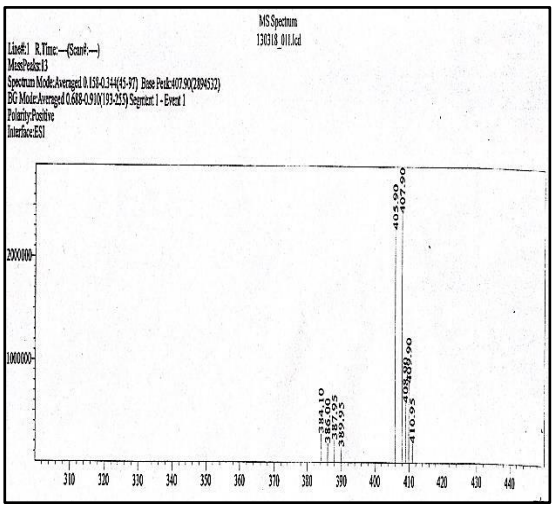

Spectrum 57. MASS of compound 54i

Compound 55a

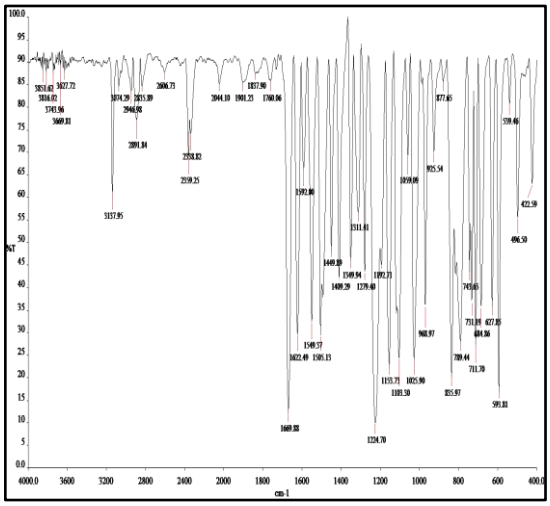

Spectrum 58. IR of compound 55a

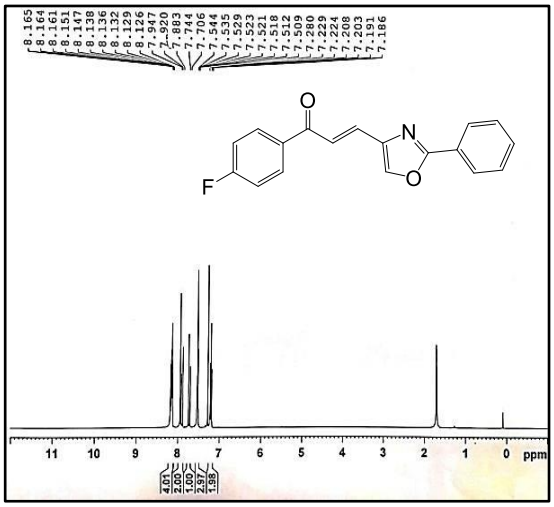

Spectrum 59. ^{1}H NMR of compound 55a

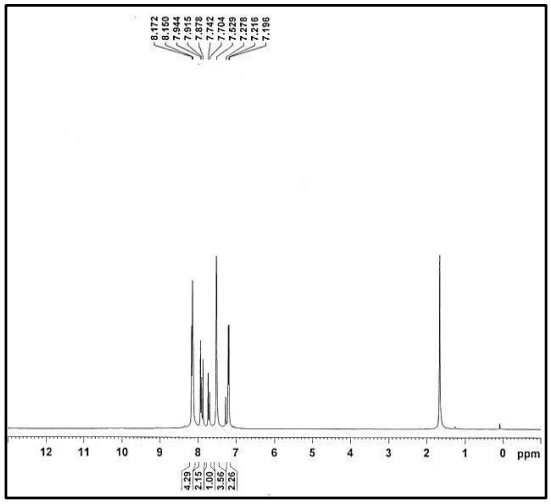

Spectrum 60. ^{19}F decoupled ^{1}H NMR of 55a

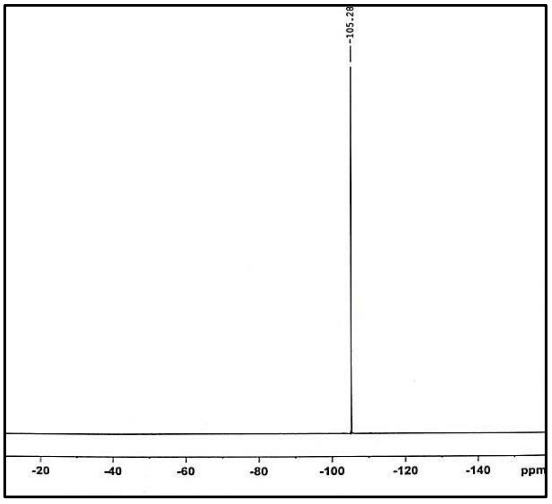

Spectrum 61. ^{19}F NMR of compound 55a

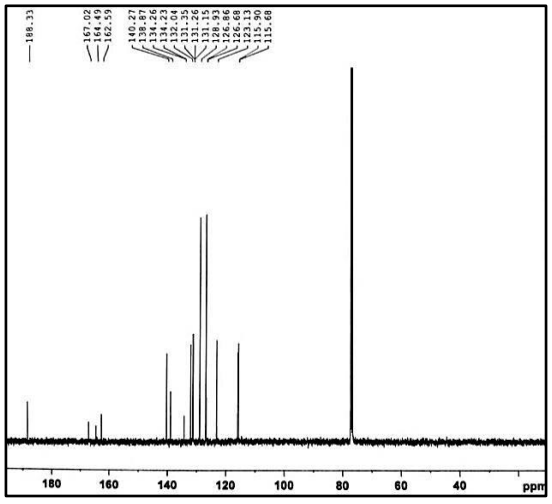

Spectrum 62. ^{13}C NMR of compound 55a

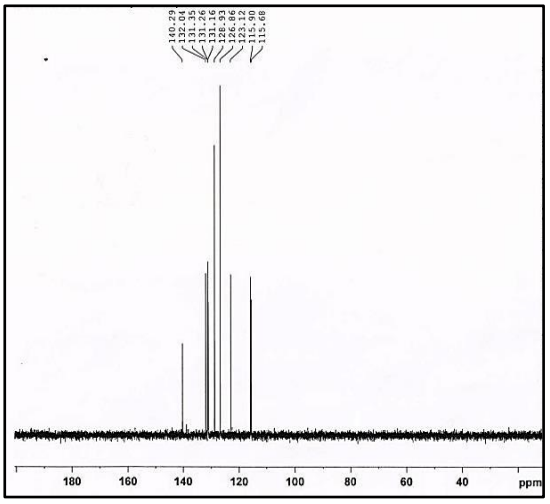

Spectrum 63. DEPT 135 of compound 55a

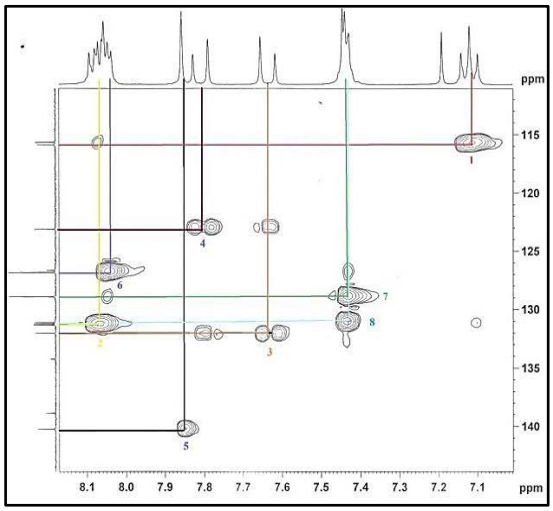

Spectrum 64. HSQC of compound 55a

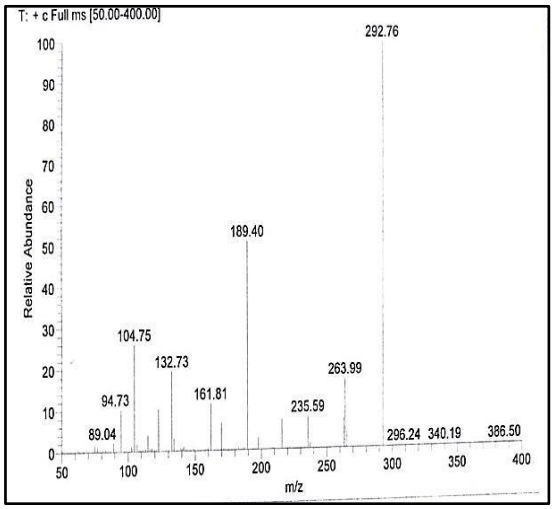

Spectrum 65. MASS of compound 55a

Compound 55b

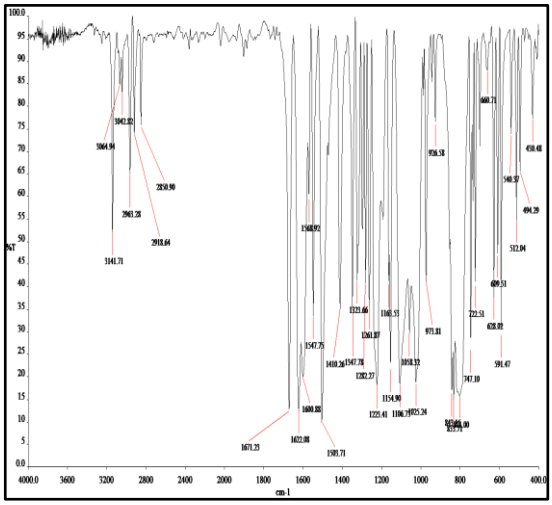

Spectrum 66. IR of compound 55b

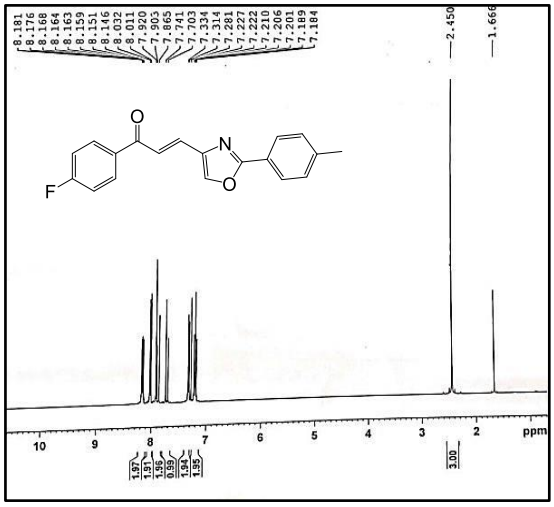

Spectrum 67. ^{1}H NMR of compound 55b

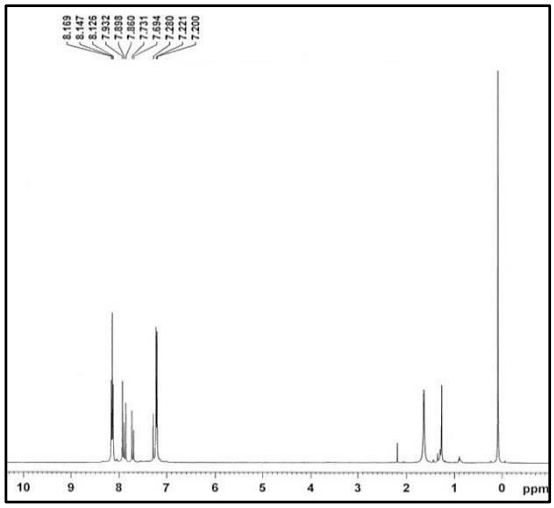

Spectrum 68. ^{19}F decoupled ^{1}H NMR of 55b

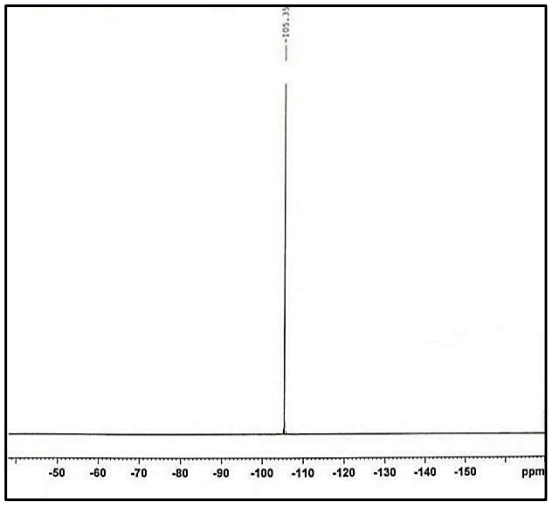

Spectrum 69. ^{19}F NMR of compound 55b

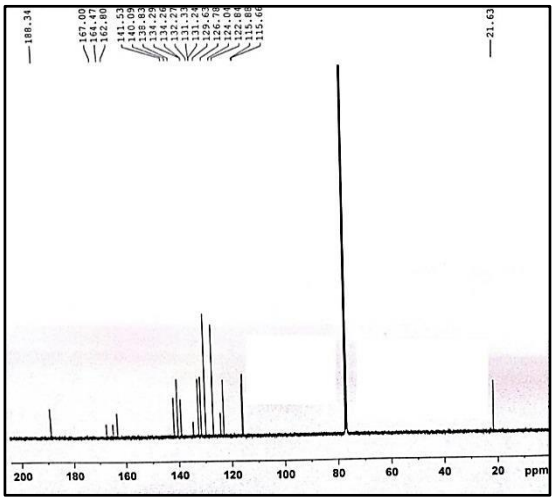

Spectrum 70. ^{13}C NMR of compound 55b

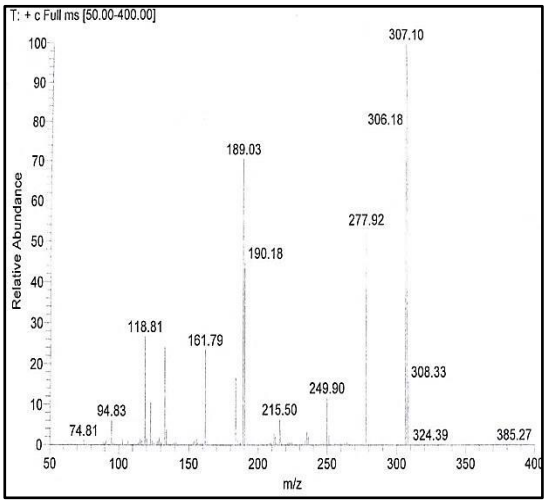

Spectrum 71. MASS of compound 55b

Compound 55c

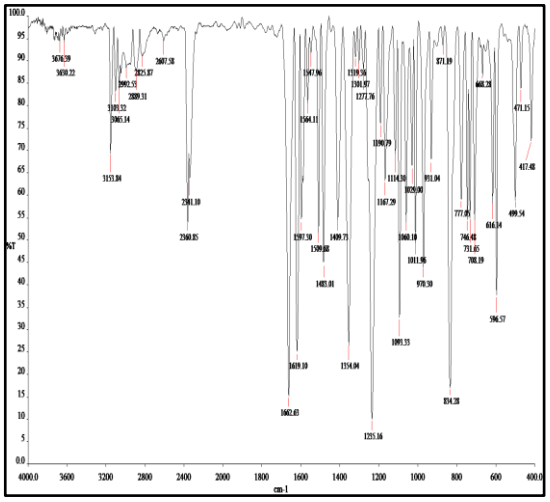

Spectrum 72. IR of compound 55c

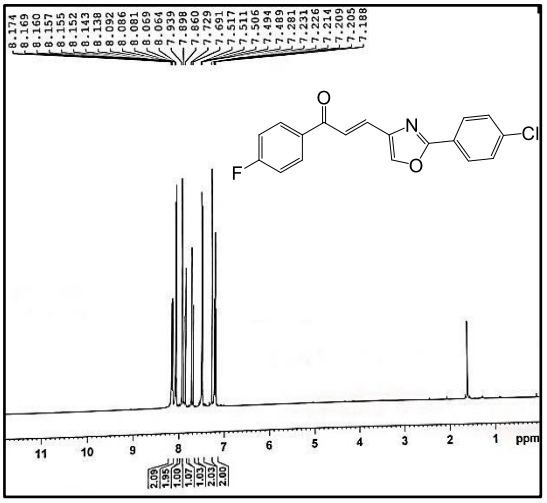

Spectrum 73. ^{1}H NMR of compound 55c

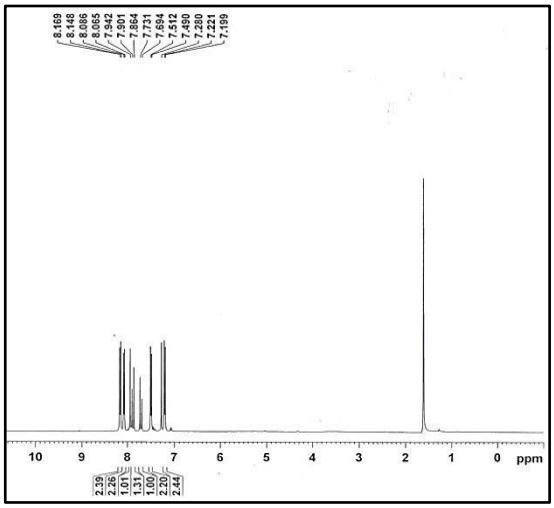

Spectrum 74. ^{19}F decoupled ^{1}H NMR of 55c

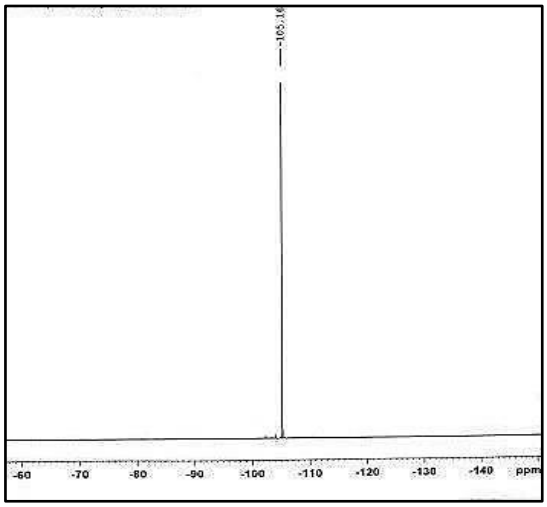

Spectrum 75. ^{19}F NMR of compound 55c

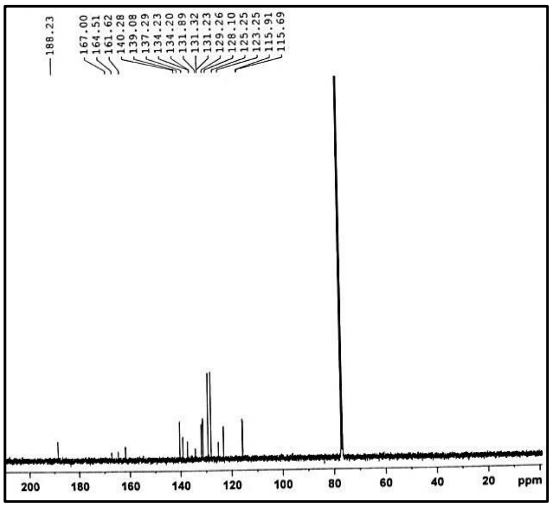

Spectrum 76. ^{13}C NMR of compound 55c

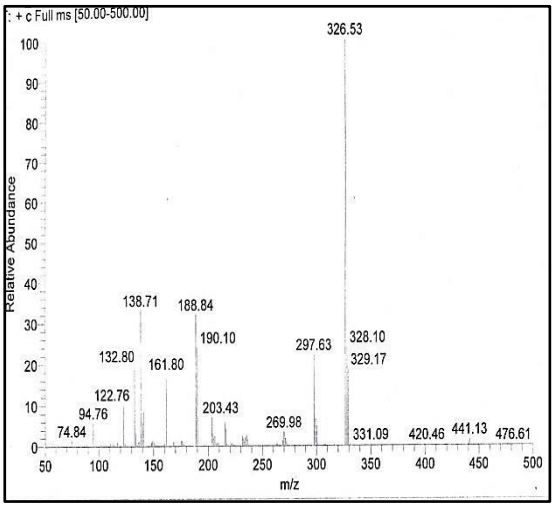

Spectrum 77. MASS of compound 55c

Compound 55d

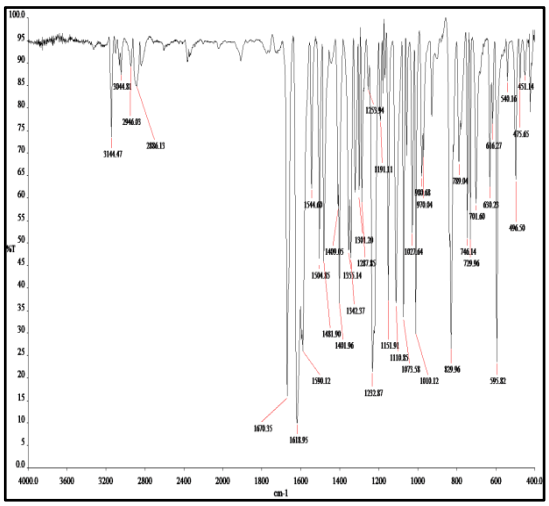

Spectrum 78. IR of compound 55d

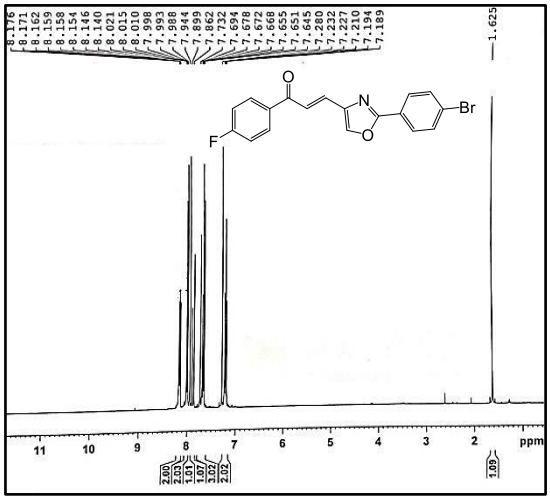

Spectrum 79. ^{1}H NMR of compound 55d

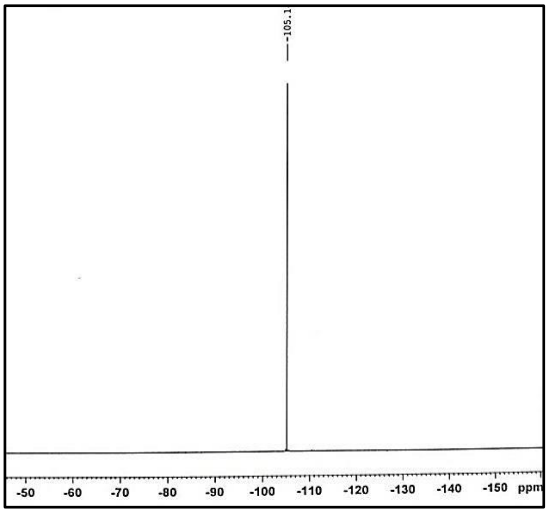

Spectrum 80. ^{19}F NMR of compound 55d

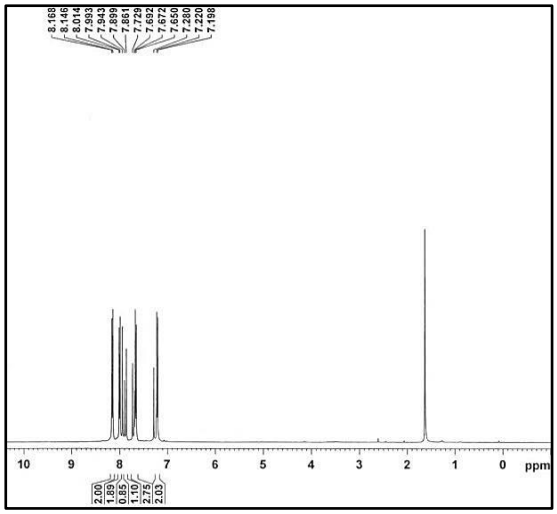

Spectrum 81. ^{19}F decoupled ^{1}H NMR of 55d

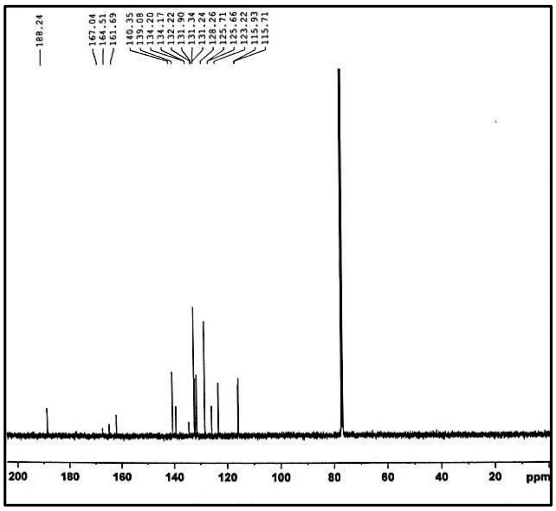

Spectrum 82. ^{13}C NMR of compound 55d

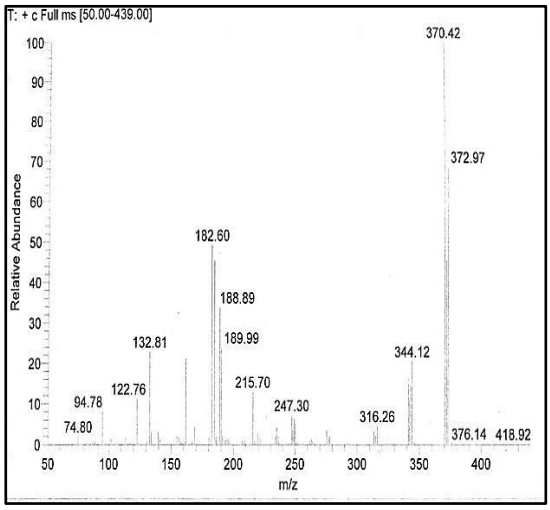

Spectrum 83. MASS of compound 55d

Compound 55e

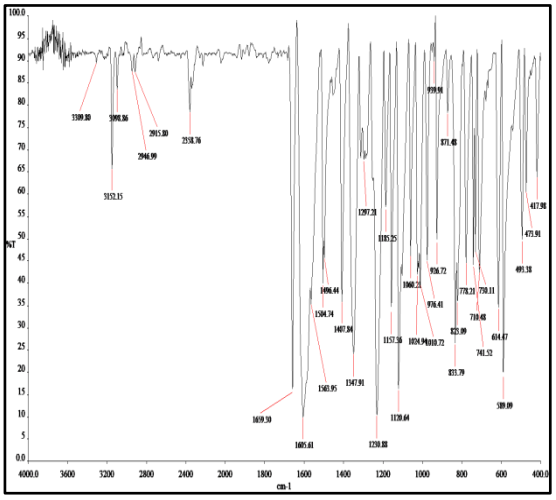

Spectrum 84. IR of compound 55e

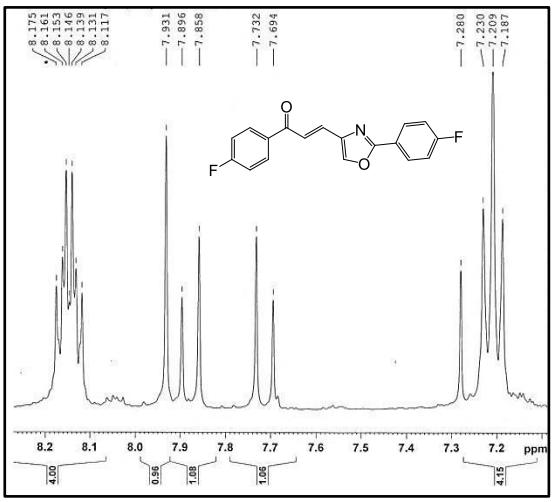

Spectrum 85. ^{1}H NMR of compound 55e

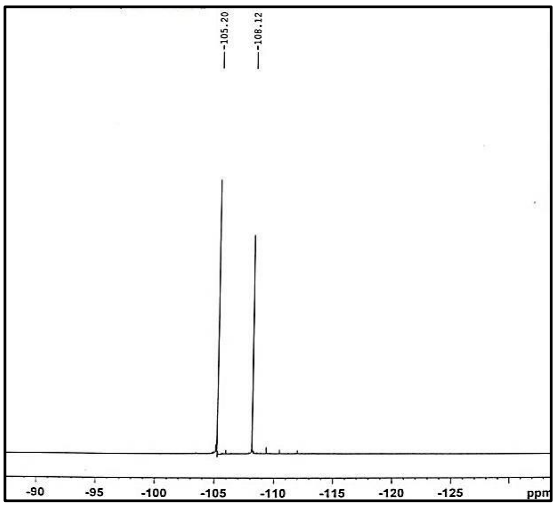

Spectrum 86. ^{19}F NMR of compound 55e

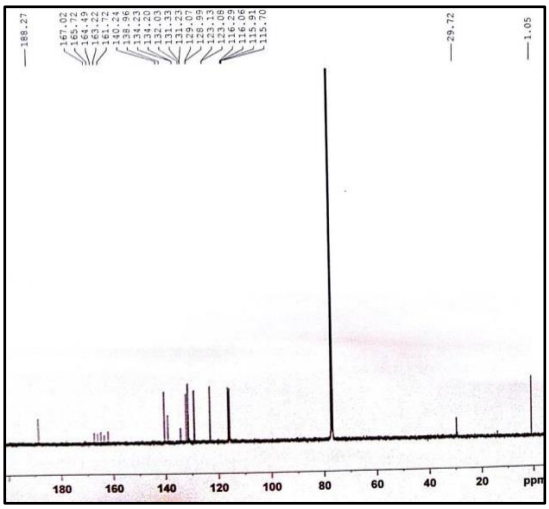

Spectrum 87. ^{13}C NMR of compound 55e

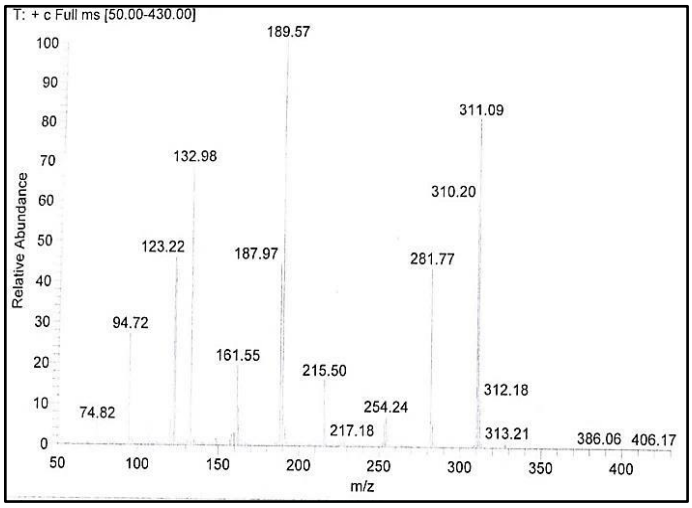

Spectrum 88. MASS of compound 55e

Compound 55f

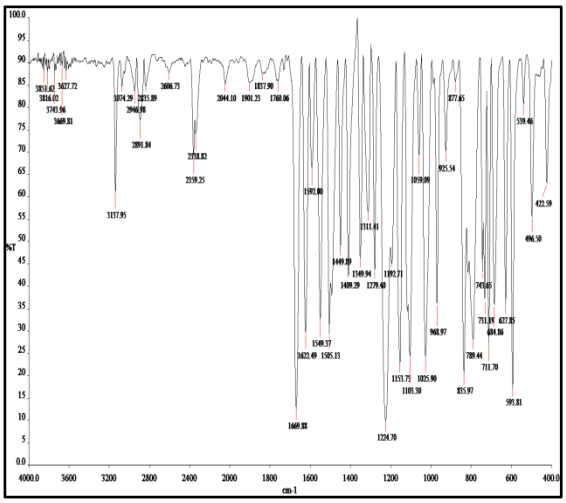

Spectrum 89. IR of compound 55f

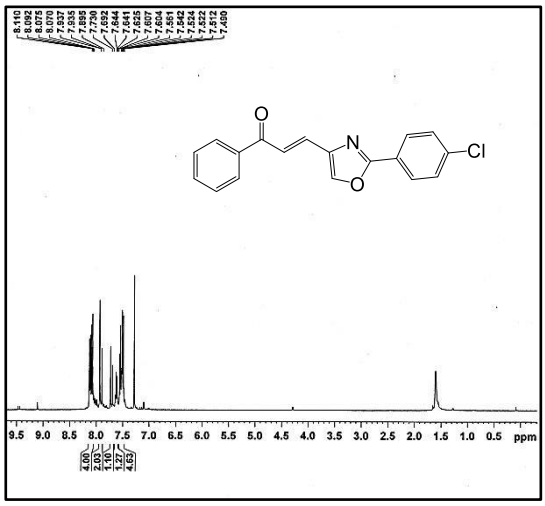

Spectrum 90. ^{1}H NMR of compound 55f

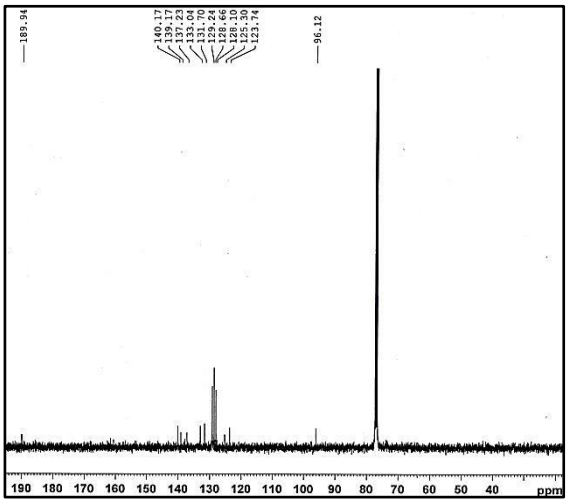

Spectrum 91. ^{13}C NMR of compound 55f

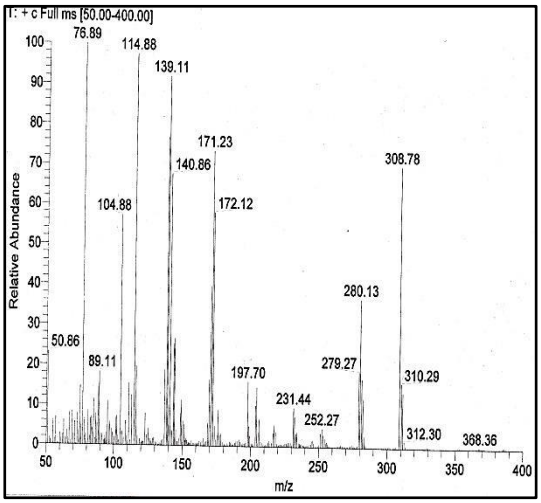

Spectrum 92. MASS of compound 55f

Compound 55g

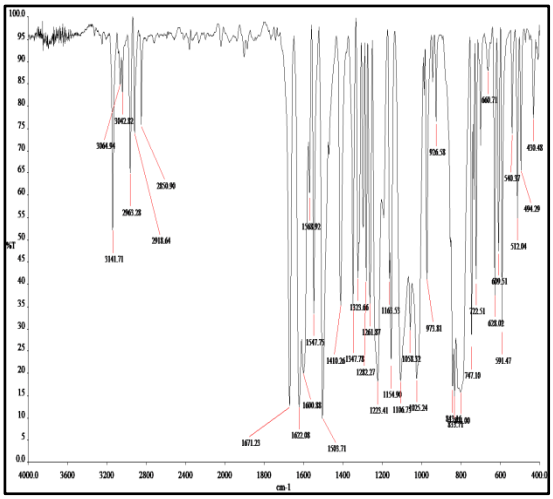

Spectrum 93. IR of compound 55g

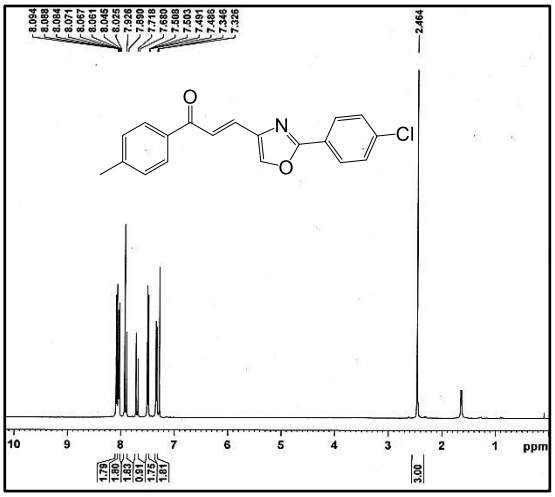

Spectrum 94. ^{1}H NMR of compound 55g

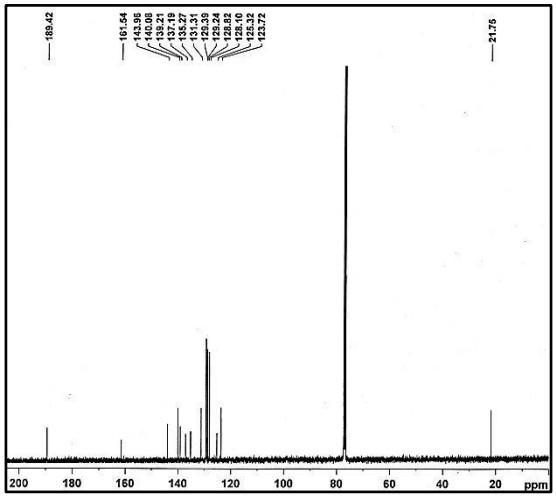

Spectrum 95. ^{13}C NMR of compound 55g

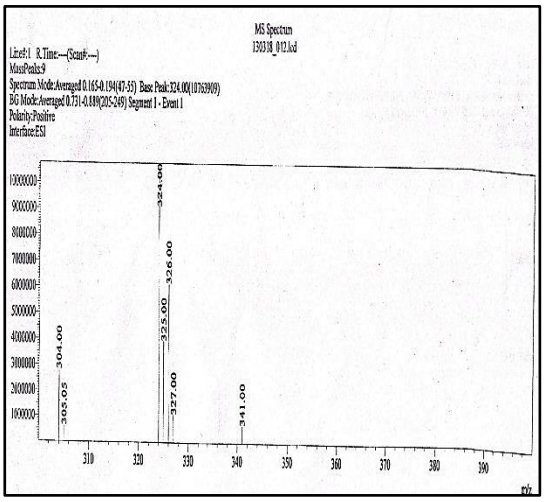

Spectrum 96. MASS of compound 55g

Compound 55h

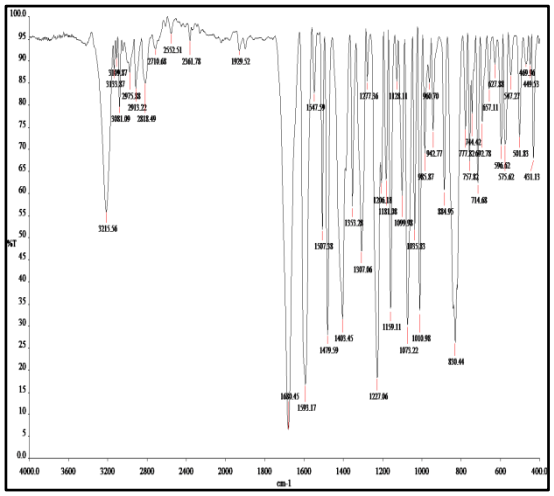

Spectrum 97. IR of compound 55h

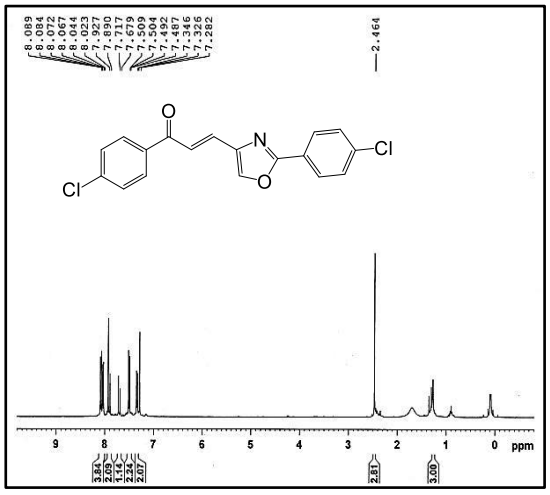

Spectrum 98. ^{1}H NMR of compound 55h

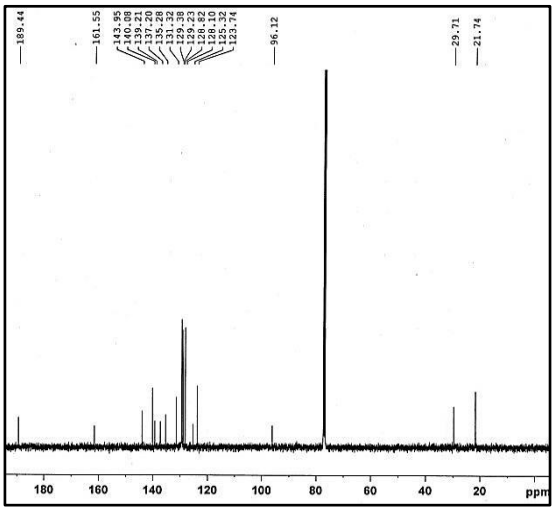

Spectrum 99. ^{13}C NMR of compound 55h

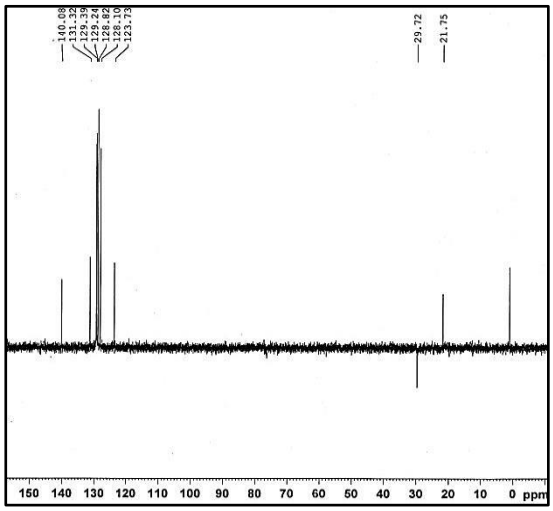

Spectrum 100. DEPT 135 of compound 55h

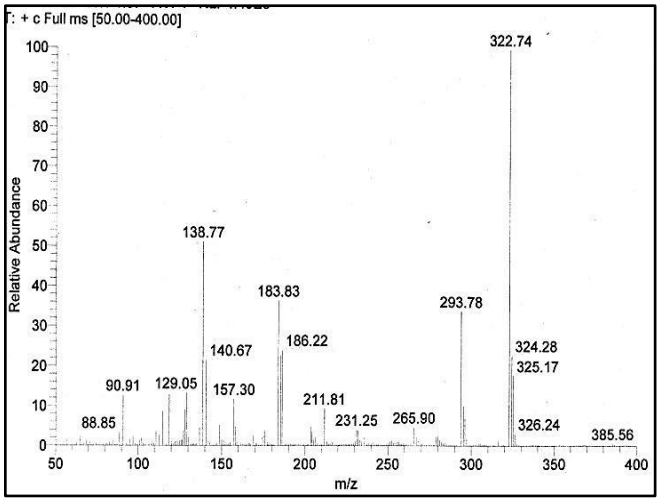

Spectrum 101. MASS of compound 55h

Compound 55i

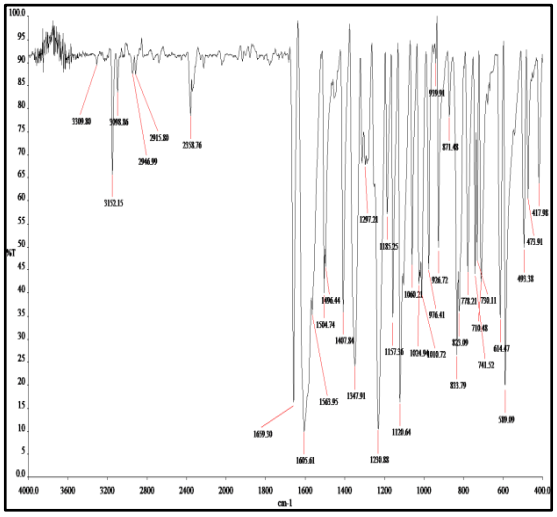

Spectrum 102. IR of compound 55i

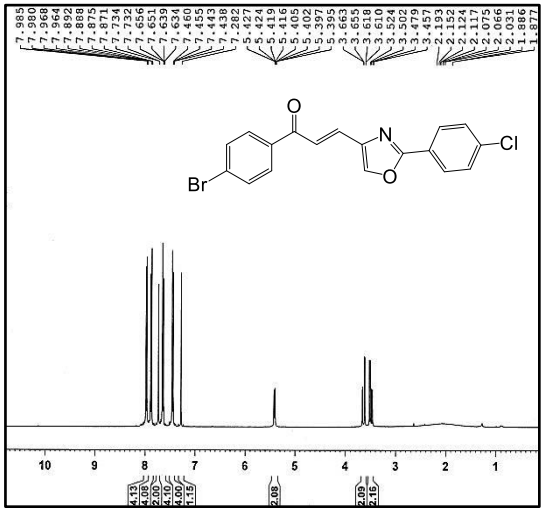

Spectrum 103. ^{1}H NMR of compound 55i

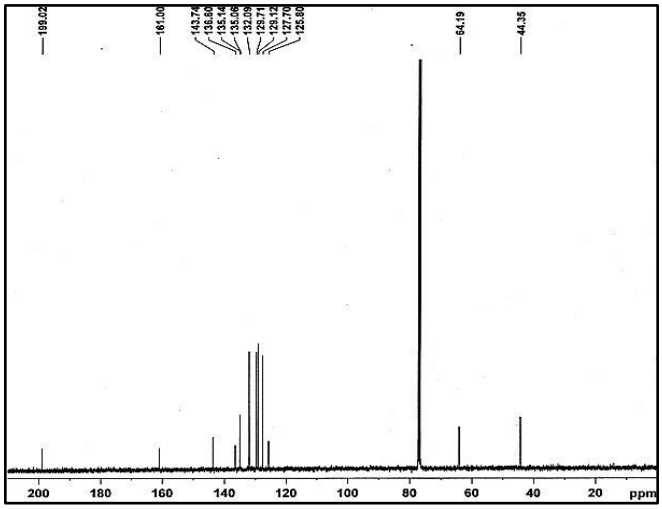

Spectrum 104. ^{13}C NMR of compound 55i

2.6 References

1 H. Zhang, Z. Zhao and C. Zhou, *Eur. J. Med. Chem.*, 2018, **144**, 444–492.

2 A. Ibrar, I. Khan, N. Abbas, U. Farooq and A. Khan, *RSC Adv.*, 2016, **6**, 93016–93047.

3 N. R. Stokes, N. Baker, J. M. Bennett, P. K. Chauhan, I. Collins, D. T. Davies, M. Gavade, D. Kumar, P. Lancett, R. Macdonald, L. Macleod, A. Mahajan, J. P. Mitchell, N. Nayal, Y. Nandan, G. R. W. Pitt, M. Singh, A. Yadav, A. Srivastava, L. G. Czaplewski and D. J. Haydon, *Bioorg. Med. Chem. Lett.*, 2014, **24**, 353–359.

4 Shamsuzzaman, M. S. Khan, M. Alam, Z. Tabassum, A. Ahmad and A. U. Khan, *Eur. J. Med. Chem.*, 2010, **45**, 1094–1097.

5 D. Yamamuro, R. Uchida, M. Ohtawa, S. Arima, Y. Futamura and M. Katane, *Bioorg. Med. Chem. Lett.*, 2015, **25**, 313–316.

6 F. Yokokawa, T. Asano and T. Shioiri, *Org. Lett.*, 2000, **2**, 4169–4172.

7 Z. J. Zhong, D. J. Zhang, Z. G. Peng, Y. H. Li, G. Z. Shan, L. M. Zuo, L. T. Wu, S. Y. Li, R. M. Gao and Z. R. Li, *Eur. J. Med. Chem.*, 2013, **69**, 32–43.

8 G. C. Moraski, M. Chang, A. Villegas-Estrada, S. G. Franzblau, U. Möllmann and M. J. Miller, *Eur. J. Med. Chem.*, 2010, **45**, 1703–1716.

9 X. Lu, X. Liu, B. Wan, S. G. Franzblau, L. Chen, C. Zhou and Q. You, *Eur. J. Med. Chem.*, 2012, **49**, 164–171.

10 I. Semenyuta, V. Kovalishyn, V. Tanchuk, S. Pilyo, V. Zyabrev, V. Blagodatnyy, O. Trokhimenko, V. Brovarets and L. Metelytsia, *Comput. Biol. Chem.*, 2016, **65**, 8–15.

11 M. J. Choi, E. S. No, D. A. Thorat, J. W. Jang, H. Yang, J. Lee, H. Choo, S. J. Kim, C. S. Lee, S. Y. Ko, J. Lee, G. Nam and A. N. Pae, *J. Med. Chem.*, 2013, **56**, 9008–9018.

12 X. H. Liu, P. C. Lv, J. Y. Xue, B. A. Song and H. L. Zhu, *Eur. J. Med. Chem.*, 2009, **44**, 3930–3935.

13 A. K. Shakya, A. Kaur, B. Al-Najjar and R. Naik, *Saudi Pharm. J.*, 2016, **24**, 616–624.

14 P. Zaware, S. R. Shah, H. Pingali, P. Makadia, B. Thube, S. Pola, D. Patel, P. Priyadarshini, D. Suthar, M. Shah, J. Jamili, K. V. V. M. Sairam, S. Giri, L. Patel, H. Patel, H. Sudani, H. Patel, M. Jain, P. Patel and R. Bahekar, *Bioorg. Med. Chem. Lett.*, 2011, **21**, 628–632.

15 V. Yeh and R. Iyengar, in *Comprehensive Heterocyclic Chemistry III*, eds. A. R. Katritzky, C. A. Ramsden, E. F. V Scriven and R. J. K. Taylor, Elsevier, Oxford, 2008, pp. 487–543.

16 R. Lakhan and B. Ternai, in *Advances in Heterocyclic Chemistry*, eds. A. R. Katritzky and A. J. Boulton, Academic Press, 1974, vol. 17, pp. 99–211.

17 L. Swellmeen, *Der Pharma Chem.*, 2016, **8**, 269–286.

18 S. Alvarez-Elcoro and J. D. C. Yao, in *Macrolide Antibiotics Chemistry, Biology, and Practice*, ed. S. B. T.-M. A. Second E. Ōmura, Academic Press, San Diego, 2003, pp. 363–402.

19 K.-S. Yeung and I. Paterson, *Angew. Chemie Int. Ed.*, 2002, **41**, 4632–4653.

20 H. Fuwa, T. Noguchi, M. Kawakami and M. Sasaki, *Bioorg. Med. Chem. Lett.*, 2014, **24**, 2415–2419.

21 M. Kita, H. Oka, A. Usui, T. Ishitsuka, Y. Mogi, H. Watanabe and H. Kigoshi, *Tetrahedron*, 2012, **68**, 8753–8760.

22 F. M. Uckun and C. J. Forsyth, *Bioorg. Med. Chem. Lett.*, 2001, **11**, 1181–1183.

23 J. Napolitano, A. Daranas, M. Norte and J. Fernandez, *Anticancer. Agents Med. Chem.*, 2009, **9**, 122–137.

24 M. Satyanarayana, Y. A. Kim, S. G. Rzuczek, D. S. Pilch, A. A. Liu, L. F. Liu, J. E. Rice and E. J. LaVoie, *Bioorg. Med. Chem. Lett.*, 2010, **20**, 3150–3154.

25 G. A. Blankson, D. S. Pilch, A. A. Liu, L. F. Liu, J. E. Rice and E. J. Lavoie, *Bioorg. Med. Chem.*, 2013, **21**, 4511–4520.

26 J. S. Sandler, P. L. Colin, M. Kelly and W. Fenical, *J. Org. Chem.*, 2006, **71**, 7245–7251.

27 D. J. Faulkner, *Nat. Prod. Res.*, 2000, **17**, 7–55.

28 Z. Jin, *Nat. Prod. Rep.*, 2006, **23**, 464–496.

29 D. Davyt and G. Serra, *Mar. Drugs*, 2010, **8**, 2755–2780.

30 J. Blunt, B. Copp, R. Keyzers, M. Munro and M. Prinsep, *Nat. Prod. Res.*, 2015, **32**, 116–211.

31 P. Wipf, *Chem. Rev.*, 1995, **95**, 2115–2134.

32 V. S. C. Yeh, *Tetrahedron*, 2004, **60**, 11995–12042.

33 S. Tilvi and K. S. Singh, *Curr. Org. Chmistry*, 2016, **20**, 1–56.

34 R. D. Norcross and I. Peterson, *Chem. Rev.*, 1995, **85**, 2041–2114.

35 K. Yeung and I. Paterson, *Chem. Rev.*, 2005, **105**, 4237–4313.

36 Z. Wang, in *Comprehensive Organic Name Reactions and Reagents*, John Wiley & Sons, Inc., 2010, pp. 2410–2413.

37 S. Gabriel, *Berichte der Dtsch. Chem. Gesellschaft*, 1907, **40**, 2647–2650.

38 R. Robinson, *J. Chem. Soc.*, 1909, 2167.

39 Z. Wang, in *Comprehensive Organic Name Reactions and Reagents*, John Wiley & Sons, Inc., 2010, pp. 1076–1079.

40 E. Fischer, *Berichte der Dtsch. Chem. Gesellschaft*, 1986, **29**, 205–214.

41 B. A. Kulkarni and A. Ganesan, *Tetrahedron Lett.*, 1999, **40**, 5637–5638.

42 W. He, C. Li and L. Zhang, *J. Am. Chem. Soc.*, 2011, **133**, 8482–8485.

43 H. Jiang, H. Huang, H. Cao and C. Qi, *Org. Lett.*, 2010, **23**, 5561–5563.

44 C. W. Cheung and S. L. Buchwald, *J. Org. Chem.*, 2012, **77**, 7526–7537.

45 C. Hempel and B. J. Nachtsheim, *Synlett*, 2013, **24**, 2119–2123.

46 Y. Ning, Y. Otani and T. Ohwada, *J. Org. Chem.*, 2017, **82**, 6313–6326.

47 M. Reddy, G. Reddy, U. Mehmood, I. Hussein, S. Rahman, K. Harrabi and B. Subba Reddy, *Synthesis*, 2015, **47**, 3315–3320.

48 A. Saito, A. Taniguchi, Y. Kambara and Y. Hanzawa, *Org. Lett.*, 2013, **3**, 1–35.

49 S. R. Shah, R. R. Thakore, T. A. Vyas and B. Sridhar, *Synlett*, 2016, **27**, 294–300.

50 Y. Pan, F. Zheng and H. Lin, *J. Org. Chem.*, 2009, **74**, 3148–3151.

51 T. Ichino, H. Arimoto and D. Uemura, *Chem. Commun.*, 2006, 1742–1744.

52 V. J. Majo and P. T. Perumal, *Tetrahedron Lett.*, 1997, **38**, 6889–6892.

53 S. R. Shah, S. S. Navathe, A. G. Dikundwar, T. N. Guru Row and A. T. Vasella, *Eur. J. Org. Chem.*, 2013, 264–267.

54 H. M. T. Albuquerque, C. M. M. Santos, J. A. S. Cavaleiro and A. M. S. Silva, *Curr. Org. Chem.*, 2014, **18**, 1–25.

55 C. Zhuang, W. Zhang, C. Sheng, W. Zhang, C. Xing and Z. Miao, *Chem. Rev.*, 2017, **117**, 7762–7810.

56 P. Singh, A. Anand and V. Kumar, *Eur. J. Med. Chem.*, 2014, **85**, 758–777.

57 D. K. Mahapatra, S. K. Bharti and V. Asati, *Eur. J. Med. Chem.*, 2015, **98**, 69–114.

58 Z. Nowakowska, *Eur. J. Med. Chem.*, 2007, **42**, 125–137.

59 X. Gan, Y. Wang, D. Hu and B. Song, *Chinese J. Chem.*, 2017, **35**, 1–8.

60 H. Kumar, V. Devaraji, R. Joshi, M. Jadhao, P. Ahirkar, R. Prasath, P. Bhavana and S. K. Ghosh, *RSC Adv.*, 2015, **5**, 65496–65513.

61 S. K. Awasthi, N. Mishra, B. Kumar, M. Sharma, A. Bhattacharya, L. C. Mishra and V. K. Bhasin, *Med. Chem. Res.*, 2009, **18**, 407–420.

62 S. Burmaoglu, O. Algul, D. Aktas, A. Gobek and G. Gulbol, *Bioorg. Med. Chem. Lett.*, 2016, **26**, 3172–3176.

63 S. L. Gaonkar and U. N. Vignesh, *Res. Chem. Intermed.*, 2017, **43**, 6043–6077.

64 C. Krishna Prasad and P. V. S. Machiraju, *Russ. J. Gen. Chem.*, 2017, **87**, 2056–2066.

65 V. R. Solomon and H. Lee, *Biomed. Pharmacother.*, 2012, **66**, 213–220.

66 S. Navathe, "*Synthesis and Study of Some New Heterocyclic Compounds with Therapeutic Interest"*, **Ph.D Thesis**, The M. S. University of Baroda, 2009.

67 H. Pingali, M. Jain, S. Shah, P. Makadia, P. Zaware, A. Goel, M. Patel, S. Giri, H. Patel and P. Patel, *Bioorg. Med. Chem.*, 2008, **16**, 7117–7127.

68 D. Patel, M. Jain, S. R. Shah, R. Bahekar, P. Jadav, B. Darji, Y. Siriki, D. Bandyopadhyay, A. Joharapurkar, S. Kshirsagar, H. Patel, M. Shaikh, K. V. V. M. Sairam and P. Patel, *ChemMedChem*, 2011, **6**, 1011–1016.

69 P. Jadav, R. Bahekar, S. R. Shah, D. Patel, A. Joharapurkar and M. Jain, *Bioorg. Med. Chem. Lett.*, 2014, **24**, 7–11.

70 L. D. Mendelsohn, *J. Chem. Inf. Comput. Sci.*, 2004, **44**, 2225–2226.

71 N. M. O. Boyle, M. Banck, C. A. James, C. Morley, T. Vandermeersch and G. R. Hutchison, *J. Cheminform.*, 2011, **3:33**, 1–14.